Mechanistic analysis of scaffold contributions to specificity and insulation in Wnt signaling

Maire Gavagan

A dissertation

submitted in partial fulfillment of the

requirements for the degree of

Doctor of Philosophy

University of Washington

2022

Reading Committee:

Jesse Zalatan, Chair

Dustin Maly

Michael Gelb

Program Authorized to Offer Degree:

Chemistry

University of Washington

Abstract

Mechanistic analysis of scaffold contributions to specificity and insulation in Wnt signaling

Maire Gavagan

Chair of the Supervisory Committee:

Dr. Jesse Zalatan

Department of Chemistry

Glycogen Synthase Kinase 3β (GSK3β) plays a pivotal role in a large number of signaling pathways. To avoid cross-pathway interference, signaling pathways that rely on GSK3β must have regulatory features that allow signals to be passed through GSK3β to the correct downstream substrates without activating other pathways. Scaffold proteins, binding platforms that assemble and regulate signaling pathways, may provide a mechanism to direct shared signaling components to specific downstream targets. In Wnt signaling, the scaffold protein Axin is thought to serve as a control point, coordinating the phosphorylation of the Wnt substrate β-catenin by GSK3β. We tested the long-standing hypothesis that Axin directs GSK3β activity in the Wnt pathway by accelerating GSK3β phosphorylation of the substrate β-catenin. We measured reaction rates in a minimal reconstituted *in vitro* system and found that, surprisingly, Axin produced only modest increases in β-catenin phosphorylation rates. Instead, Axin increases the specificity of GSK3β for β-catenin by suppressing competing kinase reactions. By

suppressing the competition, Axin can produce >10-fold increases in the β-catenin phosphorylation rate when competing substrates are present. Acting through Axin, Wnt signals could regulate just the pool of GSK3β that is bound to Axin, allowing Wnt signals to be sent without affecting other signaling pathways. Axin may also play a role in protecting Wnt-associated GSK3β from being affected by signals from other pathways. We found that binding to Axin protects GSK3β from phosphorylation at Ser9, a key regulatory event in insulin and other signaling pathways. These mechanisms allow the scaffold to create a pool of GSK3β that preferentially interacts with β-catenin and can be independently regulated through Axin without affecting, or being affected by, other signaling pathways.

Acknowledgements

Like research itself, pursuing a doctoral degree requires a high degree of collaborative effort. A huge number of people have contributed to my research and to my development as a scientist. I like to joke that everyone turns into their advisor eventually, but I am extremely fortunate to say in my case that is a good thing. My graduate advisor, Jesse Zalatan always challenged me to think and speak about complex topics and questions in my research in a manner that is both careful and precise. Although there are some topics about which we will never agree, namely the best dim sum restaurants and whether "scaffold orange" is a real color, many of the habits and skills that I have developed through Jesse's mentorship have made me a better scientist.

I'd like to thank all the people who have served on my thesis and second year committees, including Dusty Maly, Mike Gelb, Pradip Rathod, and David Kimelman. Your valuable questions and insights have helped shape this work.

I'd also like to thank all my fellow lab members, especially Betsy, Erin, and Noel. The Axin work presented here started in collaboration with Erin and without her initial work this project would have been totally different. Betsy was a former postdoc in the lab and a mentor, both scientifically and personally. Thanks for being an amazing role model as a strong female scientist but also for being a great friend. I'd also like to thank Noel for picking up the reins of this project after I leave. I can't imagine a better person to leave in charge of my projects and I'm excited to see the new directions you will take them in.

This achievement would not have been possible without the support of my family, especially my mom. Over the years she has shown me what it means to be resourceful, hard-working, and compassionate. I wouldn't be the person I am without you.

Finally, I thank my partner Danny who has been endlessly supportive throughout my time in grad school. Thanks for your endless patience with my odd hours and the “quick” stops into lab that turn into hours-long experiments. Thanks for reminding me that there’s a wonderful world of traveling, hiking, and exploring outside of lab work. Most importantly, thanks for being proud of me every day for my hard work and determination, even when none of my experiments are working.

TABLE OF CONTENTS

Chapter 1: Introduction

Cells receive a variety of information from the cellular environment and must translate these inputs through signaling pathways to produce the correct cellular behavior or output. However, signaling pathways often share components which creates the possibility of crosstalk, where one pathway inappropriately activates another. Previous work has shown that simple input-output relationships can be maintained even when components are shared by multiple signaling pathways (Guo and Wang, 2009; Mendoza et al., 2011; Ding et al., 2000). Despite years of work in this area we still do not fully understand the mechanisms and organizational features that signaling pathways use to manage shared resources and avoid crosstalk.

1.1 Scaffold Proteins and Spatial Organization

One way that signaling pathways could prevent crosstalk is by spatially organizing signaling pathways. For example, signaling components may be segregated in different parts of the cell, inside organelles, or localized inside distinct protein complexes or phase separated droplets. Scaffold proteins are multivalent proteins that serve as binding platforms to physically assemble signaling cascades (Good et al., 2011; Langeberg et al., 2015). Scaffold proteins may play a role in insulating signaling pathways against crosstalk by anchoring signaling components in different locations in the cell or by assembling protein complexes to create separate sub-pools of signaling pathway components. Scaffolds may also play a more active regulatory role in preventing crosstalk by controlling when and where signaling components are active, or by excluding negative regulators from accessing signaling components.

1.2 Scaffold Protein Functions in the Wnt Signaling Pathway

1.2.1 GSK3β is shared between multiple signaling pathways

Glycogen Synthase Kinase 3β (GSK3β) is a central kinase with over 30 known substrates in many diverse signaling pathways (Sutherland et al., 2011). Its phosphorylation of the substrate β-catenin is the defining event in canonical Wnt signaling, determining the outcome of an incoming Wnt signal (Kimelman and Xu, 2006; MacDonald et al., 2009; Moon et al., 2004; Nusse and Clevers, 2017; Polakis, 2000; Stamos and Weis, 2013). GSK3β also plays a pivotal role in an astounding number of signaling pathways, regulating development, proliferation, differentiation, cell migration, immunity, metabolism, neurobiology, and others. As might be expected from its involvement in these varied and critical cell behaviors, dysregulated GSK3β has been linked to many diseases and disorders including diabetes, Alzheimer's, heart failure, cancer, and mood disorders such as schizophrenia and bipolar disorder (Jope et al., 2007).

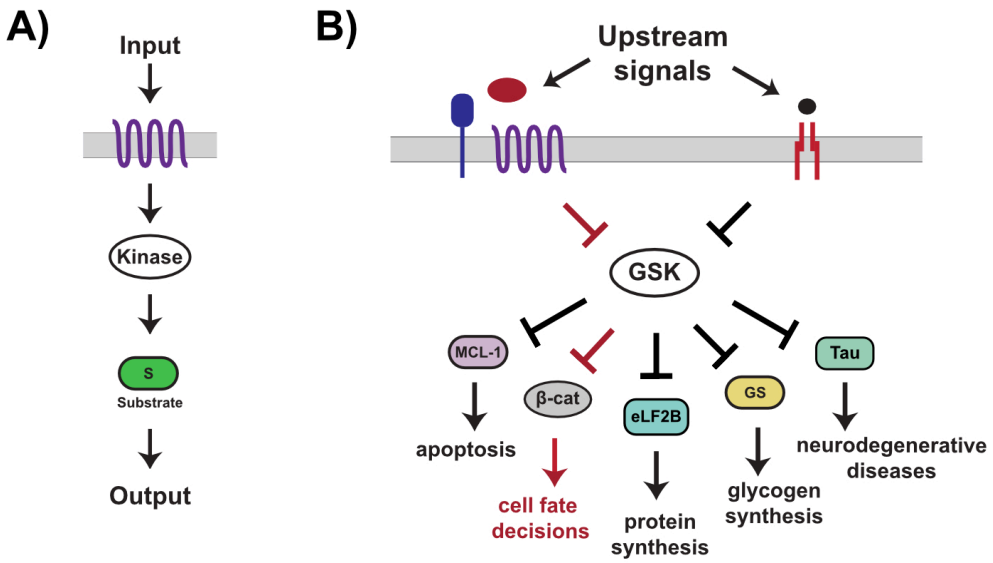

Figure 1.1. Multiple pathways transmit signals through the kinase GSK.
(A) Signaling pathways are often modeled with simple, linear input-output relationships. (B) GSK3β receives input signals from Wnt, growth factors, and hormones like insulin and acts on multiple distinct downstream targets.

Despite interest in targeting GSK3β for therapies for these diseases, efforts have been complicated by the necessity of targeting specific sub-pools of GSK3β involved in the behavior of interest. Therapeutics acting on GSK3β indiscriminately may result in toxicity because of unwanted effects on other GSK3β-involving signaling pathways (Eldar-Finkelman et al., 2011). Indeed, this lack of pathway specificity has led to the failure of many GSK3β inhibitors in clinical trials (Bhat et al., 2018). Understanding how the cellular pool of GSK3β is shared by multiple signaling pathways can help develop strategies to target just one sub-population of GSK3β that is associated with a specific activity or signaling pathway.

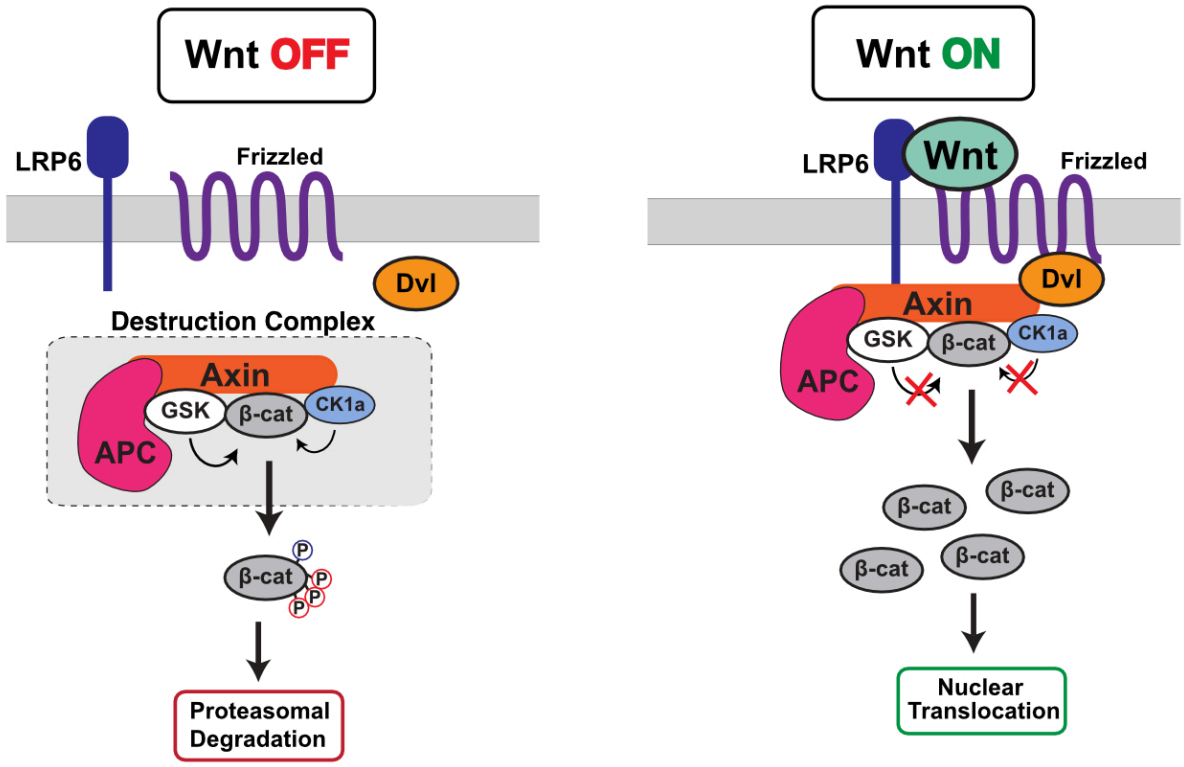

Figure 1.2. Axin assembles signaling proteins in the Wnt pathway.
GSK3β assembles into a multi-protein destruction complex containing β-catenin, CK1α, Axin, and APC. In the absence of a Wnt signal, β-catenin is phosphorylated and degraded by the proteasome. In the presence of a Wnt signal, the destruction complex is disabled, blocking β-catenin phosphorylation. β-catenin accumulates, moves into the nucleus, and activates downstream gene expression.

1.2.2 The scaffold protein Axin is crucial for Wnt signaling

If GSK3β is involved in so many signaling pathways, how can signals be sent through any one pathway without cross-activating the others? One possibility is through scaffold proteins. In Wnt signaling, the scaffold protein Axin binds and assembles the destruction complex, a Wnt-specific protein complex containing both the kinase GSK3β, the substrate β-catenin, and other Wnt proteins. This complex phosphorylates β-catenin, marking it for degradation. When a Wnt signal arrives, this machinery is disabled causing β-catenin levels to rise, move into the nucleus, and initiate a transcriptional program (Kimelman and Xu, 2006; MacDonald et al., 2009; Moon et al., 2004; Nusse and Clevers, 2017; Polakis, 2000; Stamos and Weis, 2013) The scaffold Axin is absolutely required for Wnt signaling, and normal development cannot proceed without it (Zeng et al., 1997). However, many open questions remain about the mechanistic role of Axin in Wnt signaling and its role in insulating Wnt signals from other pathways that rely on GSK3β (Nusse and Clevers, 2017).

1.3 Models for scaffold protein insulation of Wnt signaling

Promoting a specific GSK3β reaction

The scaffold protein Axin has long been hypothesized to accelerate GSK3β phosphorylation of β-catenin, the key reaction in Wnt signaling (Ikeda et al., 1998; Hart et al., 1998; Dajani et al., 2003). In this model, Axin binds to both the enzyme and substrate, bringing them closer together and increasing reaction rates (Figure 1.3A). By accelerating GSK3β activity towards only the Wnt substrate β-catenin, Axin could create a subset of GSK3β that could be independently regulated without affecting other, non-Wnt pathways. Axin could also allosterically activate GSK3β phosphorylation of β-catenin which would allow Axin to control when and where

GSK3β is active. Upstream Wnt signals could control GSK3β phosphorylation of β-catenin by regulating the scaffold instead of GSK3β.

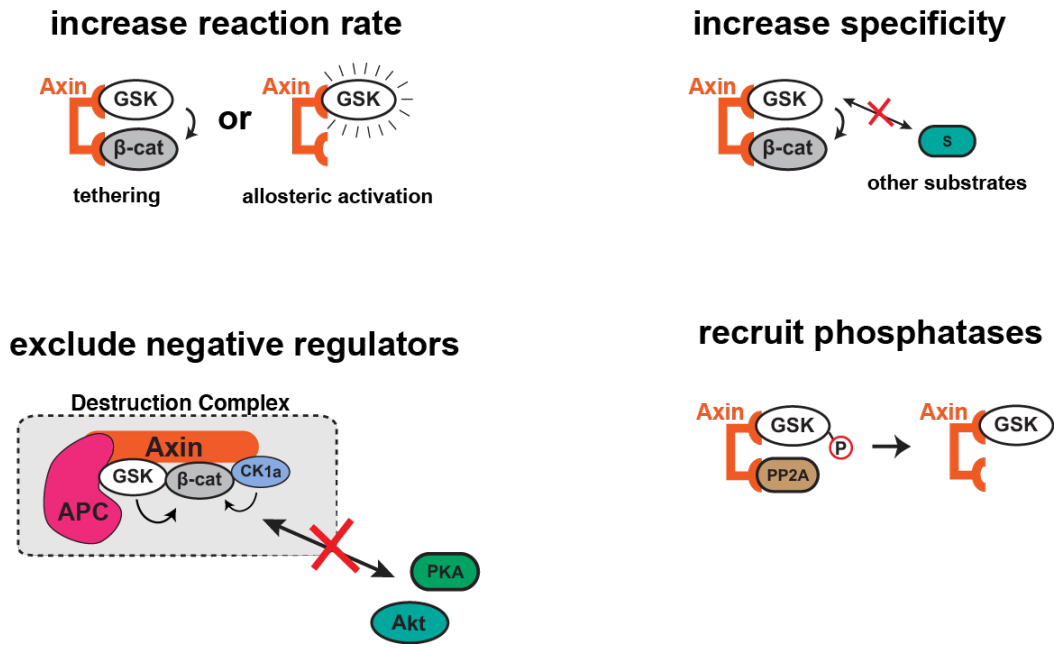

Figure 1.3. Axin assembles signaling proteins in the Wnt pathway.
(A) The scaffold Axin could increase GSK3β phosphorylation of β-catenin by tethering the kinase and substrate together, or by allosterically activating the kinase. Either mechanism would allow Axin to control when and where GSK3β is active. (B) Axin could also act by increasing the specificity of GSK3β for β-catenin. Axin could promote GSK3β binding to Wnt substrates or decrease binding to non-Wnt substrates. (C) Axin could prevent cross-activation of Wnt signaling from other pathways by preventing negative regulators such as Akt and PKA from accessing the Wnt pool of GSK3β. (D) Axin could also recruit phosphatases to remove regulatory post-translational modifications from the Wnt pool of GSK3β.

Increasing specificity of GSK3β

Instead of increasing the rate of GSK3β phosphorylation, Axin could also increase the specificity of GSK3β for β-catenin (Figure 1.3B). Enzyme specificity is a measure of how restrictive the enzyme is in its choice of substrate, or its preference for one substrate over others (Zhu et al., 2005). Axin binding could affect GSK3β's specificity towards β-catenin by making GSK3β less able to bind other substrates. Increasing the specificity of GSK3β for the Wnt substrate β-catenin would create a pool of GSK3β that preferentially interacts with β-catenin and does not interact

with other substrates. This is a relatively new model for scaffold insulation, but our recent work shows that Axin increases the specificity of GSK3β for β-catenin by suppressing reactions with non-Wnt substrates (Gavagan et al., 2020). This specificity increase could create a pool of GSK3β that could be independently regulated without affecting other signaling pathways.

Excluding negative regulators

In Wnt signaling, upstream signals are thought to inhibit GSK3β activity through changes to Axin and the destruction complex. In other signaling pathways, GSK3β is directly inhibited by upstream kinases in response to pathway activation (Stamos et al., 2014). Any changes to GSK3β's inherent activity should impact all substrates, resulting in activation of all downstream pathways. Axin could protect the Wnt pool of GSK3β from being inhibited by other pathways by blocking negative regulators from accessing GSK3β (Figure 1.3C). In this way, scaffold proteins could create a subset of GSK3β that is not affected by modifications from other signaling pathways.

Recruiting phosphatases

In non-Wnt signaling pathways such as insulin signaling, GSK3β is regulated by inhibitory phosphorylation at Ser9 and other phosphosites (Stamos et al., 2014; Thornton et al., 2008). If this inhibited GSK3β exchanges into the pool of GSK3β in the Wnt destruction complex it could result in inadvertent activation of Wnt outputs. By recruiting phosphatases such as PP2A (Thompson et al., 2018) to remove inhibitory phosphates from GSK3β, Axin could prevent non-Wnt phosphoregulation from affecting Wnt signaling (Figure 1.3D).

The following chapters describe quantitative biochemical experiments to test models for how the scaffold protein Axin prevents crosstalk in pathways that share GSK3β. In Chapter 2 we test the long-standing model that Axin increases the rate of GSK3β phosphorylation of β-catenin. Instead of increasing β-catenin phosphorylation rates, we find that Axin increases the specificity of GSK3β for β-catenin by preventing it from interacting with other, non-Wnt substrates. This Axin effect could allow signals to pass through the Wnt signaling pathway without affecting other GSK3β associated pathways. In Chapter 3 we investigate how Axin could protect Wnt signaling from changes to GSK3β when other signaling pathways are activated. We find that Axin prevents GSK3β-inactivating kinases from accessing the Wnt-associated pool of GSK3β. Together these mechanisms allow Axin to insulate Wnt signaling by creating a pool of GSK3β that 1) can be independently regulated by Wnt signals and 2) is protected from GSK3β-inactivating regulation from other signaling pathways.

Chapter 2

The Scaffold Protein Axin Promotes Signaling Specificity within the Wnt Pathway by Suppressing Competing Kinase Reactions

Maire Gavagan[1,2], Erin Fagnan[1,2], Elizabeth B. Speltz[1], and Jesse G. Zalatan[1]

[1]Department of Chemistry, University of Washington, Seattle, WA 98195, USA
[2]These authors contributed equally

2.1 Abstract

Scaffold proteins are thought to promote signaling specificity by accelerating reactions between bound kinase and substrate proteins. To test the long-standing hypothesis that the scaffold protein Axin accelerates GSK3β-mediated phosphorylation of β-catenin in the Wnt signaling network, we measured GSK3β reaction rates with multiple substrates in a minimal, biochemically-reconstituted system. We observed an unexpectedly small, ~2-fold Axin-mediated rate increase for the β-catenin reaction when measured in isolation. In contrast, when both β-catenin and non-Wnt pathway substrates are present, Axin accelerates the β-catenin reaction by preventing competition with alternative substrates. At high competitor concentrations, Axin produces >10-fold rate effects. Thus, while Axin alone does not markedly accelerate the β-catenin reaction, in physiological settings where multiple GSK3β substrates are present, Axin may promote signaling specificity by suppressing interactions with competing, non-Wnt pathway targets. This mechanism for scaffold-

mediated control of competition enables a shared kinase to perform distinct functions in multiple signaling networks.

2.2 Introduction

Glycogen synthase kinase 3β (GSK3β) is a central kinase in mammalian cell signaling networks that responds to growth factors and hormones to regulate cell growth, differentiation, and metabolism (Beurel et al., 2015; Kaidanovich-Beilin and Woodgett, 2011). GSK3β receives signals from multiple upstream inputs and acts on several distinct downstream protein targets (Figure 2.1A). GSK3β-dependent responses to Wnt and growth factor or insulin signals appear to be insulated from each other, so that Wnt signals do not activate alternative GSK3β-dependent pathways and vice versa (Ding et al., 2000; McManus et al., 2005; Ng et al., 2009). These observations raise the fundamental question of how GSK3β activity can be independently regulated by different signaling pathways. Analogous questions arise in many eukaryotic signaling networks, and understanding the mechanisms by which biochemical systems resolve this problem is a major outstanding challenge for the field.

Scaffold proteins that physically assemble protein signaling pathways provide potential mechanisms to direct shared signaling proteins to specific downstream targets (Good et al., 2011; Park et al., 2003; Zalatan et al., 2012). In the Wnt signaling network, the scaffold protein Axin coordinates the assembly of a multi-protein complex including GSK3β and its substrate β-catenin. By binding to both GSK3β and β-catenin, Axin is thought to promote β-catenin phosphorylation (Kimelman and Xu, 2006; MacDonald et al., 2009; Moon et al., 2004; Nusse and Clevers, 2017; Polakis, 2000; Stamos and Weis, 2013). Consequently, regulation of Axin

provides a possible mechanism to control GSK3β activity toward β-catenin without affecting GSK3β reactions toward other non-Wnt pathway substrates (McNeill and Woodgett, 2010).

We know a great deal about the general features of Wnt pathway activation, although the molecular mechanism by which Wnt signaling controls β-catenin phosphorylation and the precise role of Axin in this process is still debated (Nusse and Clevers, 2017). In the absence of a Wnt signal, β-catenin is sequentially phosphorylated by the kinases casein kinase 1a (CK1α) and GSK3β, which leads to proteasomal degradation of β-catenin (Figure 2.1B). Phosphorylation takes place in a multi- protein destruction complex that includes the scaffold protein Axin, the kinases CK1α and GSK3β, the substrate β-catenin, and the accessory proteins dishevelled (Dvl) and adenomatous polyposis coli (APC), which may also have scaffolding functions. Wnt pathway activation recruits the destruction complex to the membrane and disrupts its activity, allowing β-catenin to accumulate and activate downstream gene expression. Wnt signaling has been proposed to block β-catenin phosphorylation at both the CK1α and GSK3β kinase reaction steps (Hernández et al., 2012), possibly via a phosphorylation-dependent conformational change in Axin (Kim et al., 2013) or by inhibition of GSK3β when the destruction complex is recruited to the membrane (Stamos et al., 2014).

Initial support for the model that Axin promotes β-catenin phosphorylation came from *in vitro* biochemical experiments showing that the rate of GSK3β-catalyzed β-catenin phosphorylation increases substantially in the presence of Axin (Dajani et al., 2003; Hart et al., 1998; Ikeda et al., 1998). To test this hypothesis, we biochemically reconstituted GSK3β-catalyzed reactions *in vitro* and quantitatively measured reaction rates in the presence and absence of the Axin scaffold protein. By defining a minimal kinetic framework and systematically measuring rate constants

for individual reaction steps, we expected to determine whether Axin promotes binding between GSK3β and β-catenin or whether Axin allosterically modulates the activity of a GSK3β•β-catenin complex. Both mechanisms have been observed with other kinase signaling scaffolds (Good et al., 2011), and distinguishing between these possibilities is an important step toward understanding how Wnt signals might perturb Axin to regulate β-catenin phosphorylation.

Contrary to expectations, we found that Axin has small, ~2- fold effects on the steady-state rate constants for β-catenin phosphorylation *in vitro*. We observed similar effects with CK1α-phosphoprimed β-catenin, which is the preferred substrate of GSK3β *in vivo* (Amit et al., 2002; Liu et al., 2002), and with unprimed β-catenin, which was used in early biochemical studies (Dajani et al., 2003; Hart et al., 1998; Ikeda et al., 1998). The much larger effects from Axin reported in these earlier studies appear to occur only with unprimed β-catenin under highly specific conditions, and the physiological relevance of these conditions is uncertain. We further demonstrate that Axin has an unexpected ability to suppress GSK3β activity toward other non-Wnt pathway substrates, and that Axin can produce a >10-fold increase in the β-catenin phosphorylation rate when a competing substrate for GSK3β is present. This effect arises because Axin disrupts binding interactions between GSK3β and its substrates but rescues the binding defect for one specific substrate by tethering β-catenin to GSK3β. In the cell, where there are >30 substrates of GSK3β (Sutherland, 2011), the ability of Axin to suppress competing reactions provides a mechanism to specifically promote the β-catenin reaction. These findings demonstrate important biochemical features of the Wnt destruction complex and reveal a new model for how scaffold proteins can promote specificity in signaling networks.

2.3 Results

2.3.1 Reconstituting a Minimal Destruction Complex

To test the model that Axin accelerates the reaction of GSK3β with β-catenin, we biochemically reconstituted a minimal reaction system for quantitative kinetic analysis. We purified recombinant human forms of GSK3β, β-catenin, and Axin as maltose binding protein (MBP) fusions (Figure S1A). We purified active GSK3β from *E. coli* (Wang et al., 1994) and found that it was phosphorylated on the activation loop Tyr216 (Figure S1B), as had been previously reported for GSK3β purified from insect cells (Dajani et al., 2003). We purified recombinant primed, phospho-Ser45-β-catenin (pS45-β-catenin) by coexpressing β-catenin with CK1α in *E. coli* (Figure S1C). For comparison, we purified unprimed β-catenin expressed in the absence of CK1α. Finally, we purified full-length Axin and a minimal fragment of Axin (mini-Axin, residues 384–518) that includes the domains that bind both GSK3β and β-catenin (Dajani et al., 2003; Xing et al., 2003) (Figure S1D).

To confirm that recombinant Axin binds GSK3β and β-catenin in our *in vitro* system, we performed quantitative binding assays using bio-layer interferometry. We determined that full-length Axin has a K_D of 7.5 nM for GSK3β. The miniAxin fragment has a K_D of 16 nM for GSK3β (Figure S2A; Table S1). These values are similar to the previously reported K_D of 65 nM for the interaction between human GSK3β and rat Axin (Ikeda et al., 1998). Because miniAxin behaved similarly to full-length Axin, and because this construct was easier to express and purify in larger quantity than the full-length protein, we used miniAxin for most subsequent binding and kinetic assays. For several key experiments, we verified that full-length Axin demonstrated similar behavior.

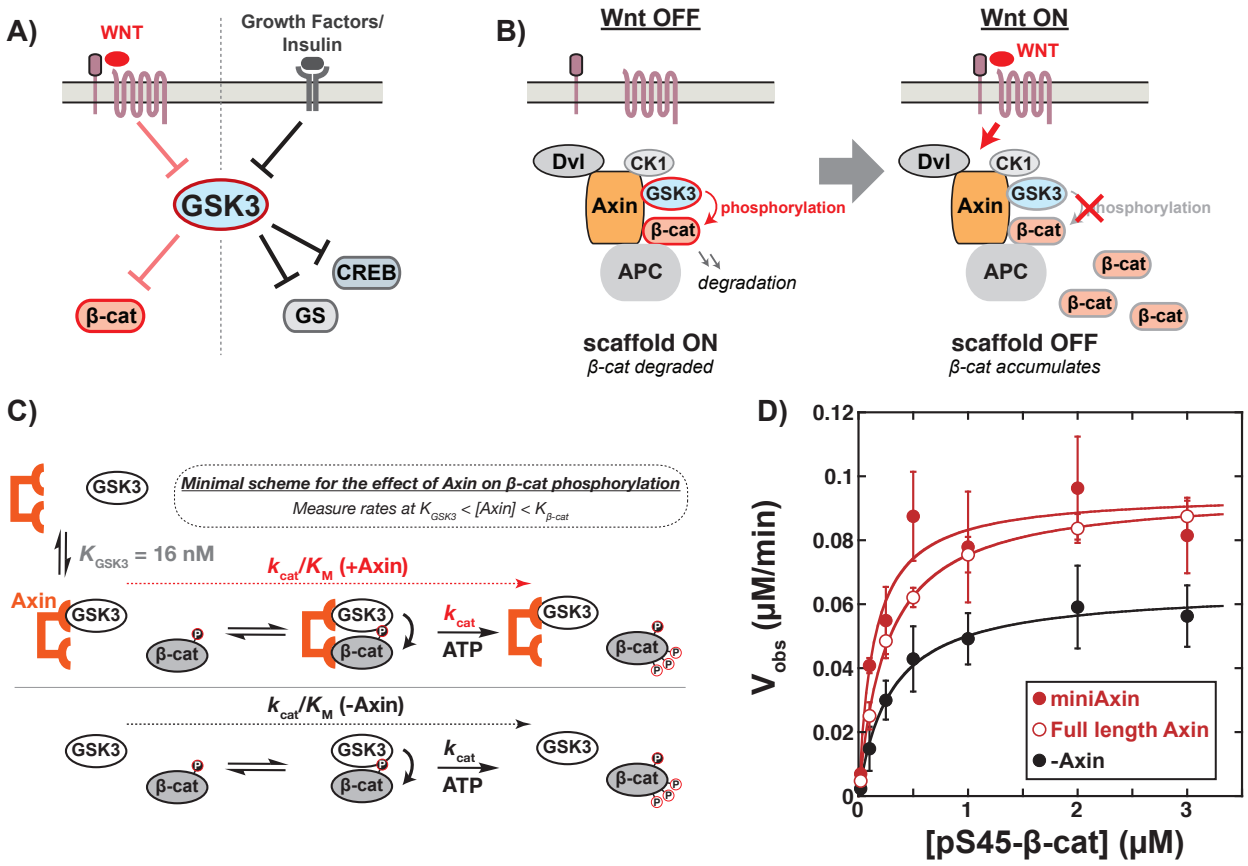

Figure 2.1. Axin assembles signaling proteins in the Wnt pathway.
(A) GSK3β receives input signals from Wnt, growth factors, and hormones like insulin and acts on multiple distinct downstream targets. (B) GSK3β assembles into a multi-protein destruction complex with β-catenin, CK1α, Axin, Dvl, and APC. In the absence of a Wnt signal, β-catenin is phosphorylated and degraded. In the presence of a Wnt signal, β-catenin phosphorylation is blocked, which allows β-catenin to accumulate. (C) Minimal kinetic scheme for the reaction of GSK3β with pS45-β-catenin in the presence and absence of Axin. GSK3β phosphorylates pS45-β-catenin at three sites: S33, S37, and T41. When K_{GSK3} < [Axin] < $K_{β\text{-cat}}$, all GSK3β is bound to Axin (when [Axin] > [GSK3β]) and there should be very little pS45-β-catenin bound to free Axin. (D) Michaelis-Menten plot of V_{obs} vs. [pS45-β-catenin] at 20 nM GSK3β in the presence and absence of 500 nM miniAxin or full length (FL) Axin. Values are mean ± SD for at least 3 measurements. See Figures S6-S8 for representative western blot images and plots of product vs. time used to obtain the initial rate values (V_{obs}) plotted here. See Table S2 for values of fitted kinetic parameters.

We proceeded to measure the affinity of miniAxin for pS45- β-catenin. The observed K_D of 4.0 μM (Figure S2B; Table S1) is similar to the reported K_D of 1.6 μM for unprimed mouse β-catenin binding to a short human Axin fragment (residues 436–498) (Choi et al., 2006). We also attempted to measure an affinity with unprimed β-catenin. We could detect miniAxin binding to unprimed β-catenin in a similar concentration range, but we were unable to accurately measure a

K_D value due to surface aggregation artifacts. Taken together, we confirmed that Axin binds to both GSK3β and β-catenin, and that Axin binds GSK3β substantially more tightly than β-catenin.

To determine how Axin affects β-catenin phosphorylation, we measured the steady-state rate constants k_{cat}/K_M and k_{cat} in the presence and absence of Axin (Figure 2.1C). Because Axin binds GSK3β much more tightly than β-catenin, we can define a minimal, simplified kinetic scheme that allows straightforward comparisons. We chose an Axin concentration above the K_D for GSK3β and below the K_D for β-catenin, which ensures that all GSK3β is bound to Axin. Although there is excess free Axin in the system, the concentration of Axin is below the K_D for β-catenin, and there should be very little β-catenin bound to free Axin. We obtained steady-state rate constants for the Axin•GSK3β complex by varying the β-catenin concentration and compared these values to a reaction of GSK3β with β-catenin in the absence of Axin. If Axin promotes binding between GSK3β and β-catenin, we expect that the observed K_M should shift to a lower concentration, and k_{cat} should remain unchanged. Alternatively, if Axin allosterically activates the GSK3β•β-catenin complex, then k_{cat} should increase without necessarily affecting K_M. This interpretation potentially oversimplifies the reality of a complex kinetic scheme that could include multiple Axin-bound states, intermediates, and rate-limiting conformational change or product release steps; it nevertheless represents a useful and straightforward starting point.

To measure β-catenin phosphorylation rates, we used quantitative western blotting. GSK3β sequentially phosphorylates pS45-β-catenin at three sites: T41, S37, and S33 (Liu et al., 2002), and product formation can be monitored using an antibody specific for pS33/pS37/pT41-β-

catenin (see STAR Methods; Figures S3–S8). This antibody preferentially recognizes the fully phosphorylated β-catenin product over any partially phosphorylated β-catenin intermediates (Figures S3 and S4), and we detected no lag in product formation that would indicate the buildup of partially phosphorylated intermediates in the reaction (Figures S6–S8). We therefore fit the observed rates to a simple Michaelis-Menten kinetic model. In the presence of miniAxin, there is a 1.5-fold increase in the observed value of k_{cat}, a 2-fold decrease in the observed value of K_M, and a 3- fold increase in k_{cat}/K_M (Figure 2.1D; Table S2). In the presence of full-length Axin, there is a 1.5-fold increase in k_{cat} and no change in K_M within error. These effects are far smaller than expected based on prior reports, one of which suggested that Axin accelerates the reaction by $>10^4$-fold (Dajani et al., 2003; Hart et al., 1998; Ikeda et al., 1998). Our observation that Axin has a small effect on the β-catenin phosphorylation reaction comes from rates measured at protein concentrations chosen to obtain defined rate constants; we also considered reactions at estimated cellular concentrations and found no effect from Axin (see Box 1; Figure S9).

When considering the role of Axin in β-catenin phosphorylation, it is important to note that the kinetics could be complicated by the fact that multisite phosphorylation reactions can proceed through distributive or processive mechanisms. Our observed rates come from detecting pS33/pS37/pT41-β-catenin accumulation (Figures S3 and S4), and we did not measure accumulation of the intermediate phosphorylation states. The observed steady-state kinetic parameters obtained from a Michaelis- Menten model could include contributions from multiple individual phosphorylation steps. Although we did not detect any lag in the initial rate assays, which could suggest the buildup of partially phosphorylated intermediates (Figure S7), it is challenging to definitively characterize multisite phosphorylation reactions (Burack and Sturgill, 1997; Ferrell and Bhatt, 1997; Selenko et al., 2008). Further, if β-catenin phosphorylation is

distributive, tethering on a scaffold protein could potentially shift the mechanism to processive (Burack and Shaw, 2000). We cannot formally distinguish between these possibilities using the approaches described here. Despite these potential complications, the lack of a large effect from Axin on the observed rate constants for β-catenin phosphorylation remains puzzling.

One possible explanation for the discrepancy between our results and prior work is that scaffold-dependent reactions can be slow if too little scaffold is present, but inhibited at excess scaffold concentrations if the kinase and substrate are not bound to the same scaffold (Levchenko et al., 2000). While we chose an Axin concentration carefully to avoid this issue, it is possible that our assumptions were incorrect. We therefore varied the concentration of miniAxin and measured reaction rates at both saturating and subsaturating pS45-β-catenin concentrations but found no miniAxin concentration that produced a larger rate enhancement (Figure S10). Thus, Axin has only a modest effect on the GSK3β reaction with pS45-β-catenin, and this effect arises from small changes in k_{cat} and K_M. The effect on K_M is relatively small, possibly because Axin binding to β-catenin is weak (K_D ~4 μM) compared with the K_M for the reaction of GSK3β with pS45-β-catenin (K_M = 0.29 μM). In order to obtain large tethering effects from a scaffold, it may be necessary for binding affinities to the scaffold to be at least comparable to the unscaffolded interaction between kinase and substrate, or for ternary complex formation to be highly cooperative.

2.3.2 Competition from GSK3β-Mediated Phosphorylation of Axin Does Not Affect Observed Rates

Axin can be phosphorylated by GSK3β (Kim et al., 2013; Willert et al., 1999), which leads to two potential complicating issues. First, Axin could compete with β-catenin as a substrate for

GSK3β, masking any potential rate acceleration mediated by Axin for β-catenin. To test this possibility, we constructed a mini- Axin mutant with Ser to Ala substitutions at all four phosphorylation sites (miniAxin-4A), which prevents any detectable phosphorylation by GSK3β (Figure S11A). The miniAxin-4A mutant had small effects on the rate constants for GSK3β-mediated phosphorylation of pS45-β-catenin, indistinguishable from the values observed in reactions with wild-type miniAxin (Figure S11B; Table S2). Thus, competition from Axin as a substrate for GSK3β does not appear to affect the observed rates, presumably because at the concentrations in our assay the Axin phosphorylation sites are not saturating the GSK3β active site.

The second potential complication is that phosphorylation of Axin increases its affinity for β-catenin (Kim et al., 2013; Willert et al., 1999), which could be necessary to enable Axin to promote β-catenin phosphorylation. Axin phosphorylation promotes β-catenin binding by relieving an autoinhibitory interaction be- tween the β-catenin binding site and the DIX domain within Axin (Kim et al., 2013). Our use of miniAxin was motivated in part to avoid complications from this effect. miniAxin does not include the DIX domain (Figure S1D), so this construct should be fully competent to bind β-catenin. However, regardless of whether the DIX domain was present (full-length Axin) or absent (miniAxin), we observed relatively small effects from Axin on GSK3β-mediated phosphorylation of β-catenin (Figure 2.1D).

2.3.3 Removing the β-catenin-Binding Site on Axin Disrupts the Activity of the Axin•GSK3β Complex

The Axin•GSK3β complex and free GSK3β have similar k_{cat} and K_M values for β-catenin, suggesting that the β-catenin-binding site on Axin should be dispensable. To test this prediction,

we removed the β-catenin-binding domain (BCD) from Axin (Figure S1D) and assessed the effect of AxinΔBCD on GSK3β activity. Because GSK3β binds to both Axin and AxinΔBCD with similar affinity (Table S1), we can use the same minimal kinetic framework as for wild-type Axin (Figure 2.1C). In the presence of AxinΔBCD, the observed rates for phosphorylation of pS45-β-catenin were substantially slower than the corresponding rates for GSK3β in the absence of Axin (Figure 2.2), indicating that the activity of the AxinΔBCD •GSK3β complex is suppressed compared with free GSK3β. The reaction does not fully saturate at high pS45-β-catenin concentrations, so we can estimate a conservative limit that $K_M \geq 1$ μM, which is >3-fold larger than the K_M of 0.29 μM in the absence of Axin (Table S2). A simple model to explain this observation is that Axin interferes with the ability of GSK3β to bind substrates. More strictly, this result suggests that Axin interferes with the steady-state accumulation of the GSK3β•β-catenin complex or a bound intermediate along the reaction pathway; our discussion below will refer to K_M effects as binding effects, but the analysis holds if the true effect is on steady-state accumulation of an intermediate.

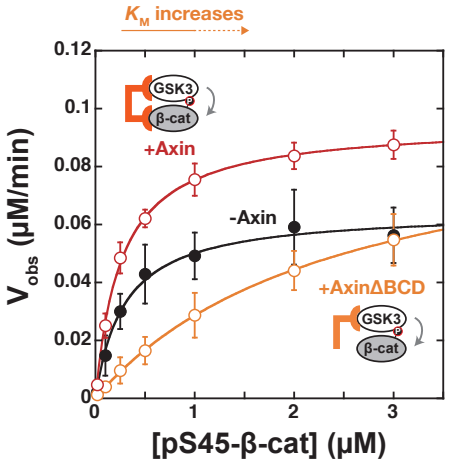

Figure 2.2. Removing the β-catenin binding site on Axin disrupts the activity of the Axin•GSK3β complex. Michaelis-Menten plot of V_{obs} vs. [pS45-β-catenin] at 20 nM GSK3β in the presence and absence of 500 nM full length Axin or AxinΔBCD. At low substrate concentrations, the AxinΔBCD reaction is slower than both the Axin reaction and the no Axin reaction. Values are mean ± SD for at least 3 measurements. See Table S2 for values of fitted kinetic parameters. The AxinΔBCD reaction does not fully saturate at high [pS45-β-catenin], which means that only the value of k_{cat}/K_M can be accurately determined. The reaction may be starting to saturate, suggesting a conservative limit of $K_M \geq$ ~1 μM.

The available literature provides some support for the idea that Axin binding can perturb GSK3β activity. A minimal Axin peptide that binds GSK3β has been reported to inhibit GSK3β activity

toward multiple substrates, including β-catenin (Zhang et al., 2003). The available crystal structures of GSK3β bound to Axin do not provide a clear explanation for this behavior. Axin does not physically occlude the substrate binding site of GSK3β, and there are no obvious structural changes in the active site between GSK3β bound to Axin and free GSK3β (Dajani et al., 2003, 2001; Stamos et al., 2014). However, the structures were obtained with a 19-amino-acid Axin peptide. The minimal fragment reported to inhibit GSK3β was 25 amino acids, and a longer Axin peptide could potentially extend toward the active site. Although we lack a complete structural model, the kinetic data strongly suggest that Axin binding to GSK3β disrupts substrate binding. This detrimental effect is rescued by Axin binding to β-catenin, which restores K_M to its original value. We initially concluded that the lack of an effect on K_M implied that Axin makes no contribution to β-catenin binding to the Axin•GSK3β complex. However, if we compare Axin•GSK3β to AxinΔBCD•GSK3β, there is a ≥ 4-fold decrease in K_M (Table S2), suggesting that the β-catenin binding domain on Axin does play a role in promoting β-catenin binding to GSK3β.

2.3.4 Axin Slows the GSK3β Reaction with Non-Wnt Pathway Substrates

If Axin has two competing functions, disrupting GSK3β substrate binding and promoting binding to β-catenin, we predicted that Axin should have a detrimental effect on the activity of GSK3β with alternative, non-Wnt pathway substrates that do not bind Axin. To determine how Axin affects interactions with these substrates, we measured reaction rates with two non-Wnt pathway substrates, glycogen synthase (GS) and cAMP response element-binding protein (CREB). GS is the canonical substrate of GSK3β in the insulin signaling pathway (Beurel et al., 2015; Kaidanovich-Beilin and Woodgett, 2011). Insulin represses GSK3β but does not activate the Wnt pathway (Ding et al., 2000; McManus et al., 2005; Ng et al., 2009). CREB is a

transcription factor that is phosphorylated by GSK3β and integrates signals from a number of pathways (Fiol et al., 1994; Shaywitz and Greenberg, 1999). In cells, PI3K/Akt signaling represses GSK3β, which affects CREB- dependent transcription but does not activate Wnt outputs (Ng et al., 2009; Tullai et al., 2007).

We expressed full-length CREB and a short CREB peptide ($CREB_{127\text{-}135}$) as MBP fusions. CREB is phosphorylated by PKA at Ser133, which serves as a priming site for GSK3β to phosphorylate Ser129 (Fiol et al., 1994) (Figure 2.3A). We phosphorylated both CREB and $CREB_{127\text{-}135}$ to completion *in vitro* with PKA to produce pS133-CREB and pS133-$CREB_{127\text{-}135}$ (Figure S12) and measured reaction rates for GSK3β-catalyzed phosphorylation of pS133-$CREB_{127\text{-}135}$. As predicted, Axin substantially decreased CREB phosphorylation rates (Figures 2.3B, 2.3C, S13, and S14). Axin decreased k_{cat}/K_M by factors of 13-fold for pS133-CREB and 23-fold for pS133-$CREB_{127\text{-}135}$, relative to the same reaction in the absence of Axin (Table S2). The reactions did not detectably saturate in the presence of Axin, suggesting that the K_M has shifted to a much larger value and that at least some of the decrease in k_{cat}/K_M arises from a disruption of binding interactions between GSK3β and pS133-CREB. An alternative possibility is that Axin binds directly to CREB and prevents it from binding GSK3β, but there are no reports of CREB binding to Axin, and we did not detect any binding in a pull-down assay (Figure S13).

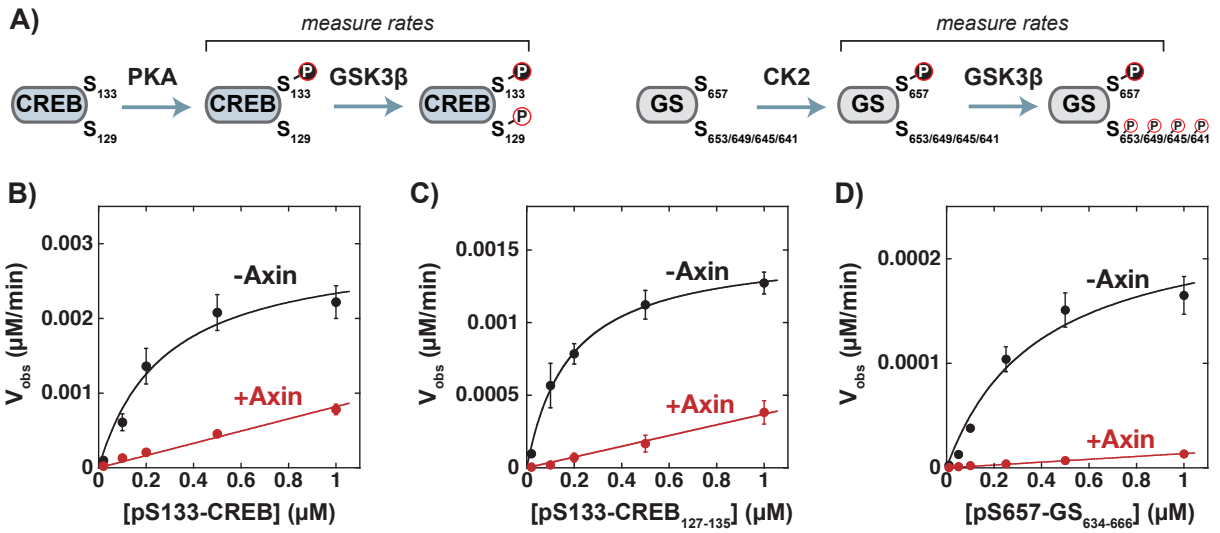

Figure 2.3. Axin decreases phosphorylation rates of non-Wnt pathway GSK3β substrates.
(A) Minimal schemes for phosphorylation of CREB and GS. PKA phosphorylates CREB at S133. pS133 serves as a priming site for GSK3β, which phosphorylates pS133-CREB at S129. CK2 phosphorylates GS at S657, which primes sequential GSK3β reactions at S653/S649/S645/S641. (B-D) Michaelis-Menten plots of V_{obs} vs. substrate for (B) [pS133-CREB], (C) [pS133-CREB$_{127-135}$], and (D) [pS657-GS$_{634-666}$] at 20 nM GSK3β in the presence and absence of 500 nM miniAxin. Values are mean ± SD for at least 3 measurements. See Table S2 for values of fitted kinetic parameters. There is no detectable saturation of the reactions in the presence of miniAxin up to 1 μM substrate, which means that only the value of k_{cat}/K_M can be determined from the slope of a linear fit to the data. We were unable to detect GSK3β-catalyzed phosphorylation of unprimed CREB$_{127-133}$ ($V_{obs} \leq 3 \times 10^{-5}$ μM/min at 0.5 μM CREB$_{127-133}$) or GS$_{634-666}$ ($V_{obs} \leq 6 \times 10^{-7}$ μM/min at 0.2 μM GS$_{634-666}$).

We also expressed a GS peptide (GS$_{634-666}$) as an MBP fusion. GS is phosphorylated by casein kinase 2 (CK2) at Ser657 and then sequentially phosphorylated at S653, S649, S645, and S641 by GSK3β (Fiol et al., 1987, 1990) (Figure 2.3A). We phosphorylated GS$_{634-666}$ on S657 to completion *in vitro* with CK2 to produce pS657-GS$_{634-666}$ (Figure S12) and measured reaction rates for GSK3β-catalyzed phosphorylation of pS657-GS$_{634-666}$ using an antibody specific for pS641 (Figures 2.3D, S13, and S14). As with β-catenin, multisite phosphorylation of GS has the potential to be quite mechanistically complicated. Nevertheless, the initial rates for pS641 accumulation were linear and could be fit to a simple Michaelis-Menten model to obtain observed steady-state kinetic parameters. Similar to the reaction with CREB, Axin decreased

k_{cat}/K_M for pS657-$GS_{634-666}$ phosphorylation by a factor of 46-fold. Again, the reaction did not detectably saturate in the presence of Axin.

Taken together, these results are consistent with a model where Axin binding inhibits GSK3β activity by increasing the K_M of GSK3β for its substrates and preventing accumulation of GSK3β•substrate complexes. For the reaction with β-catenin, Axin compensates for this inhibition by binding directly to β-catenin and stabilizing the GSK3β•β-catenin complex. Consistent with this model, an Axin mutant that cannot bind to β-catenin (AxinΔBCD) increases the K_M for the reaction by ≥4-fold (Figure 2.2; Table S2). In reactions with the non-Wnt pathway substrates CREB and GS, Axin does not compensate for GSK3β inhibition because it has no native binding interactions to these substrates. Thus, Axin increases the K_M of GSK3β for CREB and GS and substantially decreases the phosphorylation rate at low substrate concentrations below the K_M.

2.3.5 Axin Accelerates the β-catenin Reaction When Competing Substrates Are Present

The Axin-mediated inhibition of GSK3β activity for non-Wnt pathway substrates has a large effect on the specificity of GSK3β for alternative substrates, which can result in large effects on β-catenin phosphorylation rates. Because Axin decreases the k_{cat}/K_M of GSK3β ~10–50-fold for non-Wnt pathway substrates (Figure 2.3) and increases the k_{cat}/K_M of GSK3β for pS45-β-catenin 3-fold (Figure 2.1D), the Axin•GSK3β complex is ~10^2-fold more specific toward β-catenin than free GSK3β (Figure S15). When both β-catenin and an alternative GSK3β substrate are present at low, subsaturating concentrations, this specificity increase from Axin will manifest largely as a decrease in the rate for the alternative substrate reaction

However, when the non-Wnt pathway substrate is present at saturating concentrations and in excess over β-catenin, Axin can produce larger rate increases for β-catenin phosphorylation. This effect arises because any other GSK3β substrate can act as a competitive inhibitor of the β-catenin reaction. When Axin is added to the system, the K_M for the competitor will increase, resulting in more GSK3β available to react with β-catenin and increasing the rate of β-catenin phosphorylation (Figures 2.4A and S16). To test this prediction, we measured pS45-β-catenin phosphorylation in a competitive reaction with excess, saturating pS133-$CREB_{127-135}$ present. In this system, adding Axin produced a 20-fold increase in pS45-β-catenin phosphorylation, much larger than the 3-fold increase in the absence of competitor (Figure 2.4B). As predicted, this larger effect results entirely from a decrease in the β-catenin phosphorylation rate in the absence of Axin. When Axin is present, the β-catenin phosphorylation rates are similar in the presence or absence of competitor because Axin suppresses the competition effect. In the absence of Axin, pS133-$CREB_{127-135}$ competes for GSK3β and inhibits the β-catenin reaction. We observed a similar effect in the presence of pS657-$GS_{634-666}$ (Figure 2.4B), although slightly smaller than with CREB because GS does not fully saturate GSK3β in the reaction conditions tested (Figure S16C). Thus, while Axin alone has a modest effect on the β-catenin reaction rate, in the presence of competing substrates Axin can produce much larger increases in β-catenin phosphorylation. This competition-mediated scaffold effect may be relevant *in vivo*, where GSK3β has many potential competing substrates (Sutherland, 2011) (Figure S16D).

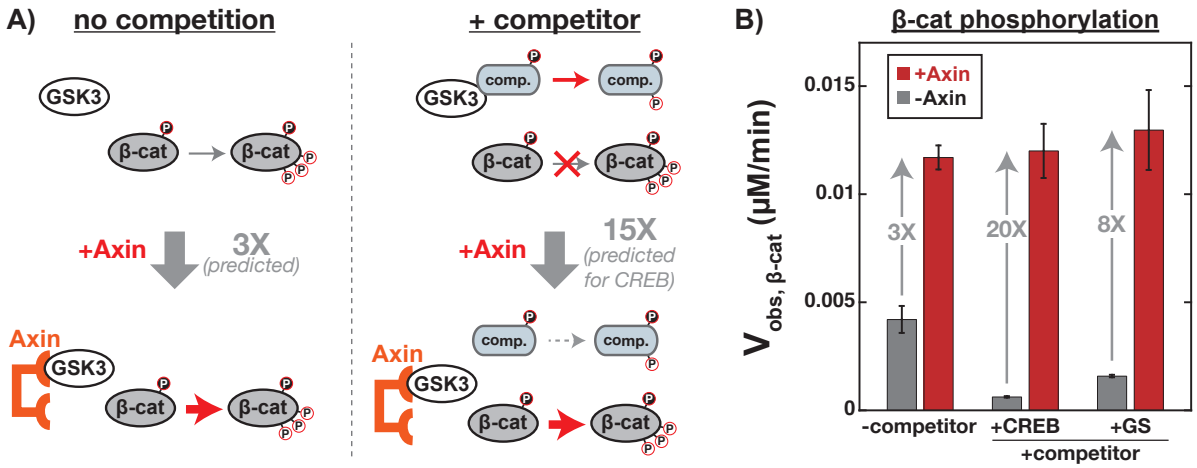

Figure 2.4. Axin accelerates the β-catenin reaction when competing substrates are present. (A) Prediction for the effect of Axin on pS45-β-catenin phosphorylation when a competing substrate is present. When a competitor is present at saturating concentrations and pS45-β-catenin is present at subsaturating concentrations, the competitor forms a complex with GSK3β and inhibits the reaction with pS45-β-catenin. Axin disrupts the interaction of GSK3β with the competitor, preventing buildup of the GSK3β•competitor complex. Using a Michaelis-Menten model with a pS133-CREB$_{127\text{-}135}$ competitive inhibitor present at 1 μM concentration (Figure S16B), we predict that Axin should produce a 15-fold increase on the β-catenin phosphorylation rate in the presence of pS133-CREB$_{127\text{-}135}$, much larger than the 3-fold increase in the absence of competitor. A similar analysis with pS657-GS$_{634\text{-}666}$ as the competitor predicts an 8-fold increase in β-catenin (Figure S16C); the predicted effect is smaller than for CREB because the K_M of GSK3β for GS is larger (Table S2) and 1 μM GS is not fully saturating. (B) β-catenin phosphorylation rates (V_{obs}) measured at 20 nM GSK3β and 50 nM pS45-β-catenin (subsaturating) in the presence and absence of 500 nM miniAxin with either no competitor, 1 μM pS133-CREB$_{127\text{-}135}$, or 1 μM pS657-GS$_{634\text{-}666}$. Values are mean ± SD for at least 3 measurements. In the absence of competitor, Axin produces a 3-fold rate increase. In the presence of CREB or GS competitors, Axin produces 20-fold or 8-fold rate increases, respectively, similar to the predicted values.

2.3.6 An Inactive GSK3β•β-catenin Complex Accumulates in the Reaction with Unprimed β-catenin

Our quantitative kinetic data described above suggest a new model for how the destruction complex specifically accelerates the β-catenin reaction, but a major question remains unanswered: if Axin has only ~2-fold effects on k_{cat} and K_M values for β-catenin phosphorylation, why did early biochemical studies in this system observe much larger rate

increases? One notable difference is that the initial biochemical studies on Axin were performed with unprimed β-catenin as a substrate (Dajani et al., 2003; Hart et al., 1998; Ikeda et al., 1998), prior to or concurrent with the discovery of phosphopriming by CK1 (Amit et al., 2002; Liu et al., 2002). An early mechanistic model for Axin suggested that its function might be to bypass the need for phosphopriming (Frame et al., 2001). In this case, either phosphopriming of β-catenin or Axin-mediated tethering would promote the reaction of GSK3β with β-catenin, but there might not be an additional effect from Axin when β-catenin is phosphoprimed. When we measured reaction rates with unprimed β-catenin, we found that the unprimed reaction was ~10^2-fold slower than the primed reaction, as expected. However, the steady-state rate constants for unprimed β-catenin were not affected by the presence of Axin (Figure S18; Table S2).

Additional experiments with unprimed β-catenin revealed an unexpected behavior that can explain previous reports of large Axin-mediated rate enhancements. In most circumstances, enzymatic reaction rates should increase linearly with increasing enzyme concentration, and this behavior occurs in the reactions with pS45-β-catenin, pS133-CREB, pS133-$CREB_{127\text{-}135}$, and pS657-$GS_{634\text{-}666}$ (Figure S19). However, when we varied the GSK3β concentration in reactions with unprimed β-catenin, we observed that the rate does not increase linearly with GSK3β concentration. Instead, in the absence of Axin the observed rates level off sharply above ~100 nM GSK3β. In contrast, in the presence of Axin the observed rates increase linearly with GSK3β concentration (Figure S20). This concentration-dependent inactivation of GSK3β could be due to the formation of an inactive dimer or oligomer, and Axin binding to GSK3β could prevent the formation of this inactive state. Thus, if reaction rates are measured at relatively high levels of GSK3β and with unprimed β-catenin, which was the case in the early biochemical studies

(Dajani et al., 2003; Hart et al., 1998; Ikeda et al., 1998), Axin produces a large increase in the observed rates.

Based on the kinetic data, the inactive state could be a reversible, oligomeric GSK3β•β-catenin complex (Figures S20 and S21). If the inactive state were a dimer or oligomer of GSK3β alone, we would have expected to see a similar inactivation effect in all GSK3β reactions, but this effect is not observed in reactions with pS45-β-catenin, pS133-CREB, pS133-$CREB_{127\text{-}135}$, or pS657-$GS_{634\text{-}666}$ (Figure S19). Thus, the inactive state likely includes both GSK3β and unprimed β-catenin. Further, kinetic modeling suggests that the inactive state is a higher-order oligomer. The observed rates level off too sharply with increasing GSK3β concentration to fit to a dimer model (Figure S20). The proposed inactive oligomer is consistent with the kinetic data, but we cannot exclude alternative models.

The physiological relevance of an oligomeric, inactive GSK3β•β-catenin complex is uncertain. Cellular GSK3β concentrations estimated from mass spectrometry proteomics datasets (Beck et al., 2011; Itzhak et al., 2016; Nagaraj et al., 2011) vary in the range of ~10–300 nM for human HeLa and U2OS cells (cell volumes from BioNumbers BNID 103725 and 108088 [Milo et al., 2010]; see also Box 1). These values are similar to the ~100 nM concentration where we see the active to inactive transition *in vitro*, and additional experiments to determine if an oligomeric GSK3β•β-catenin complex exists *in vivo* could be justified. However, the observation that Axin accelerates the β-catenin reaction *in vitro* was the initial foundation to explain the function of the Wnt pathway destruction complex *in vivo* (Kimelman and Xu, 2006; MacDonald et al., 2009; Moon et al., 2004; Nusse and Clevers, 2017; Polakis, 2000; Stamos and Weis, 2013). Our data suggest that the mechanistic origin of this original observation is only applicable to the specific

condition of high GSK3β concentrations reacting with unprimed β-catenin, which is likely not relevant to the preferred physiological reaction of GSK3β with CK1-phosphoprimed pS45-β-catenin.

2.4 Discussion

To understand how Wnt signals regulate Axin to modulate GSK3β activity, we biochemically reconstituted GSK3β-mediated reactions *in vitro* and attempted to reproduce the long- standing result that Axin substantially accelerates the reaction of GSK3β with β-catenin (Dajani et al., 2003; Hart et al., 1998; Ikeda et al., 1998). Although prior reports suggested large effects as high as 10^4-fold, we found modest 2- to 3-fold effects from Axin on the rate constants for the phosphorylation reaction (Table S2). Two key features of our work can explain this discrepancy. First, we measured *in vitro* reaction rates with the phosphoprimed form of β-catenin, while most prior work used unprimed β-catenin (one study included both CK1 and GSK3β in a reaction with β-catenin in the presence and absence of Axin [Ha et al., 2004]. The effect of Axin on the observed rates reported in that work is consistent with the rate constants we observe here). A large Axin-dependent rate enhancement can be observed with unprimed β-catenin, but only in the specific condition of high GSK3β concentration, where Axin prevents the formation of an oligomeric, inactive GSK3β•β-catenin complex (Figure S20). Second, we measured well-defined rate constants in the presence and absence of Axin, while previous reports made indirect comparisons between observed rates, leading to the estimate of a 10^4-fold effect from Axin (Dajani et al., 2003).

The small effect of Axin on GSK3β activity toward β-catenin is the result of two opposing effects. First, Axin binding to GSK3β nonspecifically disrupts substrate binding, as seen in the

reactions with GS and CREB in the presence of Axin and with β-catenin in the presence of AxinΔBCD (Figures 2.2 and 2.3). Second, Axin has a β-catenin binding site that rescues substrate binding specifically for β-catenin. These opposing effects result in ≤2- fold changes in K_M when comparing the β-catenin reactions of Axin•GSK3β to GSK3β, but a larger >4-fold decrease when comparing Axin•GSK3β to AxinΔBCD•GSK3β. Thus, it is reasonable to view Axin as a tethering scaffold that specifically promotes binding of GSK3β to β-catenin, even though there is no net effect of Axin on K_M.

How do we reconcile the finding that Axin has small effects on reaction rates *in vitro* with the vast literature that supports the importance of Axin in Wnt signaling (MacDonald et al., 2009; Nusse and Clevers, 2017; Stamos and Weis, 2013)? We know that Axin has substantial effects on Wnt signaling and vertebrate development (Anvarian et al., 2016; Peterson-Nedry et al., 2008; Zeng et al., 1997), and Axin mutants are associated with cancer (Anastas and Moon, 2013; Satoh et al., 2000). Moreover, the idea that the destruction complex acts to accelerate β-catenin phosphorylation is a cornerstone of functional models for Wnt signaling (Kim et al., 2013; Lee et al., 2003). One important point to consider is that we do not have a clear framework to evaluate how large of an *in vitro* effect is necessary to account for phenotypic effects *in vivo*, and a 2-fold increase in reaction rates might actually be physiologically meaningful. In cell culture models, treatment with high levels of Wnt ligand can produce ~5–10-fold increases in total β-catenin levels (Hannoush, 2008; Hernández et al., 2012), with a corresponding ~5-fold decrease in GSK3β-β-catenin phosphorylation rate (Hernández et al., 2012). 2-fold changes in β-catenin levels also have detect- able effects on transcription *in vivo* (Jacobsen et al., 2016). However, the observation that *in vivo* changes in β-catenin levels and phosphorylation rate can substantially

exceed 2-fold suggests that we should be able to identify mechanisms that produce correspondingly larger effects *in vitro*.

While Axin alone does not appear to have a sufficiently large effect on β-catenin phosphorylation *in vitro* to account for *in vivo* observations, additional proteins and components that are present *in vivo* could lead to larger effects. We demonstrate one such possible contribution here: Axin produces large increases in reaction rates when another GSK3β substrate is present at saturating concentrations. The β-catenin reaction with GSK3β is inhibited by the presence of competing substrates, and Axin relieves this inhibition to produce much larger increases in the β-catenin phosphorylation rate than observed in the absence of competition (Figure 2.4). This effect arises because Axin nonspecifically disrupts GSK3β binding to its substrates while simultaneously binding to β-catenin to maintain this specific interaction with GSK3β. The possibility that this effect occurs *in vivo* does not require large physiological GS or CREB concentrations. In a cellular environment, where >30 competing substrates of GSK3β are present (Sutherland, 2011), many possible non-Wnt pathway substrates could contribute to saturating GSK3β and inhibiting the reaction with β-catenin (Figure S16D). Cellular Axin abundances are 10 to 10^3-fold lower than GSK3β (Beck et al., 2011; Geiger et al., 2012; Itzhak et al., 2016; Lee et al., 2003; Nagaraj et al., 2011; Wang et al., 2019), which means that a small fraction of the total GSK3β could be bound to Axin and preferentially phosphorylate β-catenin at rates much faster than the Axin-independent pool. The precise magnitude of this effect depends on the concentrations of GSK3β, Axin, and the competing GSK3β substrates. The Axin-dependent rate enhancement will also depend on how much GSK3β in the Axin-independent pool is free to phosphorylate β-catenin. Other scaffold and adapter proteins are known to engage GSK3β (Beurel et al., 2015), which could produce multiple distinct sub- populations that each

promote a specific GSK3β reaction and suppress competitors. We emphasize that the proposed model is a prediction based on a simplified *in vitro* system, which allows us to evaluate the functional behaviors that are possible for biological molecules (see Box 1). Determining whether this mechanism is operative in cells will require experiments that can modulate competition in an *in vivo* setting.

A model where Axin promotes β-catenin phosphorylation by suppressing competing reactions is consistent with our understanding of Wnt and GSK3β function *in vivo*. Wnt signals that disrupt binding interactions to Axin or perturb the conformation of Axin would be predicted to prevent β-catenin phosphorylation. We would also still predict that Wnt signals do not activate other GSK3β-dependent signaling pathways (Ding et al., 2000; McManus et al., 2005; Ng et al., 2009). A Wnt signal that disrupts the Axin•GSK3β complex and relieves the non-specific inhibition of GSK3β could lead to faster reactions with non-Wnt GSK3β substrates, but since the amount of Axin•GSK3β is small relative to the total amount of GSK3β, the overall change in rates toward alternative substrates is likely to be negligible.

Other components from the Wnt pathway could make additional contributions to reactivity and specificity for β-catenin phosphorylation in the destruction complex, although their precise contributions have not yet been quantified. APC is a particularly intriguing candidate (Figure 2.1B), as it binds Axin and has multiple binding sites for β-catenin in the low nM affinity range (Liu et al., 2006; Xing et al., 2004). By binding tightly to β-catenin, the Axin•APC complex could be more effective than Axin alone at tethering β-catenin to GSK3β (Hinoi et al., 2000; Ji et al., 2018; Kishida et al., 1998), leading to larger rate effects. Post-translational modifications of Axin and the formation of higher-order assemblies could also affect reaction rates (Kim et al.,

2013; Schaefer et al., 2018). It is possible that the destruction complex also promotes the CK1α-mediated phosphopriming step (Amit et al., 2002; Liu et al., 2002), which would increase the GSK3β-mediated β-catenin phosphorylation rate. There are conflicting reports on whether Axin accelerates the CK1α-catalyzed reaction *in vitro* (Amit et al., 2002; Ha et al., 2004; Sobrado et al., 2005), and there is evidence that Wnt signals affect both the CK1α and GSK3β-mediated reactions *in vivo* (Hernández et al., 2012). Finally, Wnt signals may lead to competition for GSK3β by the co-receptors LRP5/6, which can inhibit activity toward β-catenin (Stamos et al., 2014). An important feature of our work is that we have established a clear and quantitative kinetic framework to evaluate the functional effects of Axin on β-catenin phosphorylation, and we can now introduce additional components to evaluate their functional effects, including other kinases, scaffold proteins, and phosphatases.

In addition to providing new insights into Wnt pathway signaling, our results have broad implications for understanding scaffold protein function. Axin was among the earliest proteins identified as a signaling scaffold (Ikeda et al., 1998) and was initially discussed as a prototypical model for tethering a kinase and substrate together to accelerate a phosphorylation reaction (Pawson and Nash, 2003). There is now an emerging consensus that scaffold proteins can have many functions beyond simply tethering a kinase to its substrate, including allosterically modulating the activity of their target proteins (Good et al., 2011). Here, we show that Axin does have a tethering function, but the opposing effect from nonspecifically perturbing GSK3β binding to its substrates results in a modest net effect when the activity of Axin is studied in isolation. The functional advantage from

Axin-mediated tethering only emerges in a more complex system with multiple competing substrates, which may more accurately reflect the *in vivo* environment. These insights arose from reconstitution and quantitative kinetic characterization of a minimal biochemical system *in vitro*, which highlighted an apparent discrepancy between *in vitro* and *in vivo* behavior and enabled us to identify a possible solution. Future biochemical studies that introduce additional Wnt pathway and GSK3β-interacting proteins will likely provide further insights and rigorous tests to expand our understanding of complex, interconnected cell signaling networks.

2.5 Supplemental Information

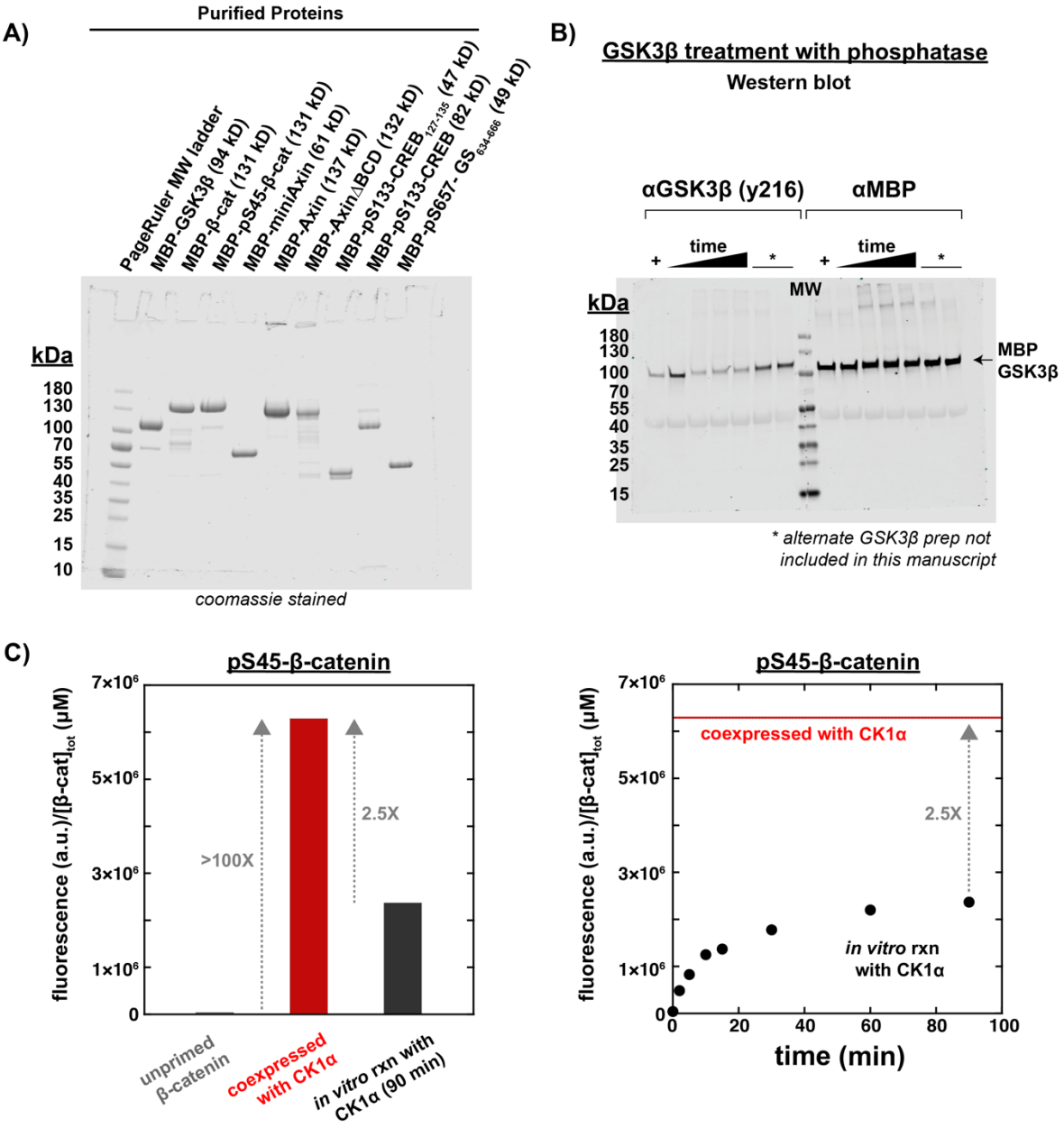

Figure S1. Characterization of purified proteins, related to Figures 1-3.
(A) Coomassie-stained SDS-PAGE of purified proteins used in this work. MBP-pS45-β-catenin is the material purified after coexpression with CK1α. Phosphorylated CREB and GS constructs were purified after *in vitro* phosphorylation (see Methods). Each lane was loaded with 15 μL of 5 μM protein.
(B) GSK3β purified from *E. coli* is phosphorylated on the activation loop Tyr216. Purified GSK3β was incubated with the tyrosine phosphatase YopH and analyzed by western blot using an antibody specific for pY216 GSK3β. Purified GSK3β produced a detectable signal at the expected molecular weight (94 kD), and the signal decreases substantially upon YopH treatment. Timepoints are 0, 0.5, 1, and 4 hrs. The lane labeled (+) was incubated for 0.5 hr with 100 μM ATP, which had no apparent effect. The loading control indicates no change in total GSK3β, using an anti-MBP antibody that detects the MBP tag on purified GSK3β. Samples were run together on a single gel. After the western blot transfer, the membrane was cut down the center of the MW ladder lane so each half of the gel could be incubated with separate antibodies. The membrane halves were placed back together for imaging.
(C) β-catenin co-expressed with CK1α in *E. coli* is phosphorylated on Ser45. The extent of S45 phosphorylation was detected by western blot using an antibody specific for pS45-β-catenin. Phosphoprimed β-catenin can also be obtained by incubating unprimed β-catenin with purified CK1α. In this reaction, we observe partial phosphorylation of Ser45, with a total pS45 signal (normalized to total protein concentration) reaching only ~40% of that obtained when β-catenin is co-expressed with CK1α.
(D) Schematics of full length human Axin (isoform 2, Uniprot O15169-2), AxinΔBCD, and $Axin_{384\text{-}518}$ (miniAxin), which contains the binding sites for both GSK3β and β-catenin (see Methods for an explanation of domain boundaries).

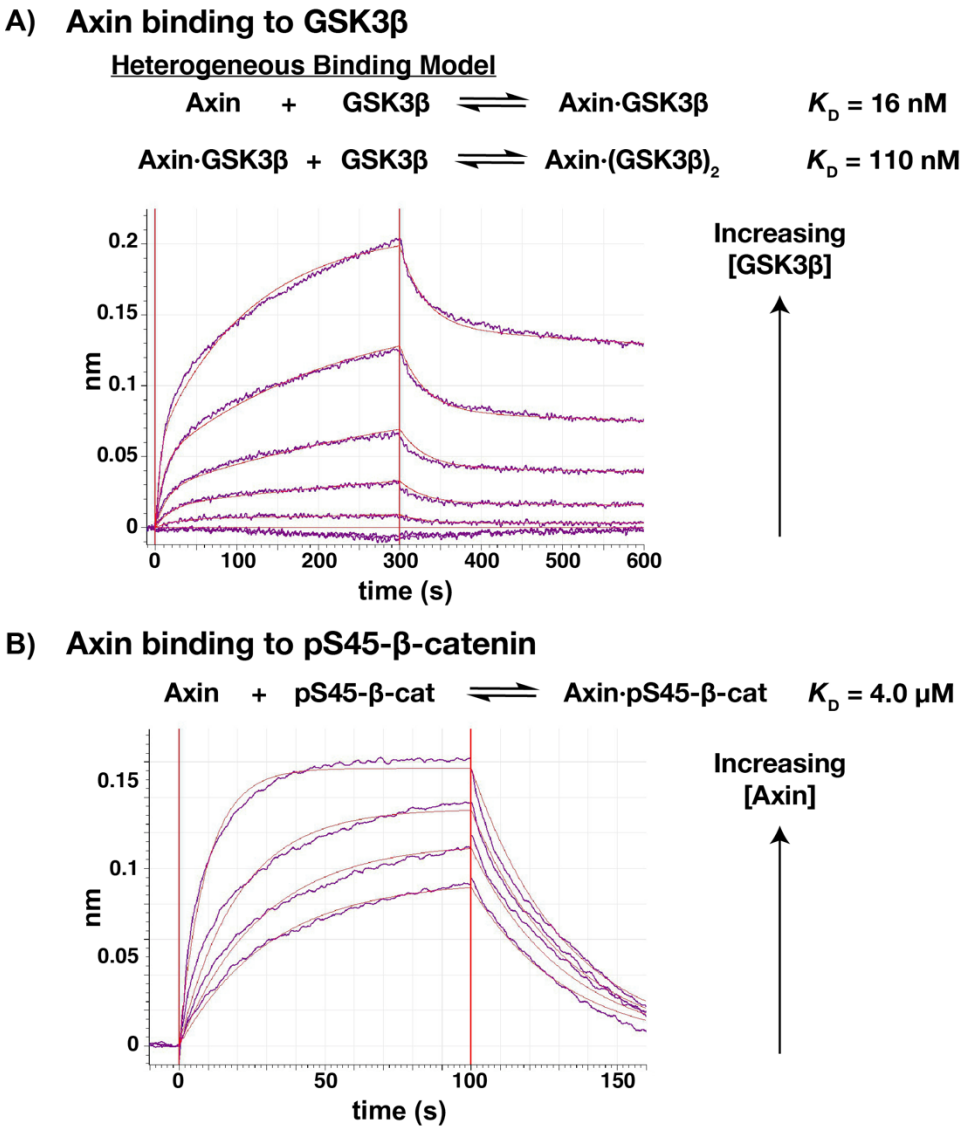

Figure S2. Axin binding to GSK3β and β-catenin, related to Figure 1.
(A) Bio-layer interferometry traces showing association and dissociation of GSK3β to immobilized biotinylated miniAxin. Similar data were obtained with full length Axin and AxinΔBCD. The data were fit to a Heterogeneous Binding Model (Data Analysis HT 11.0, ForteBio) that accounts for GSK3β binding to Axin and GSK3β dimerization, which has been previously reported (Fraser et al., 2002). This fit gives a K_D of 16 nM for miniAxin binding to GSK3β. The fitted K_D for GSK3β dimerization is 110 nM, which is somewhat tighter than the low μM value estimated from crosslinking experiments (Fraser et al., 2002). A 1:1 binding model that neglects GSK3β dimerization gives a poor fit to the data. Values of fitted binding constants are reported in Table S1.
(B) Bio-layer interferometry traces showing association and dissociation of miniAxin to immobilized biotinylated pS45-β-catenin. This binding event produced a negative shift in the interferometry signal (the data are displayed with an inverted y-axis), indicating a compression in the surface which could result from a conformational change in the bound complex. The data were fit using a 1:1 binding model. This fit gives a K_D of 4.0 μM for Axin binding to pS45-β-catenin.

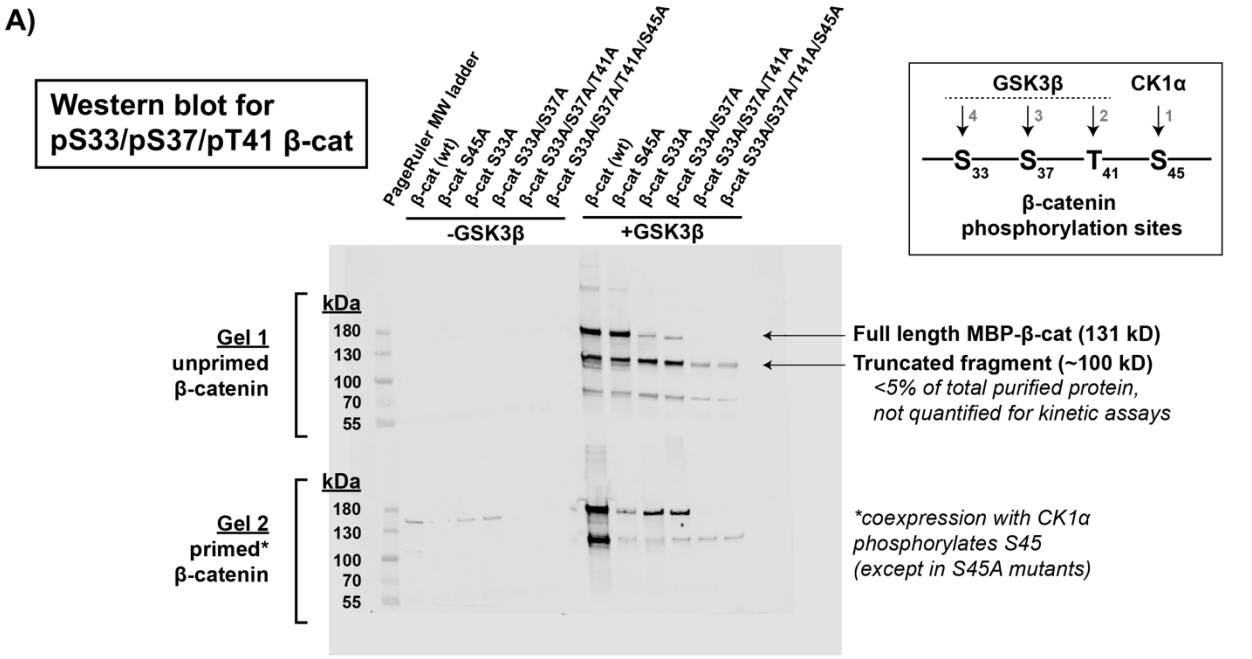
A)
Western blot for pS33/pS37/pT41 β-cat
PageRuler MW ladder
β-cat (wt)
β-cat S45A
β-cat S33A
β-cat S33A/S37A
β-cat S33A/S37A/T41A
β-cat S33A/S37A/T41A/S45A
-GSK3β
+GSK3β
GSK3β
CK1α
S33 S37 T41 S45
β-catenin phosphorylation sites
Gel 1 unprimed β-catenin
Gel 2 primed* β-catenin
kDa
180
130
100
70
55
Full length MBP-β-cat (131 kD)
Truncated fragment (~100 kD)
<5% of total purified protein, not quantified for kinetic assays
*coexpression with CK1α phosphorylates S45 (except in S45A mutants)

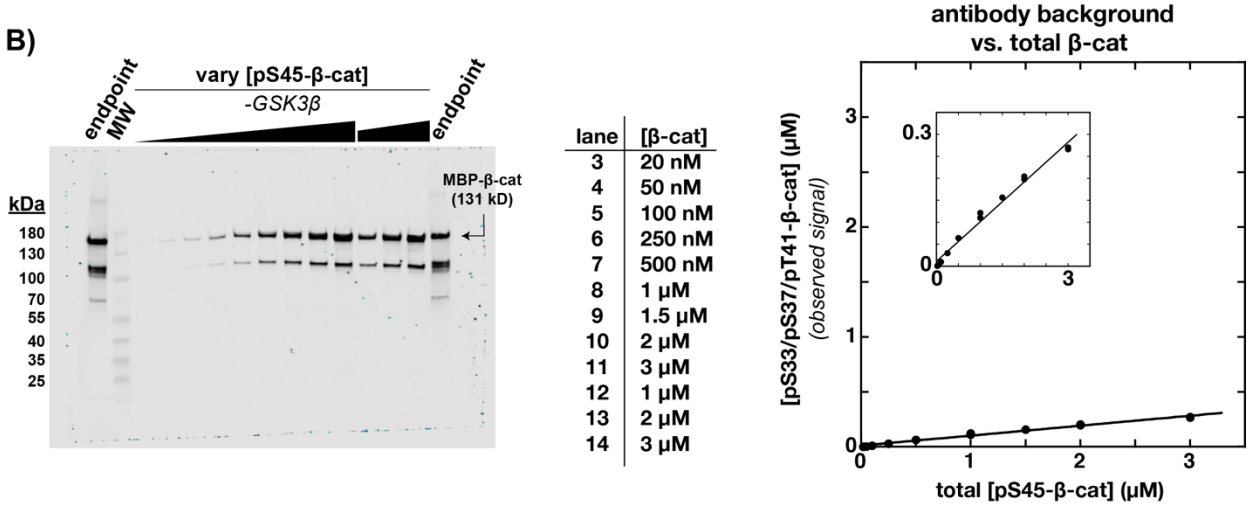
B)
endpoint MW
vary [pS45-β-cat]
-GSK3β
endpoint
kDa
180
130
100
70
55
40
35
25
MBP-β-cat (131 kD)
lane [β-cat]
3 20 nM
4 50 nM
5 100 nM
6 250 nM
7 500 nM
8 1 μM
9 1.5 μM
10 2 μM
11 3 μM
12 1 μM
13 2 μM
14 3 μM
antibody background vs. total β-cat
[pS33/pS37/pT41-β-cat] (μM)
(observed signal)
total [pS45-β-cat] (μM)

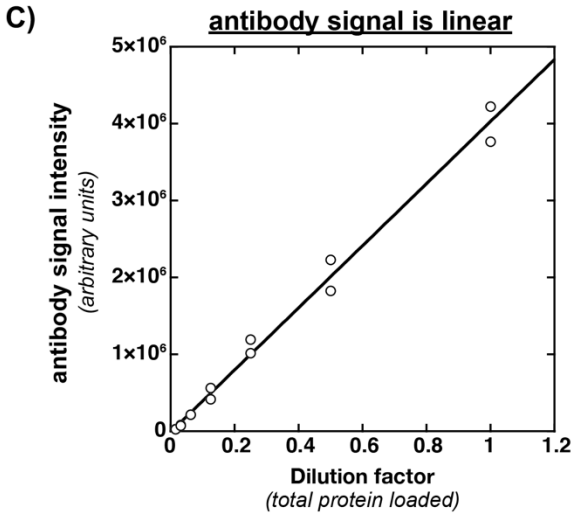
C)
antibody signal is linear
antibody signal intensity
(arbitrary units)
5x10⁶
4x10⁶
3x10⁶
2x10⁶
1x10⁶
0
0.2
0.4
0.6
0.8
1
1.2
Dilution factor
(total protein loaded)

Figure S3. Characterization of the anti-Phospho-β-Catenin (Ser33/37/Thr41) antibody (Cell Signaling Technology #9561), related to Figure 1.

CK1α phosphorylates β-catenin at S45. GSK3β sequentially phosphorylates pS45-β-catenin at three sites: T41, S37, and S33 (C. Liu et al., 2002), and product formation can be monitored using an antibody specific for pS33/pS37/pT41-β-catenin.

(A) Western blot of wild type and phosphosite mutants of β-catenin to assess specificity for the triply phosphorylated (S33/S37/T41) state. Gel 1 shows unprimed β-catenin without GSK3β and after a GSK3β reaction to completion (50 nM β-catenin, 100 nM GSK3β, 100 nM miniAxin, and 100 μM ATP at 25 ºC for 16 hrs, see quantification in Figure S4B. Gel 2 shows primed β-catenin without GSK3β and after a GSK3β reaction to completion (50 nM β-catenin, 100 nM GSK3β, 100 nM miniAxin, and 100 μM ATP at 25 ºC for 30 min, see quantification in Figure S4A. Each primed β-catenin protein was prepared by coexpression with CK1α, which phosphorylates S45 on all constructs except the S45A mutants. After long incubations with GSK3β, two bands can be observed by western blotting. The top band corresponds to the expected 131 kD molecular weight of full length MBP-β-catenin. The lower band (~100 kD) is likely to be a truncated fragment of β-catenin that co-purifies with the full length protein, as the signal disappears in the β-catenin phosphosite point mutants. Based on coomassie staining for total protein (Figure S1), the 100 kD fragment is present at <5% of total purified protein, and phosphorylation of this band is not significant in initial rate assays (see Figures S6 & S8). Mutation of any of the GSK3β phosphorylation sites substantially reduces the detectable signal, indicating that the antibody preferentially recognizes triply phosphorylated (S33/S37/T41) β-catenin.

(B) In the absence of GSK3β, there is detectable antibody signal in the pS45-β-catenin sample (see panel (A); this signal disappears when all three GSK3β phosphosites are mutated, suggesting that it results from weak CK1α–mediated phosphorylation of the GSK3β sites). The background signal corresponds to ~10% of the total protein. All samples on this gel were loaded at 1:5 dilution (see Methods).

(C) The antibody signal is linear over a broad range spanning the observed signal in all kinetic assays. The plot shows a set of 2-fold serial dilutions from a reaction with 3 μM pS45-β-catenin, 20 nM GSK3β and 500 nM miniAxin at the 1.5 minute timepoint. This is the longest timepoint at the highest pS45-β-catenin concentration used in any assay and corresponds to the largest raw signal analyzed in any experiment. There are 6 dilutions; the largest dilution factor is 1:64. All samples on this gel were loaded at 1:5 dilution (see Methods). Each dilution sample was run in duplicate (2 points at every dilution factor).

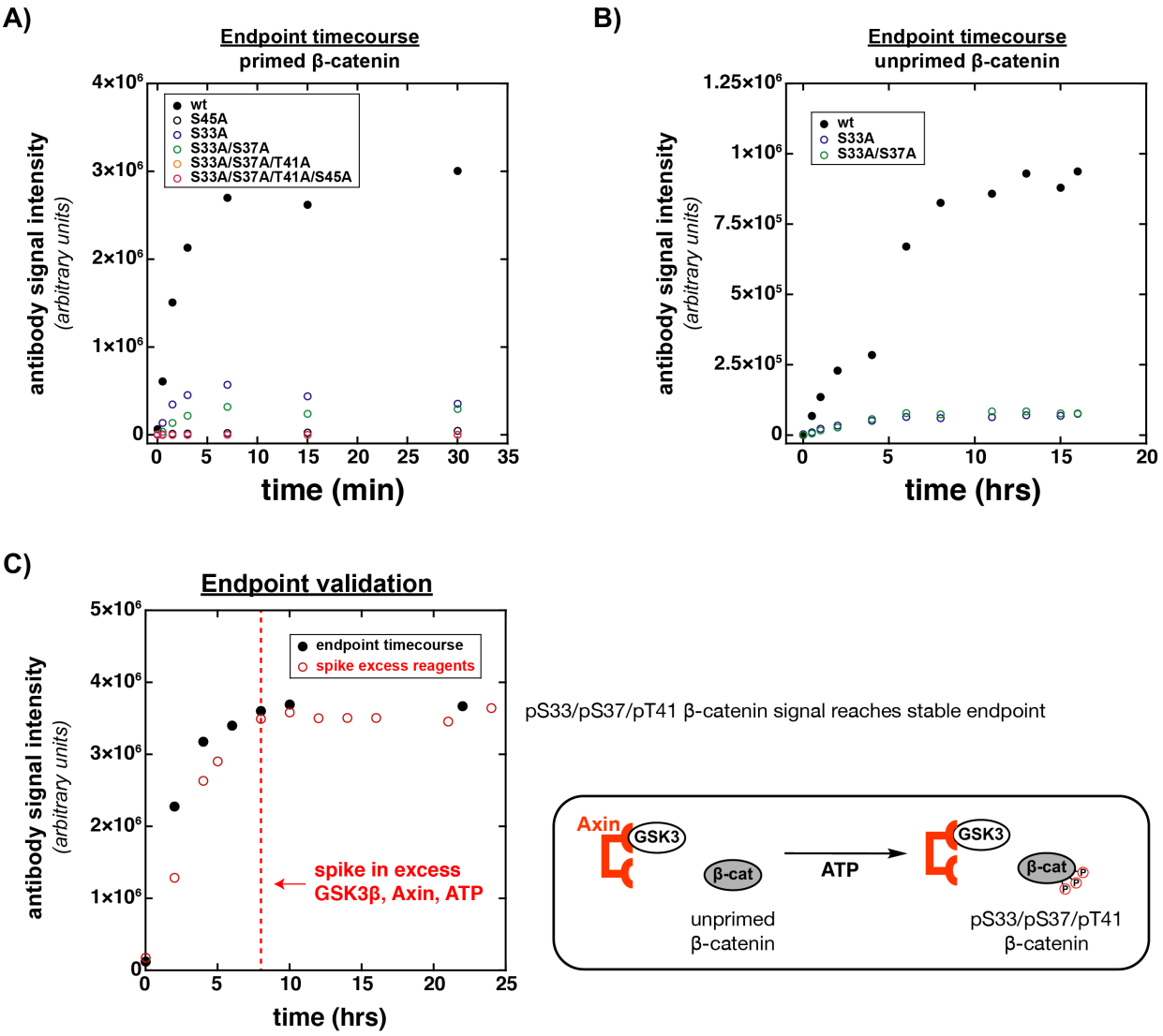

Figure S4. Endpoint standards for GSK3β-phosphorylated β-catenin, related to Figure 1.
(A) Timecourse of phosphorylation of an endpoint standard of pS45-β-catenin and quantification of antibody signal relative to β-catenin phosphosite mutants. Reaction conditions are 50 nM pS45-β-catenin, 100 nM GSK3β, and 100 μM ATP at 25 ºC. The reaction approaches completion in ~10 minutes. Phosphosite mutants produce at most ~10% of the signal of wild type β-catenin.
(B) Timecourse of phosphorylation of an endpoint standard of unprimed β-catenin and quantification of antibody signal relative to β-catenin phosphosite mutants. Reaction conditions are 50 nM β-catenin, 100 nM GSK3β, 100 nM miniAxin, and 100 μM ATP at 25 ºC. The reaction approaches completion in ~10 hours. Phosphosite mutants produce at most ~10% of the signal of wild type β-catenin.
(C) Validation of the endpoint standard of unprimed β-catenin. The endpoint standard is 50 nM β-catenin, 100 nM GSK3β, 100 nM miniAxin, and 100 μM ATP at 25 ºC. The "spike excess reagents" standard is 50 nM β-catenin, 1 μM GSK3β, 1 μM miniAxin, and 100 μM ATP at 25 ºC, with an additional 500 nM GSK3β, 500 nM miniAxin, and 100 μM ATP added at 8 hrs.

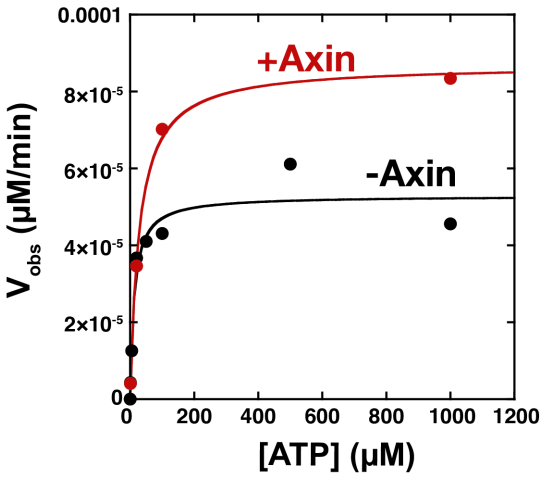

Figure S5. The concentration of ATP used for quantitative kinetic experiments (100 μM) is saturating for GSK3β in the presence and absence of Axin, related to Figure 1.
Michaelis-Menten plot of V_{obs} vs. [ATP] at 20 nM GSK3β and 500 nM unprimed β-catenin in the presence and absence of 100 nM miniAxin. Fits to the Michaelis-Menten equation give $K_{M,\ ATP}$ values of 12 ± 4 μM and 28 ± 3 μM in the presence and absence of Axin, respectively.

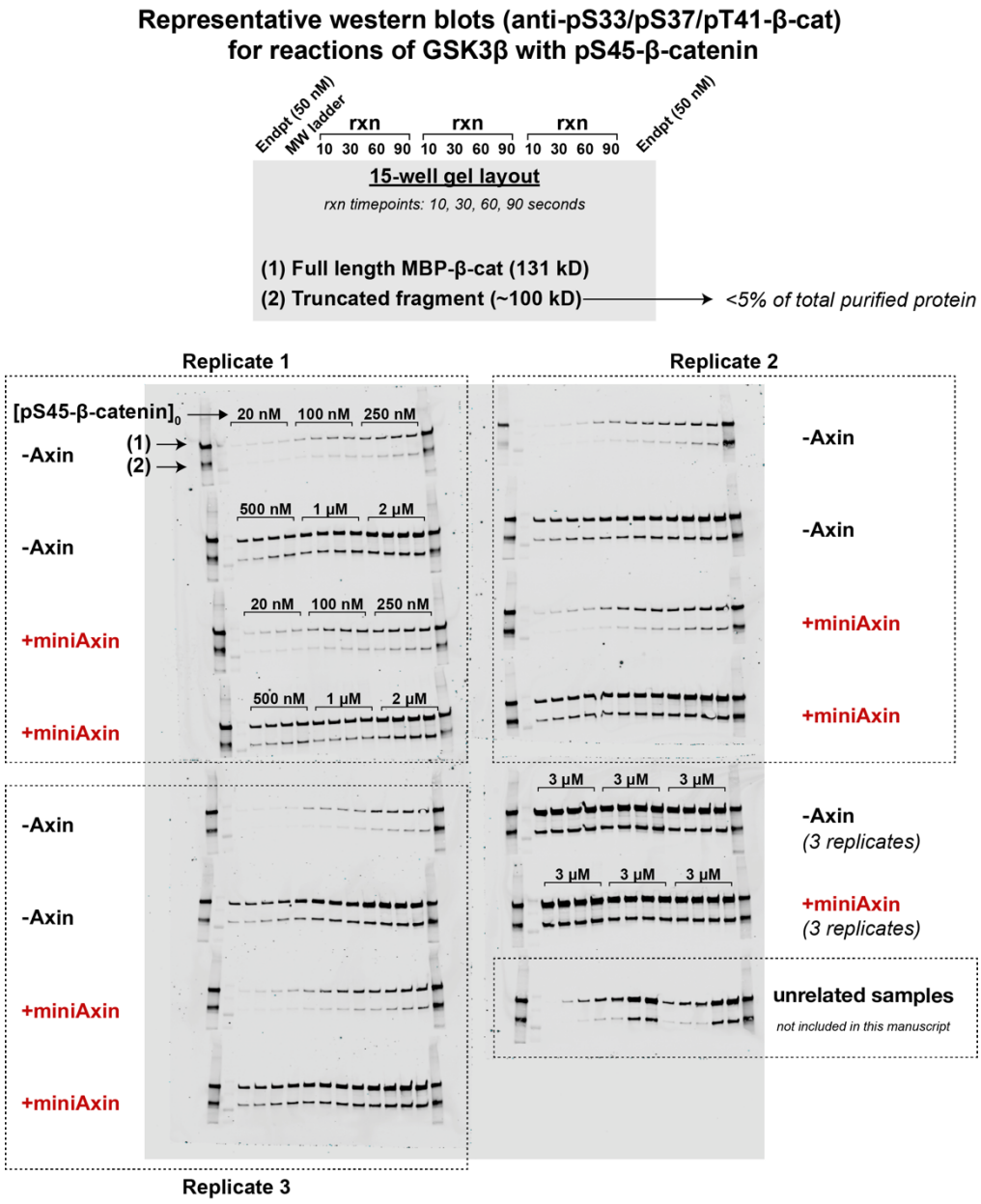

Figure S6. Representative western blots for the reaction of GSK3β with pS45-β-catenin in the presence and absence of Axin, related to Figure 1.

Western blots for reactions of varying concentrations of pS45-β-catenin at 20 nM GSK3β in the presence and absence of 500 nM miniAxin. Two phospho-β-catenin bands can be observed by western blotting (see Figure S3A). The top band corresponds to full length MBP-β-catenin and was quantified for all rate measurements. For reactions with [p-S45-β-catenin] ≥ 500 nM, gel samples were diluted 1:5 to prevent a gel smearing artifact (see Methods). See Figure S7 for quantification. The conclusions from this work are not affected if the lower, truncated β-catenin species is included in the analysis. The Axin effects on truncated β-catenin phosphorylation rates are indistinguishable from the effects on full length β-catenin in all experimental conditions tested. Further, in an alternative prep of pS45- β-catenin, accumulation of the truncated band is negligible and we observe the same Axin effects (Figures S8 & S17).

A) Product vs. time plots for reactions of GSK3β with pS45-β-catenin (-Axin)

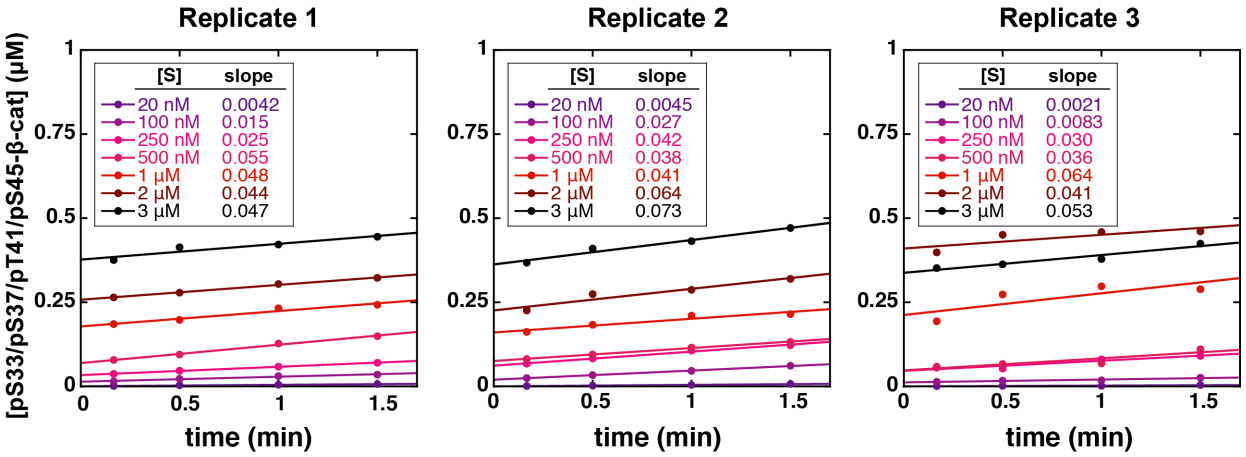

B) Product vs. time plots for reactions of GSK3β with pS45-β-catenin (+miniAxin)

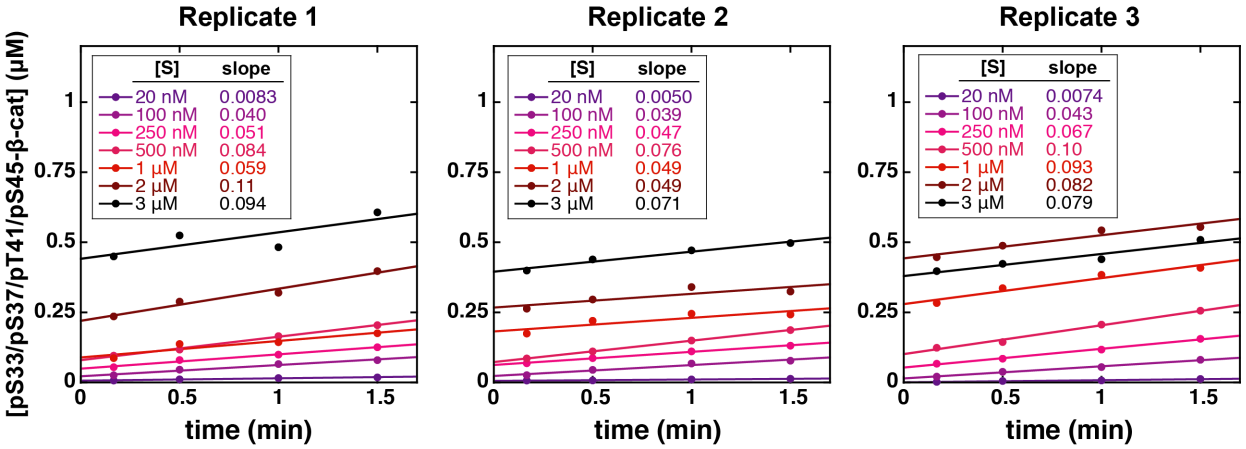

Figure S7. Plots of product vs. time for reaction of GSK3β with pS45-β-catenin in the presence and absence of Axin, related to Figure 1.

(A) Product vs. time plots for reactions of GSK3β with pS45-β-catenin in the absence of Axin. (B) Product vs. time plots for reactions of GSK3β with pS45-β-catenin in the presence of 500 nM miniAxin. Data in (A) and (B) correspond to the reaction conditions and western blots shown in Figure S6. The reported slopes are initial rates in units of μM/min. At high concentrations of substrate, there is detectable background signal (y-intercepts are not 0 at t=0). This background arises from partial phosphorylation of the GSK3β sites during expression of pS45-β-catenin (see Figure S3D); this signal is <10% of the possible total conversion and should not affect initial rate measurements. To confirm that this background does not affect the measured rates or the conclusions drawn, we also performed kinetic assays with *in vitro* phosphorylated pS45-β-catenin, which is partially phosphorylated at S45 (Figure S1C) and does not have detectable background at t=0 (see Figure S8). The effects of Axin with *in vitro* phosphorylated pS45-β-catenin were similar to the effects observed with the pS45-β-catenin obtained from coexpression with CK1α (Figure S8; see also Figure S17 for competition reaction, related to Figure 4).

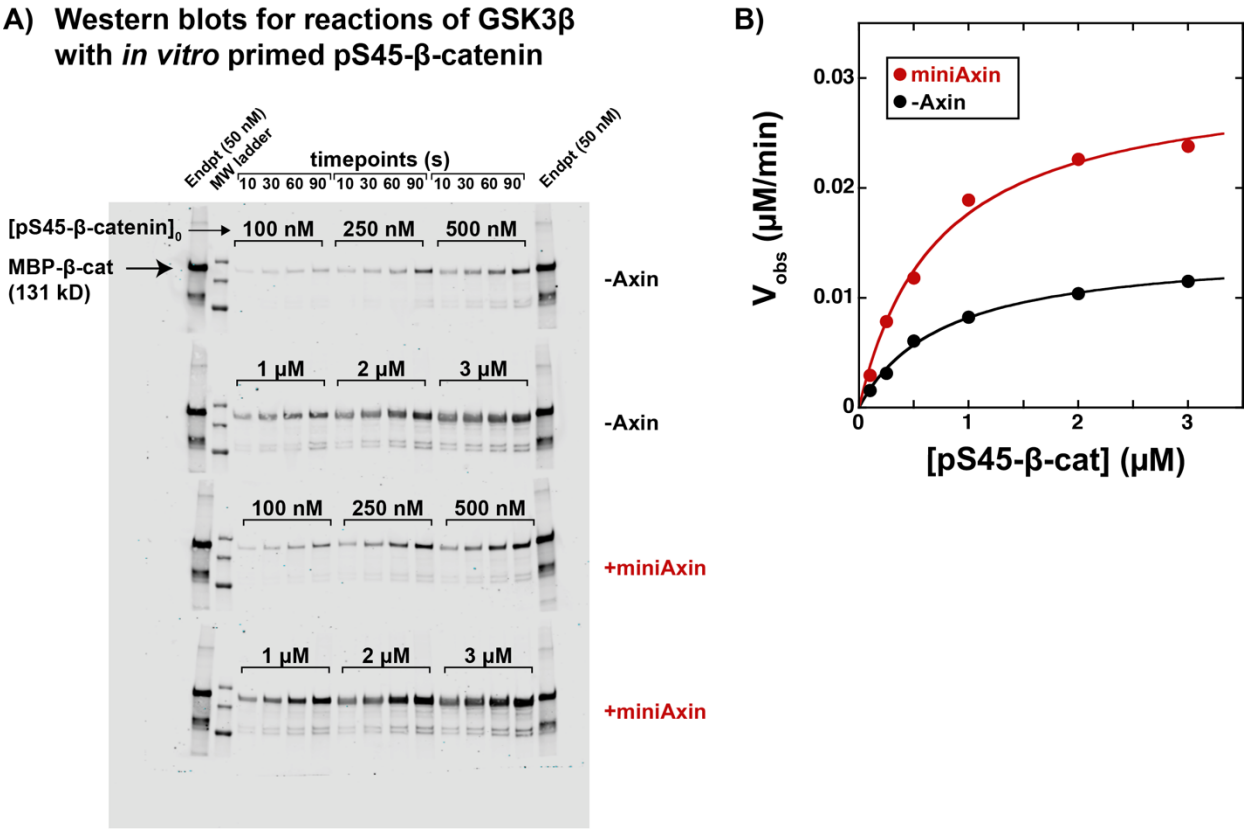

Figure S8. Representative western blots and quantification for the reaction of GSK3β with pS45-β-catenin using *in vitro* phosphorylated pS45-β-catenin, related to Figure 1.
pS45-β-catenin prepared by coexpression with CK1α has background signal from partial phosphorylation of the GSK3β sites (see Figures S3D, S6, and S7). pS45-β-catenin prepared from an *in vitro* reaction of β-catenin with CK1α does not have significant background signal.
(A) Western blots for reactions of varying concentrations of *in vitro* CK1α -phosphorylated pS45-β-catenin at 20 nM GSK3β in the presence and absence of 500 nM miniAxin. For reactions with [p-S45-β-catenin] ≥ 500 nM, gel samples were diluted 1:5 to prevent a gel smearing artifact (see Methods).
(B) Michaelis-Menten plot of V_{obs} vs. [pS45-β-catenin] at 20 nM GSK3β. Values are initial rates from the western blots in panel (A); only one replicate was performed at each substrate concentration. As observed with pS45-β-catenin prepared by coexpression, Axin has only small effects on the steady state rate constants (Table S3).

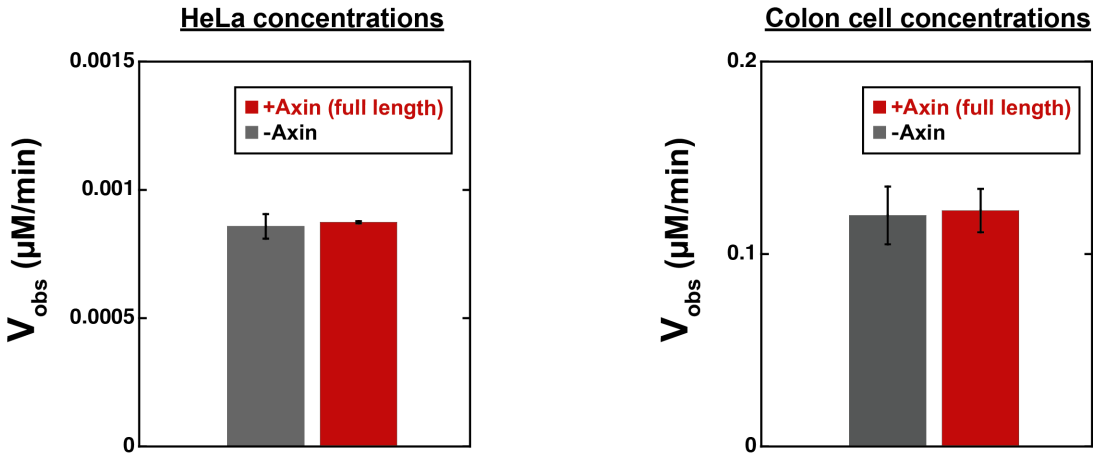

Figure S9. Comparisons of observed rates for GSK3β reactions with pS45-β-catenin at estimated physiological concentrations, related to Figure 1.
Observed rates for GSK3β reactions with pS45-β-catenin in the presence or absence of Axin using concentrations estimated for HeLa or colon cells (see main text box 1 and Table 2). Values are mean ± SD for 3 measurements.

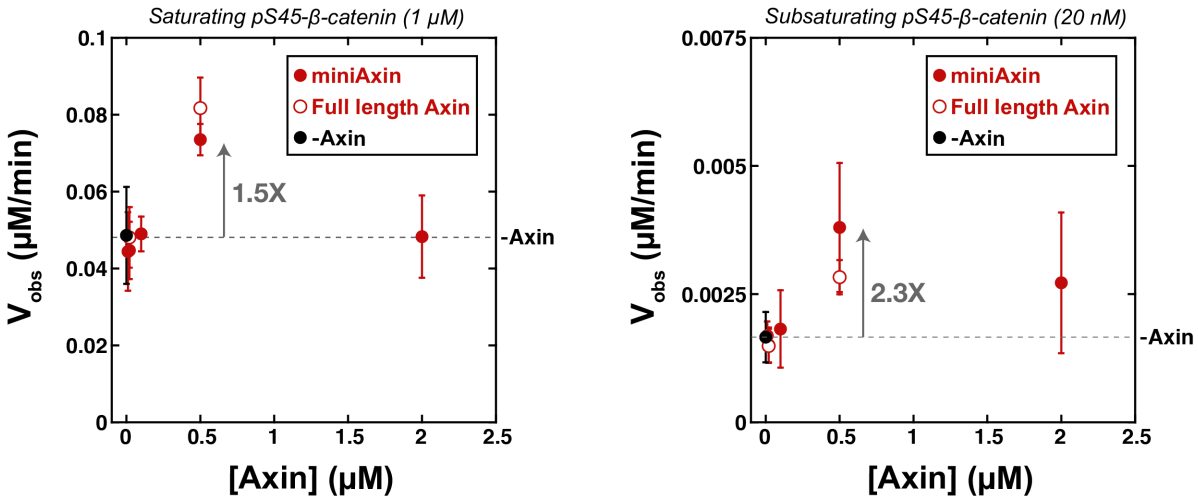

Figure S10. Varying the concentration of Axin for the reaction of GSK3β with pS45-β-catenin does not produce larger rate effects than observed with 500 nM Axin , related to Figure 1.

Plots of V_{obs} vs. [Axin] with either miniAxin or full length Axin, 20 nM GSK3β, and 1 μM or 20 nM pS45-β-catenin. It is important to test both saturating concentrations (i.e. k_{cat} conditions, 1 μM pS45-β-catenin) and subsaturating concentrations (i.e. k_{cat}/K_M conditions, 20 nM pS45-β-catenin) because if Axin has a large effect on K_M it would not be detectable in saturating conditions. For full length Axin, only a subset of Axin concentrations were measured (20 and 500 nM). Error bars are mean ± SD for at least 3 measurements.

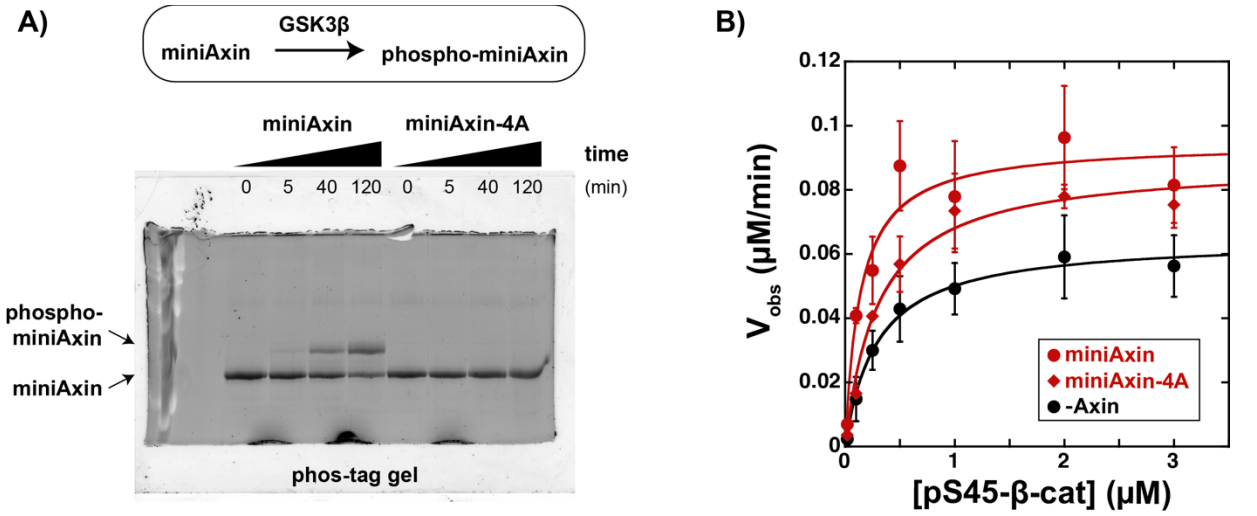

Figure S11. GSK3β phosphorylates Axin, related to Figure 1.
(A) GSK3β phosphorylates Axin at residues T481, S486, S493, and S496 GSK3β (S.-E. Kim et al., 2013; Willert et al., 1999). Mutation of each of these residues to A (miniAxin-4A) prevents detectable phosphorylation. Reactions were prepared with 20 nM GSK3β, 500 nM miniAxin or miniAxin-4A, and 100 μM ATP. 20 μL aliquots were quenched at the indicated timepoints and loaded on a Phos-tag gel (see Methods). The slower-migrating species in the miniAxin reation is phosphorylated miniAxin.
(B) Michaelis-Menten plot of V_{obs} vs. [pS45-β-catenin] at 20 nM GSK3β in the presence and absence of 500 nM miniAxin or miniAxin-4A. Values are mean ± SD for at least 3 measurements. See Table S2 for values of fitted kinetic parameters.

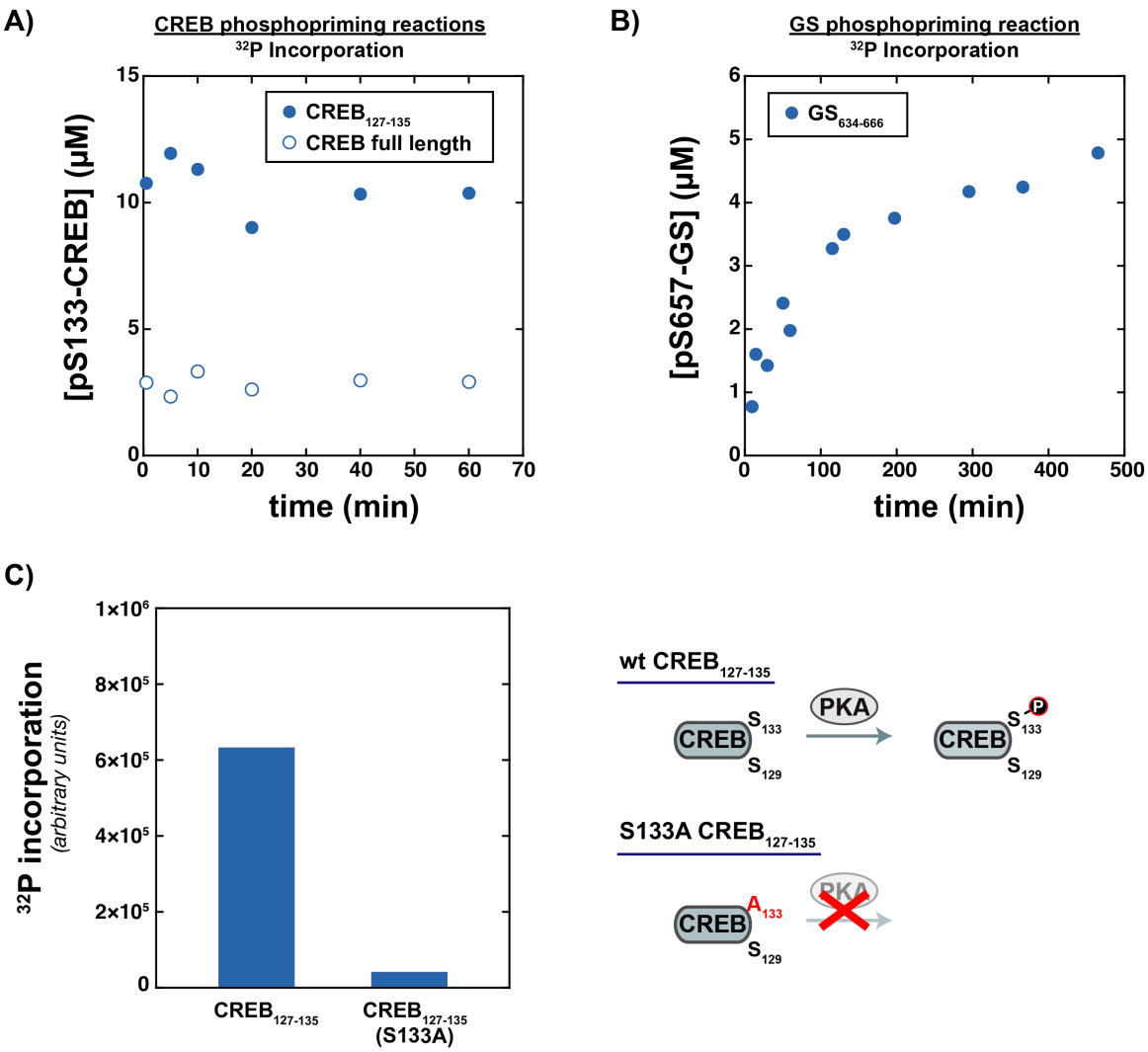

Figure S12. Phosphopriming reactions of alternative GSK3β substrates, related to Figure 3.
(A) PKA phosphorylates CREB. Reactions were performed with 10 μM CREB or $CREB_{127-135}$, 2 μM PKA, 100 μM ATP, and trace γ-^{32}P-ATP as described in the Methods section. ^{32}P incorporation into CREB rapidly approaches completion within the first 30 seconds of the reaction. ^{32}P counts were converted to concentration using an independent endpoint standard from a PKA reaction with an optimal substrate (see Methods). Full length CREB approaches a limit at 3 μM conversion. Each reaction has 10 μM CREB, but the material in the full length CREB reaction was <50% pure from Ni-NTA resin, so 3 μM conversion is plausible.
(B) CK2 phosphorylates GS. The reaction was performed in a 50 μL volume with 5 μM $GS_{634-666}$, 250 units of CK2 (0.5 μL 500 U/μL CK2, NEB catalog #P6010), 100 μM ATP, and trace γ-^{32}P-ATP as described in the Methods section. ^{32}P incorporation into GS approaches completion in ~200 minutes. ^{32}P counts were converted to concentration as described in (A) above.
(C) No significant ^{32}P incorporation is detectable in S133A $CREB_{127-135}$, which confirms that wt $CREB_{127-135}$ is phosphorylated on Ser_{133}. Reaction conditions were as in panel (A), with samples taken at 60 minutes.

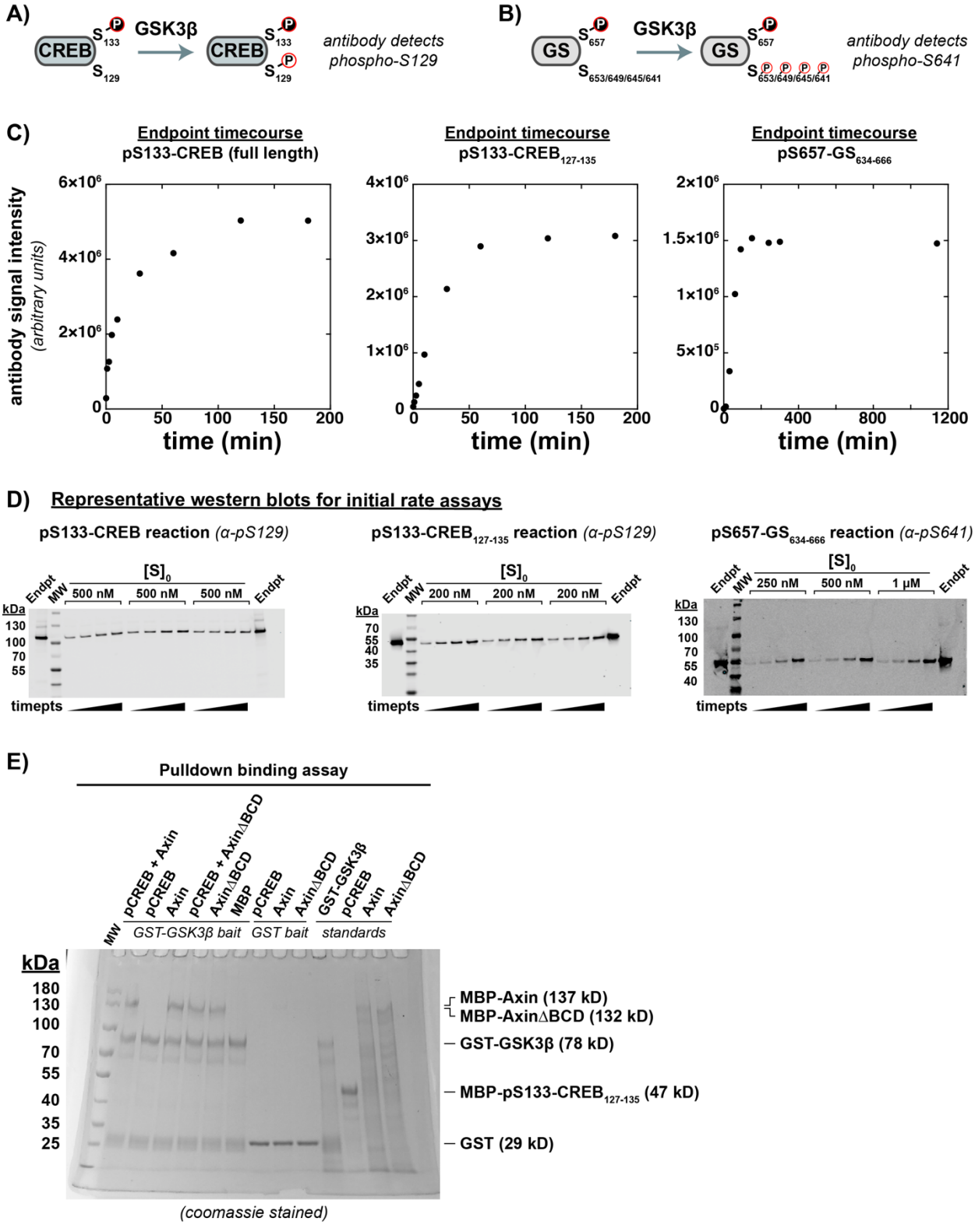
A)
CREB
S133
S129
GSK3β
CREB
S133
S129
antibody detects phospho-S129
B)
GS
S657
S653/649/645/641
GSK3β
GS
S657
S653/649/645/641
antibody detects phospho-S641
C)
Endpoint timecourse
pS133-CREB (full length)
Endpoint timecourse
pS133-CREB127-135
Endpoint timecourse
pS657-GS634-666
antibody signal intensity (arbitrary units)
time (min)
time (min)
time (min)
D)
Representative western blots for initial rate assays
pS133-CREB reaction (α-pS129)
pS133-CREB127-135 reaction (α-pS129)
pS657-GS634-666 reaction (α-pS641)
[S]0
Endpt
MW
500 nM
200 nM
250 nM
1 μM
kDa
timepts
E)
Pulldown binding assay
MW
pCREB + Axin
pCREB
Axin
pCREB + AxinΔBCD
AxinΔBCD
MBP
pCREB
Axin
AxinΔBCD
GST-GSK3β
pCREB
Axin
AxinΔBCD
GST-GSK3β bait
GST bait
standards
kDa
180
130
100
70
55
40
35
25
MBP-Axin (137 kD)
MBP-AxinΔBCD (132 kD)
GST-GSK3β (78 kD)
MBP-pS133-CREB127-135 (47 kD)
GST (29 kD)
(coomassie stained)

Figure S13. Timecourses for endpoint standards of GSK3β-phosphorylated CREB and GS, related to Figure 3.

(A) GSK3β phosphorylates pS133-CREB on S129 (Fiol et al., 1994), which can be detected with anti-Phospho-CREB (Ser129) antibody (Thermo Scientific #PA5-36843).

(B) GSK3β sequentially phosphorylates pS657-GS on S653, S649, S645, and S641 (Fiol et al., 1990; 1987). The anti-phospho-GS antibody (Cell Signaling Technology #3891) detects phospho-S641.

(C) Timecourses of phosphorylation of endpoint standards for GSK3β reactions with pS133-CREB, pS133-$CREB_{127\text{-}135}$, and pS657-$GS_{634\text{-}666}$. Reactions were conducted with 50 nM substrate, 100 nM GSK3β, and 100 μM ATP.

(D) Representative western blots for reactions of GSK3β with pS133-CREB, pS133-$CREB_{127\text{-}135}$, and pS657-$GS_{634\text{-}666}$ in the absence of Axin. Reactions were conducted with 20 nM GSK3β and the substrate concentrations indicated. The images shown are the complete, uncropped blot membrane images; each gel was cut before transferring to the membrane to facilitate multiple simultaneous transfers in the same apparatus (as seen in Figure S6).

(E) pS133-$CREB_{127\text{-}135}$ does not detectably bind to Axin. In a pulldown assay, GST-GSK3β binds to Axin and AxinΔBCD. When pS133-$CREB_{127\text{-}135}$ is included in a binding assay with Axin, there is no detectable co-precipitation of pS133-$CREB_{127\text{-}135}$ with Axin or AxinΔBCD (lanes 2 and 5). There is also no detectable binding of pS133-$CREB_{127\text{-}135}$ directly to GST-GSK3β (lane 3). The observed K_M of GSK3β for pS133-$CREB_{127\text{-}135}$ in phosphorylation assays is ~0.2 μM; if the K_D is similar then this result suggests the detection limit for binding affinity in this assay is ≤0.2 μM. Protein standards included for reference on the right side of the gel are the partially-purified samples (by Ni-NTA only, see Methods) used in the binding assays.

A) Product vs. time plots for reactions of GSK3β with pS657-GS (-Axin)

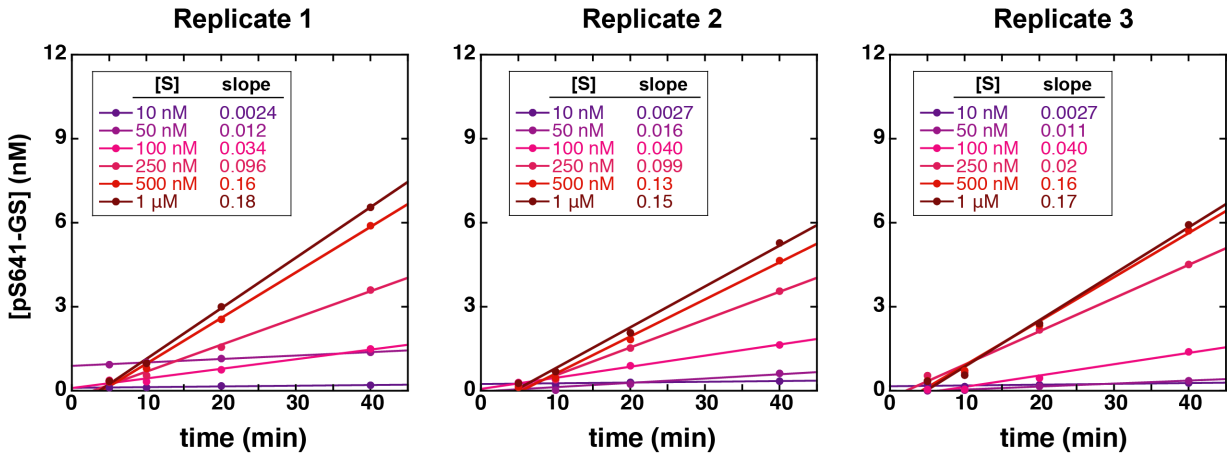

B) Product vs. time plots for reactions of GSK3β with pS657-GS (+miniAxin)

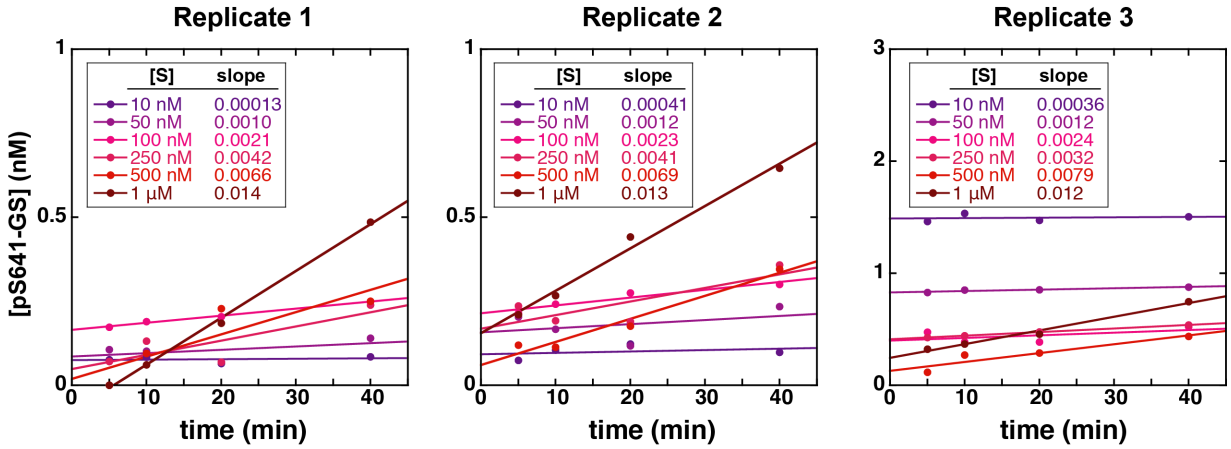

Figure S14. Plots of product vs. time for reaction of GSK3β with pS657-GS$_{634\text{-}666}$ in the presence and absence of Axin, related to Figure 3.
(A) Product vs. time plots for reactions of 20 nM GSK3β with varying concentrations of pS657-GS$_{634\text{-}666}$ in the absence of Axin.
(B) Product vs. time plots for reactions of 20 nM GSK3β with varying concentrations of pS657-GS$_{634\text{-}666}$ in the presence of 500 nM miniAxin. The reported slopes are initial rates in units of nM/min. See main text Figure 3D for Michaelis-Menten plots of V_{obs} vs. [pS657-GS$_{634\text{-}666}$].

A)

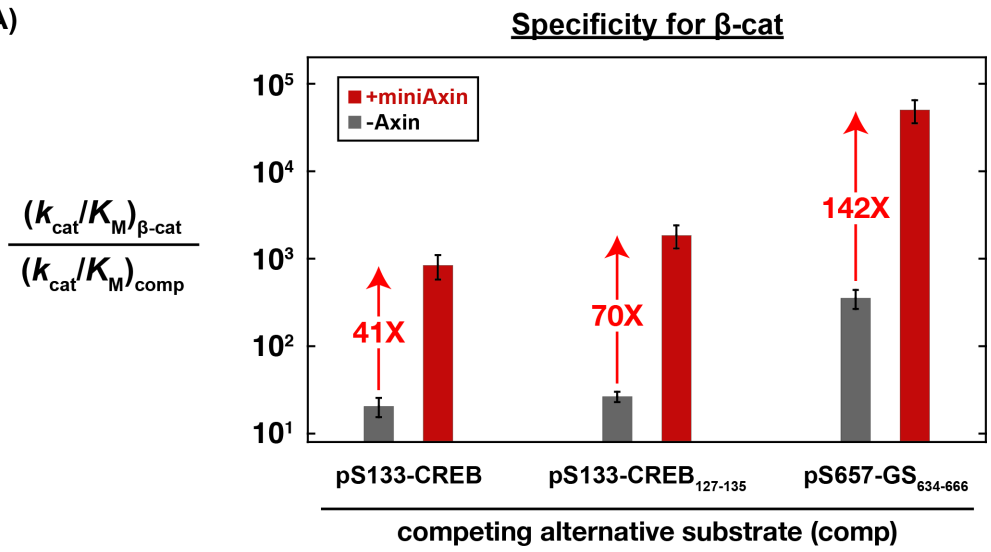

B)

$$\frac{V_{obs,\,\beta\text{-cat}}}{V_{obs,\,comp}} = \frac{\dfrac{k_{cat,\,\beta\text{-cat}}[GSK3]_0[\beta\text{-cat}]}{K_{M,\,\beta\text{-cat}}\left(1+\dfrac{[comp]}{K_{M,\,comp}}\right)+[\beta\text{-cat}]}}{\dfrac{k_{cat,\,comp}[GSK3]_0[comp]}{K_{M,\,comp}\left(1+\dfrac{[\beta\text{-cat}]}{K_{M,\,\beta\text{-cat}}}\right)+[comp]}} = \frac{(k_{cat}/K_M)_{\beta\text{-cat}}[\beta\text{-cat}]}{(k_{cat}/K_M)_{comp}[comp]}$$

Figure S15. Specificity of GSK3β for β-catenin, related to Figure 3.
(A) The specificity of GSK3β for pS45-β-catenin relative to competing alternative substrates is the ratio of the corresponding k_{cat}/K_M values. Specificity increases by ~10^2-fold in the presence of miniAxin. Values are from Table S2.
(B) The rate equations for enzyme specificity, where the relative rates are determined by the substrate concentrations and the ratio of the k_{cat}/K_M values (Fersht, 1999). See also Figure S16A.

A)

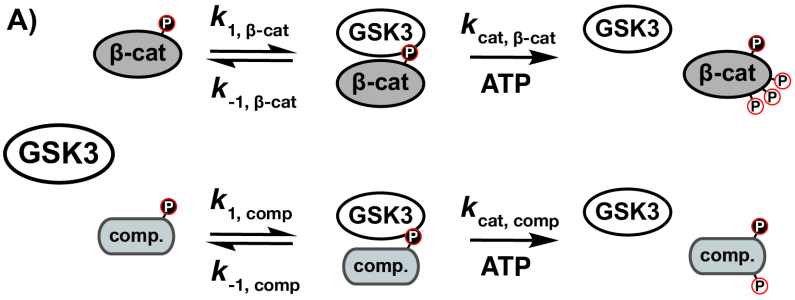

$$V_{obs,\beta\text{-cat}} = \frac{k_{cat,\beta\text{-cat}}[GSK3]_0[\beta\text{-cat}]}{K_{M,\beta\text{-cat}}\left(1+\frac{[comp]}{K_{M,comp}}\right)+[\beta\text{-cat}]}$$

$$V_{obs,comp} = \frac{k_{cat,CREB}[GSK3]_0[comp]}{K_{M,CREB}\left(1+\frac{[\beta\text{-cat}]}{K_{M,\beta\text{-cat}}}\right)+[comp]}$$

B) **Predicted β-catenin reaction rate vs. [CREB]**

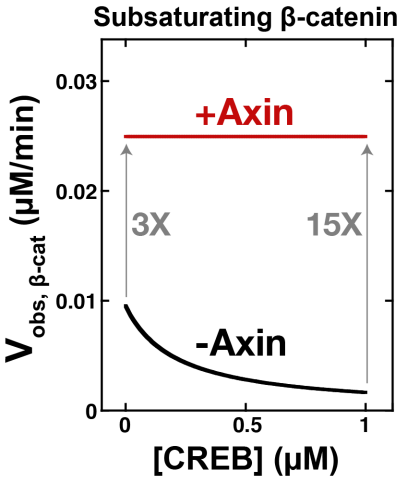

$$V_{obs} = \frac{k_{cat,+Axin}[GSK3]_0[\beta\text{-cat}]}{K_{M,+Axin}+[\beta\text{-cat}]}$$

$$V_{obs} = \frac{k_{cat,-Axin}[GSK3]_0[\beta\text{-cat}]}{K_{M,-Axin}\left(1+\frac{[CREB]}{K_{M,CREB}}\right)+[\beta\text{-cat}]}$$

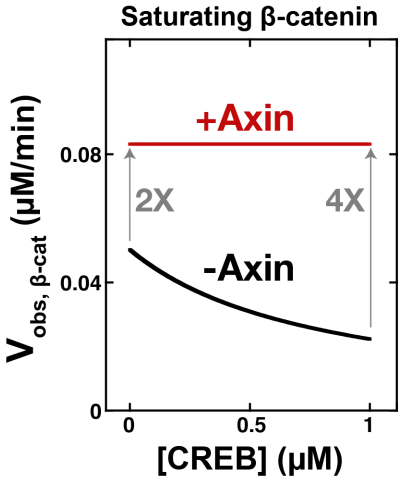

C) **Predicted β-catenin reaction rate vs. [GS]**

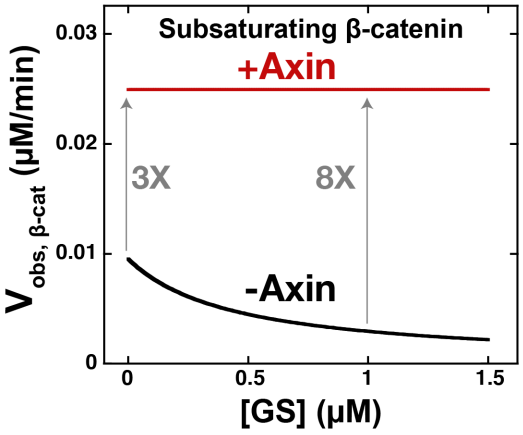

$$V_{obs} = \frac{k_{cat,+Axin}[GSK3]_0[\beta\text{-cat}]}{K_{M,+Axin}+[\beta\text{-cat}]}$$

$$V_{obs} = \frac{k_{cat,-Axin}[GSK3]_0[\beta\text{-cat}]}{K_{M,-Axin}\left(1+\frac{[GS]}{K_{M,GS}}\right)+[\beta\text{-cat}]}$$

D)

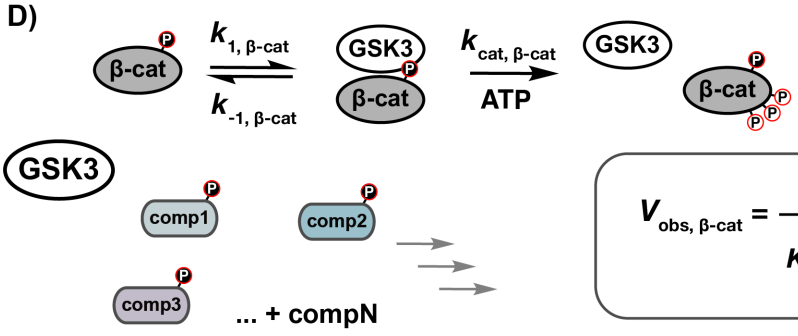

$$V_{obs,\beta\text{-cat}} = \frac{k_{cat,\beta\text{-cat}}[GSK3]_0[\beta\text{-cat}]}{K_{M,\beta\text{-cat}}\left(1+\sum\frac{[comp]}{K_{M,comp}}\right)+[\beta\text{-cat}]}$$

Figure S16. Kinetic model for a GSK3β reaction with β-catenin in the presence of competing substrates, related to Figure 4.

(A) Kinetic scheme for a competitive reaction. Each substrate effectively acts as a competitive inhibitor for the other substrate. See also Figure S15.

(B) Predicted rates for β-catenin phosphorylation as a function of $CREB_{127\text{-}135}$ concentration at 20 nM GSK3β and 50 nM (subsaturating) or 1 μM (saturating) pS45-β-catenin. Increasing concentrations of $CREB_{127\text{-}135}$ inhibit the β-catenin reaction in the absence of Axin. The expected values of V_{obs} were calculated using the equations from (A) and the kinetic parameters from Table S2. For the +miniAxin reaction, where $K_{M,\ CREB} \geq 1$ μM, we assumed that the term $[CREB_{127\text{-}135}]/K_{M,\ CREB}$ is negligible over the $[CREB_{127\text{-}135}]$ concentration range shown. When β-catenin is present at saturating concentrations, $CREB_{127\text{-}135}$is less effective at competing for GSK3β, leading to a smaller effect from Axin at high $[CREB_{127\text{-}135}]$.

(C) Predicted rates for β-catenin phosphorylation as a function of $GS_{634\text{-}666}$ concentration at 20 nM GSK3β and 50 nM (subsaturating) pS45-β-catenin. The expected values of V_{obs} were calculated using the equations from (A) and the kinetic parameters from Table S2, as described in (B) for the reaction with $CREB_{127\text{-}135}$ competitor. The predicted effect at 1 μM competitor is smaller than for CREB because the K_M of GSK3β for GS is larger (Table S2) and a 1 μM concentration of GS is not fully saturating.

(D) Kinetic scheme for a competitive reaction with multiple competitors. The competitive inhibition term is the sum of all inhibition terms for each individual competitor.

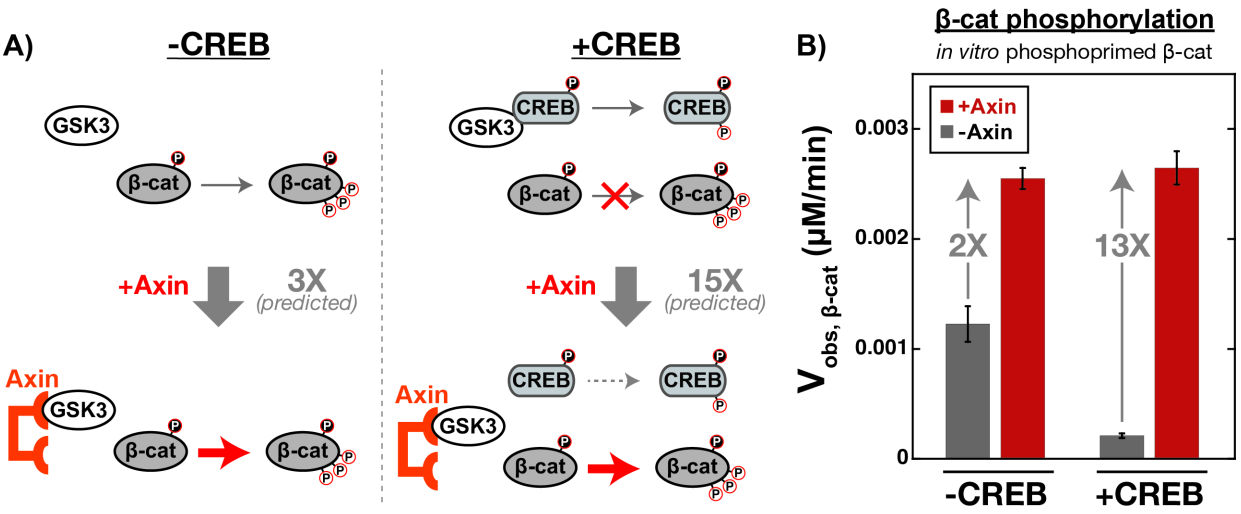

Figure S17. Axin accelerates the β-catenin reaction when competing substrates are present., related to Figure 4.

(A) Prediction for the effect of Axin on pS45-β-catenin phosphorylation when a competing substrate is present, as in main text Figure 4A.

(B) β-catenin phosphorylation rates (V_{obs}) measured at 20 nM GSK3β and 50 nM pS45-β-catenin in the presence and absence of 500 nM miniAxin with no competitor or 1 μM pS133-CREB$_{127\text{-}135}$. Values are mean ± SD for at least 3 measurements. These reactions were performed with *in vitro* phosphorylated pS45-β-catenin (see Figure S8) for comparison with the values obtained with fully-phosphorylated pS45-β-catenin obtained from coexpression with CK1α (main text Figure 4B). In the absence of competitor, Axin produces a 2-fold rate increase. In the presence of CREB competitor, Axin produces a 13-fold rate increase, similar to the 20-fold increase observed with fully-phosphorylated pS45-β-catenin.

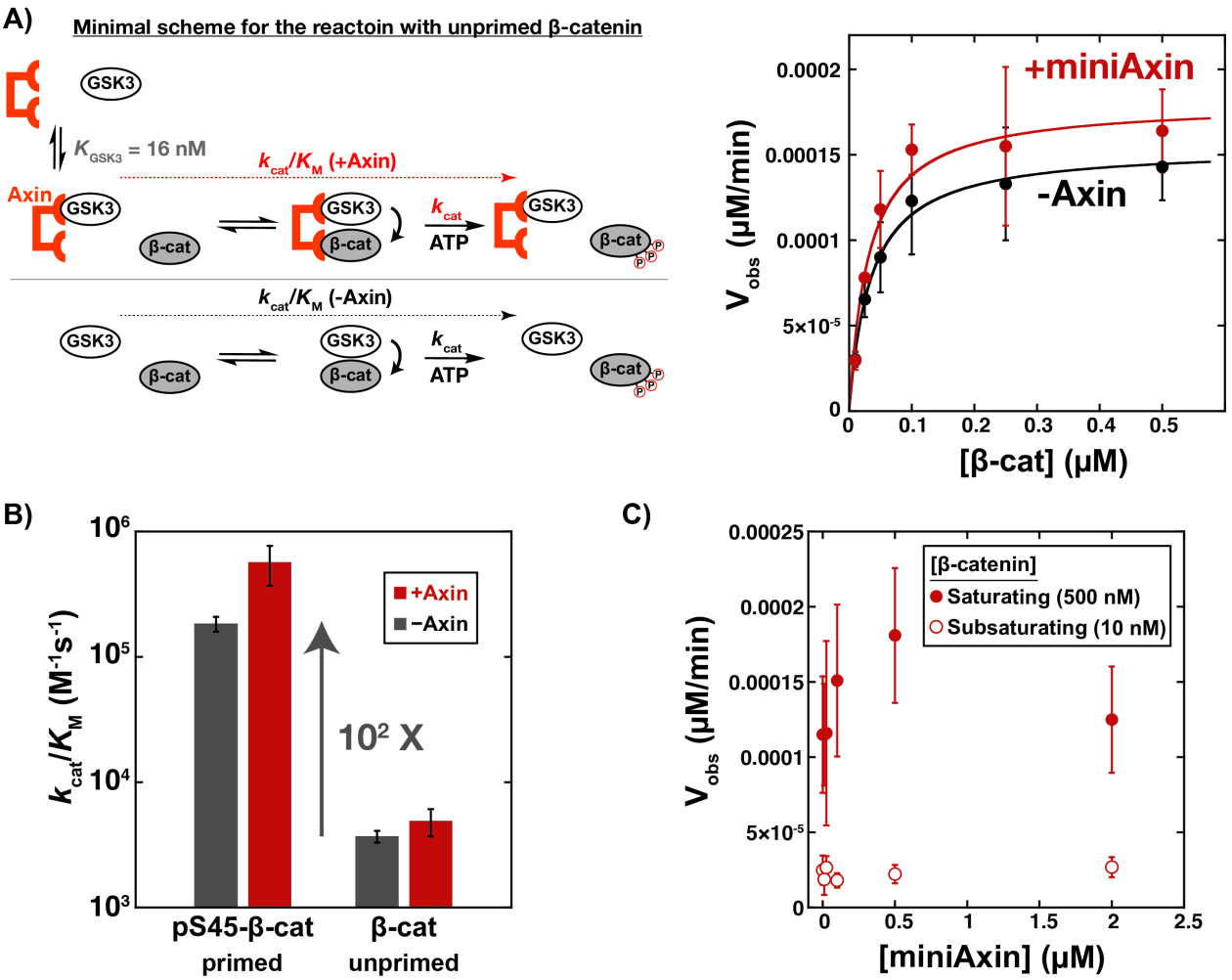

Figure S18. Axin has no significant effect on the reaction of GSK3β with unprimed β-catenin, related to Figure 1.

(A) Michaelis-Menten plot of V_{obs} vs. [β-catenin] at 20 nM GSK3β in the presence and absence of 500 nM miniAxin. See Table S2 for values of fitted kinetic parameters.

(B) Comparison of k_{cat}/K_M values (Table S2) for phosphoprimed and unprimed β-catenin.

(C) Varying the concentration of Axin for the reaction of GSK3β with unprimed β-catenin does not produce significant rate effects. Plot of V_{obs} vs. [miniAxin] at 20 nM GSK3β and 10 nM (subsaturating) or 500 nM (saturating) β-catenin. Error bars are mean ± SD for at least 3 measurements.

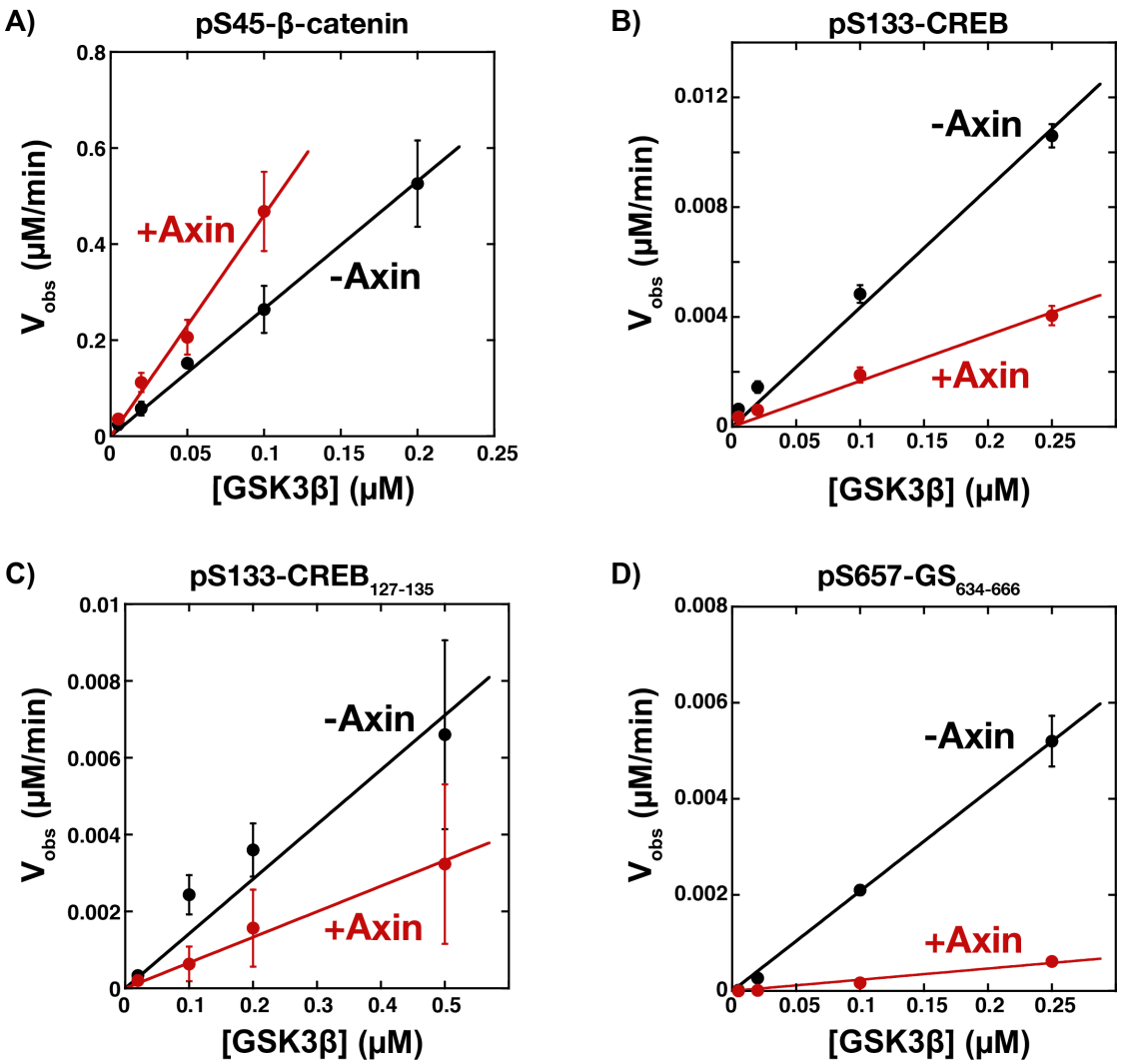

Figure S19. V_{obs} vs. [GSK3β], related to Figure 1 & Figure 3.
V_{obs} for fixed concentrations of substrate with varying concentrations of GSK3β in the presence or absence of Axin.
(A) Plot of V_{obs} vs. [GSK3β] at 1 μM pS45-β-catenin in the presence and absence of 500 nM miniAxin. V_{obs} increases linearly with enzyme concentration, as expected. An accurate initial rate for 0.2 μM GSK3β with Axin could not be measured because the reaction exceeded 40% conversion before two timepoints could be collected.
(B) Plot of V_{obs} vs. [GSK3β] at 500 nM pS133-CREB in the presence and absence of 500 nM miniAxin.
(C) Plot of V_{obs} vs. [GSK3β] at 500 nM pS133-CREB$_{127-135}$ in the presence and absence of 500 nM miniAxin.
(D) Plot of V_{obs} vs. [GSK3β] at 500 nM pS657-GS$_{634-666}$ in the presence and absence of 500 nM miniAxin. Values in (A-D) are mean ± SD for at least 3 measurements.

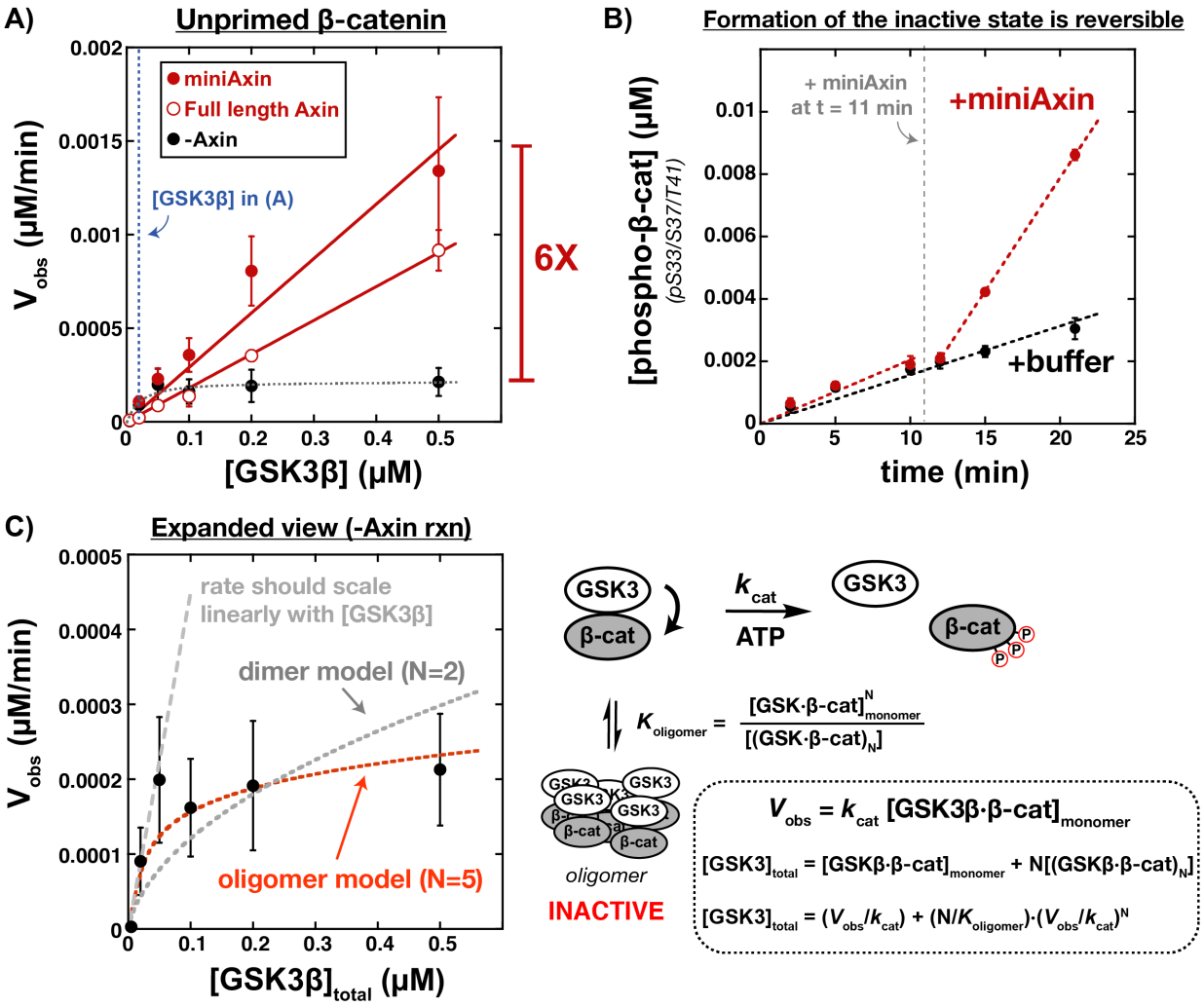

Figure S20. Axin prevents the buildup of an inactive GSK3β•β-catenin complex in the reaction with unprimed β-catenin, related to Figure 1.

(A) Plot of V_{obs} vs. [GSK3β] at 500 nM unprimed β-catenin in the presence and absence of 500 nM miniAxin or full length Axin. V_{obs} for the -Axin reaction does not increase linearly with enzyme concentration, suggesting that an inactive state forms at high [GSK3β].

(B) Formation of the inactive state is reversible. Product vs. time plot for a reaction with 500 nM GSK3β and 500 nM unprimed β-catenin. At t = 11 min, miniAxin was added to a final concentration of 500 nM and the reaction rate sharply increases. A control reaction (+buffer) shows no change in rate.

(C) Expanded view of panel (A) in the absence of Axin with unprimed β-catenin and a kinetic model with an inactive, oligomeric state. The model starts from the saturated GSK3β•β-catenin complex (see Figure S21 for further discussion of this point). In the absence of the inactive state, V_{obs} should increase linearly with [GSK3β]. Fitting the data to a model with an inactive GSK3β•β-catenin dimer (N=2) gives non-linear behavior but still shows substantial deviations from the data. Fitting the data to a model with a higher-order inactive GSK3β•β-catenin oligomer (N=5) gives a reasonable fit. Larger values of N give indistinguishable fits to the data. The N=5 fit is also shown in panel (A). Error bars in (A-C) are mean ± SD for at least 3 measurements.

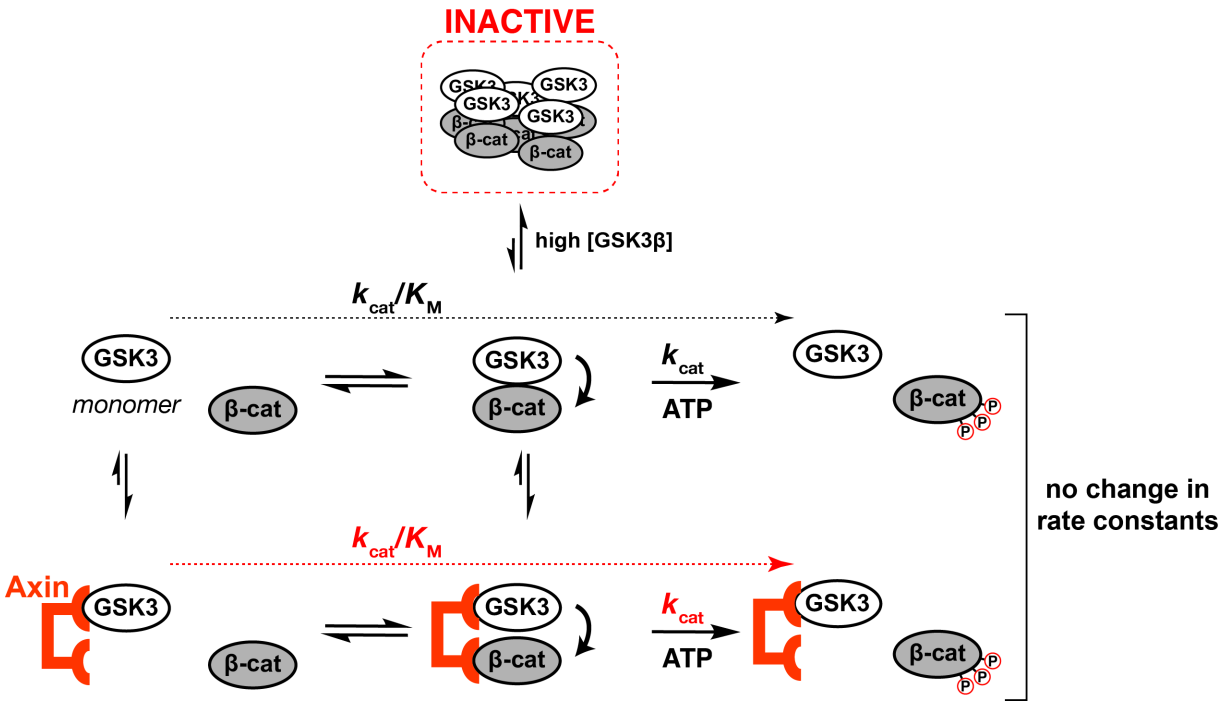

Figure S21. Kinetic model for the effect of Axin at high concentrations of GSK3β in reactions with unprimed β-catenin, related to Figure 1.

The observed Axin-dependent rate enhancement in the reaction of GSK3β with unprimed β-catenin occurs only at high GSK3β concentration and arises because Axin increases active enzyme concentration, not because of a tethering effect between kinase and substrate. At low GSK3β concentrations, Axin has no significant effect on the steady state rate constants for the reaction (Figure S18). At high GSK3β concentrations, we propose that the GSK3β•β-catenin complex cooperatively assembles into an inactive, higher-order oligomer. Axin prevents the formation of this higher-order oligomer, which leads to an increase in observed rates for the reaction of GSK3β with β-catenin (Figure S20). The inactive state includes both GSK3β and unprimed β-catenin; if the inactive state were a dimer or oligomer of GSK3β alone, we would have expected to see a similar inactivation effect in all GSK3β reactions, but this effect is not observed in reactions with pS45-β-catenin, pS133-CREB, pS133-CREB$_{127\text{-}133}$, or pS657-GS$_{634\text{-}666}$ (Figure S19). Thus, the kinetic model does not include a hypothetical inactive oligomer of free GSK3β.

Supplemental Tables

Table S1. Binding constants for Axin interacting with GSK3β and β-catenin, related to Figure 1.[a]

Immobilized Substrate	**Binding Partner**	K_D	k_a ($M^{-1}s^{-1}$)	k_d (s^{-1})
miniAxin	GSK3β	16 ± 0.2 nM	$(1.7 \pm 0.009) \times 10^4$	$(2.7 \pm 0.02) \times 10^{-4}$
Axin (full length)	GSK3β	7.5 ± 0.09 nM	$(2.7 \pm 0.01) \times 10^4$	$(2.0 \pm 0.02) \times 10^{-4}$
AxinΔBCD	GSK3β	11 ± 0.2 nM	$(1.9 \pm 0.01) \times 10^4$	$(2.1 \pm 0.03) \times 10^{-4}$
pS45-β-catenin	miniAxin	4.0 ± 0.05 μM	$(7.7 \pm 0.08) \times 10^3$	$(3.1 \pm 0.009) \times 10^{-2}$

[a] Binding constants were determined using bio-layer interferometry as described in the Methods. See Figure S2. Standard errors are from global fits to the bio-layer interferometry traces. All fits had χ^2 values < 1 and R^2 values > 0.98.

Table S2. Kinetic parameters for GSK3β reactions, related to Figures 1-3.[a]

Substrate	**Reaction**	k_{cat} (s^{-1})	K_M (μM)	k_{cat}/K_M ($M^{-1}s^{-1}$)
pS45-β-catenin	–Axin	$(5.4 \pm 0.2) \times 10^{-2}$	0.29 ± 0.04	$(1.8 \pm 0.2) \times 10^5$
	+miniAxin	$(7.9 \pm 0.6) \times 10^{-2}$	0.14 ± 0.05	$(5.7 \pm 1.7) \times 10^5$
	+miniAxin-4A	$(7.4 \pm 0.4) \times 10^{-2}$	0.30 ± 0.06	$(2.4 \pm 0.4) \times 10^5$
	+full length Axin	$(7.9 \pm 0.1) \times 10^{-2}$	0.26 ± 0.01	$(3.0 \pm 0.1) \times 10^5$
	+AxinΔBCD	n.d.	n.d. (≥1 μM)	$(3.4 \pm 0.1) \times 10^4$
β-catenin	–Axin	$(1.3 \pm 0.04) \times 10^{-4}$	0.034 ± 0.004	$(3.7 \pm 0.3) \times 10^3$
	+miniAxin	$(1.5 \pm 0.09) \times 10^{-4}$	0.031 ± 0.007	$(4.9 \pm 0.9) \times 10^3$
pS133-CREB	–Axin	$(2.5 \pm 0.3) \times 10^{-3}$	0.28 ± 0.09	$(9.0 \pm 2.0) \times 10^3$
	+miniAxin	n.d.	n.d. (≥1 μM)	$(6.8 \pm 0.3) \times 10^2$
pS133-$CREB_{127-135}$	–Axin	$(1.3 \pm 0.2) \times 10^{-3}$	0.18 ± 0.02	$(7.0 \pm 0.6) \times 10^3$
	+miniAxin	n.d.	n.d. (≥1 μM)	$(3.1 \pm 0.1) \times 10^2$
pS657-$GS_{634-666}$	–Axin	$(2.4 \pm 0.4) \times 10^{-4}$	0.38 ± 0.14	$(5.2 \pm 1.1) \times 10^2$
	+miniAxin	n.d.	n.d. (≥1 μM)	11 ± 0.4

[a] See Figures 1, 2, 3, & S11 for data and the Methods section for the kinetic model used to fit the data to obtain observed values of k_{cat}, K_M, and k_{cat}/K_M. Standard errors are from non-linear least squares fits to the initial rate data as described in the Methods. The CREB and GS reactions in the presence of Axin did not detectably saturate up to 1 μM substrate (Figure 3), and only the values of k_{cat}/K_M could be accurately determined. Similarly, the pS45-β-catenin reaction in the presence of AxinΔBCD did not fully saturate (Figure 2). Partial saturation was observed at 3 μM pS45-β-catenin, suggesting a conservative limit of $K_M \geq 1$ μM.

Table S3. Observed kinetic parameters for the GSK3β reaction with pS45-β-catenin, related to Figure 1.[a]

Substrate	Reaction	k_{cat} (s^{-1})	K_M (μM)	k_{cat}/K_M ($M^{-1}s^{-1}$)
pS45-β-catenin	–Axin	$(1.2 \pm 0.04) \times 10^{-2}$	0.77 ± 0.07	$(1.6 \pm 0.2) \times 10^{4}$
	+miniAxin	$(2.5 \pm 0.12) \times 10^{-2}$	0.71 ± 0.1	$(3.5 \pm 0.5) \times 10^{4}$

[a] The values shown in this table are for pS45-β-catenin prepared by *in vitro* phosphorylation with CK1α (Figure S8); see Table S2 for kinetic parameters obtained with pS45-β-catenin obtained by coexpression with CK1α. Standard errors for k_{cat} and K_M are from non-linear least squares fits to the initial rate data. The error for k_{cat}/K_M is propagated from the individual k_{cat} and K_M values.

In vitro prepped pS45-β-catenin is not phosphorylated to completion at S45; we estimate that the *in vitro* CK1α reaction goes to ~40% completion (Figure S1C). The presence of significant quantities of unprimed β-catenin will affect the observed values of the steady state parameters because unprimed β-catenin can compete for GSK3β with a K_M ~30 nM (in the presence or absence of Axin). This relatively low K_M value means that significant quantities of GSK3β will be occupied by unprimed β-catenin at all concentrations of pS45-β-catenin (because increasing [pS45-β-catenin] will also increase unprimed [β-catenin]). This effect will result in a decrease in the observed k_{cat} and an increase the observed K_M relative to a reaction with 100% pure pS45-β-catenin. Nevertheless, the relative values of the observed rate constants in the presence or absence of Axin should not be affected by the presence of unprimed β-catenin.

Table S4. Estimated cellular concentrations for Wnt pathway proteins, related to Box 1.[a]

	HeLa cells	Colon cells
GSK3β	9.5 nM	64 nM
β-catenin	22 nM	719 nM
Axin	1.3 nM	1.3 nM

[a] Cellular concentrations can be estimated using the number of molecules per cell, obtained from mass spectrometry data, and a cell volume from microscopy data (Itzhak et al., 2016). HeLa cell protein concentrations were calculated from protein abundance values (Nagaraj et al., 2011) and a cell volume of 2425 μm^3 (BNID 103725 (Milo et al., 2010)). Colon cell protein concentrations were calculated from abundances obtained from human tissue samples (D. Wang et al., 2019) and a cell volume of 1400 μm^3 (BNID 111216 (Wisniewski et al., 2012)).

Table S5. Protein expression plasmids, related to STAR Methods.

Plasmid	Protein[a]	Expressed Protein	Vector[b]	Source
pES001	GSK3β	MBP-GSK3β-HA-His	pMBP-MG	*This study*
pMG033	GSK3β	GST-GSK3β-HA-His	pETARA	*This study*
pEF073	Axin	MBP-Axin-His	pMBP-MG	*This study*
pMG023	$Axin_{384-518}$ (miniAxin)	MBP-$Axin_{384-518}$-His	pMBP-MG	*This study*
pMG031	$Axin_{384-518}$ T481A/S486A/S493A/S496A	MBP-$Axin_{384-518}$ T481A/S486A/S493A/S496A-His	pMBP-MG	*This study*
pMG035	$Axin_{\Delta 465-518}$ (AxinΔBCD)	MBP-$Axin_{\Delta 465-518}$-His	pMBP-MG	*This study*
pEF019	β-catenin	MBP-β-catenin-His	pMBP-MG	*This study*
pMG050	β-catenin S45A	MBP-β-catenin S45A-His	pMBP-MG	*This study*
pMG047	β-catenin S33A	MBP-β-catenin S33A-His	pMBP-MG	*This study*
pMG057	β-catenin S33A/S37A	MBP-β-catenin S33A/S37A-His	pMBP-MG	*This study*
pMG061	β-catenin S33A/S37A/T41A	MBP-β-catenin S33A/S37A/T41A-His	pMBP-MG	*This study*
pMG062	β-catenin S33A/S37A/T41A/S45A	MBP-β-catenin S33A/S37A/T41A/S45A-His	pMBP-MG	*This study*
pMG051[c]	β-catenin CK1α	MBP-β-catenin-His GST-CK1α	pMBP-MG	*This study*
pMG063	β-catenin S45A CK1α	MBP-β-catenin S45A-His GST-CK1α	pMBP-MG	*This study*
pMG064	β-catenin S33A CK1α	MBP-β-catenin S33A-His GST-CK1α	pMBP-MG	*This study*
pMG065	β-catenin S33A/S37A CK1α	MBP-β-catenin S33A/S37A-His GST-CK1α	pMBP-MG	*This study*
pMG066	β-catenin S33A/S37A/T41A CK1α	MBP-β-catenin S33A/S37A/T41A-His GST-CK1α	pMBP-MG	*This study*
pMG067	β-catenin S33A/S37A/T41A/S45A CK1α	MBP-β-catenin S33A/S37A/ T41A/S45A-His GST-CK1α	pMBP-MG	*This study*
pMG046	CK1α	GST-CK1α-His	pETARA	*This study*
pEF086	CREB (127-135)	MBP-$CREB_{127-135}$-His	pMBP-MG	*This study*
pEF087	CREB (127-135) S133A	MBP-$CREB_{127-135}$(S133A)-His	pMBP-MG	*This study*
pMG059	CREB	MBP-CREB-His	pMBP-MG	*This study*
pMG058	Glycogen Synthase (634-666)	MBP-$GS_{634-666}$-His	pMBP-MG	*This study*
H_6-rC	PKA catalytic subunit	His-PKA-rC	pET15b	Addgene #14921
pES010	Kemptide	MBP-Kemptide-His	pMBP-MG	(Speltz and Zalatan, 2020)
YopH	YopH	YopH (untagged)	pCDFDuet	(Seeliger et al., 2005)
pJZ101	MBP	MBP-His	pMBP-MG	*This study*
pJZ102	GST	GST-His	pETARA	*This study*

[a] All proteins are human sequences except PKA, which is the mouse sequence.

[b] pMBP-MG is a modified version of pMAL-p2X (New England Biolabs) with an N-terminal TEV-cleavable MBP tag and a C-terminal His6 tag. pETARA contains an N-terminal TEV-cleavable GST tag and a C-terminal His6 tag. pMBP-MG and pETARA were described previously (Good et al., 2009).

[c] pMG051 was constructed by inserting the GST-CK1α expression cassette (without the His tag) from pMG046 into the pEF019 backbone. B-catenin mutants (pMG063-67) were cloned into this dual expression cassette.

Chapter 3

The Axin scaffold protects the kinase GSK3β from cross-pathway inhibition

Maire Gavagan[1] and Jesse G. Zalatan[1]

[1]Department of Chemistry, University of Washington, Seattle, WA 98195, USA

3.1 Abstract

Multiple signaling pathways regulate the kinase GSK3β by inhibitory phosphorylation at Ser9, which then occupies the priming pocket and is thought to block substrate binding. Since this mechanism should affect GSK3β activity towards all of its primed substrates, it is unclear why Ser9 phosphorylation does not affect other signaling outputs downstream of GSK3β, such as Wnt signaling. To test models for how GSK3β in the Wnt pathway is insulated from potential cross-activation by other signals, we evaluated the role of the Wnt-specific scaffold protein Axin in multiple reaction steps. Using an *in vitro* reconstituted system, we found that Axin protects GSK3β from phosphorylation at Ser9 by upstream kinases, which could prevent accumulation of pS9-GSK3β in the Axin-GSK3β complex. Scaffold proteins that protect bound proteins from reactions with other signaling molecules could provide a general mechanism to insulate signaling pathways from improper crosstalk.

3.2 Introduction

Glycogen Synthase Kinase 3β (GSK3β) is a ubiquitously expressed and evolutionarily conserved kinase with important roles in multiple signaling pathways. GSK3β acts on a wide range of substrates in different pathways with downstream effects ranging from cell growth and differentiation to metabolism to apoptosis. GSK3β has also been implicated in a wide variety of diseases and disorders, including schizophrenia, bipolar disorder, type 2 diabetes, Alzheimer's, cancer, and others (Nusse and Clevers, 2017; Beurel et al., 2015). Despite strong interest in therapies targeting GSK3β for these diseases, these efforts have been complicated by the difficulty of targeting only one of the cellular processes regulated by GSK3β (Bhat et al., 2018). Understanding how the cellular pool of GSK3β is regulated by multiple signaling pathways is a critical first step towards developing strategies to target distinct sub-populations of GSK3β.

GSK3β plays a key role in the Wnt pathway, a signaling pathway that regulates development and stem cell growth (Nusse and Clevers, 2017). Dysregulated Wnt signaling has been linked to several types of cancer, including acting as the primary driver of tumorigenesis in colorectal cancer (Zhan et al., 2017). In Wnt signaling, the scaffold protein Axin binds and assembles GSK3β, its substrate β-catenin, and other Wnt pathway proteins in a Wnt-specific protein complex called the destruction complex. In this complex, the kinases CK1α and GSK3β sequentially phosphorylate β-catenin, marking it for degradation. Wnt signals inhibit these kinase reactions, allowing β-catenin to accumulate and activate transcription of Wnt target genes (Kimelman and Xu, 2006; MacDonald et al., 2009; Moon et al., 2004; Nusse and Clevers, 2017; Polakis, 2000; Stamos and Weis, 2013, Hernández et al., 2012) (Figure 1A). Axin has been proposed to serve as a control point in Wnt signaling, promoting β-catenin phosphorylation in

the Wnt off state and coordinating the deactivation of β-catenin phosphorylation in response to Wnt signals (Kimelman and Xu, 2006; Nusse and Clevers, 2017).

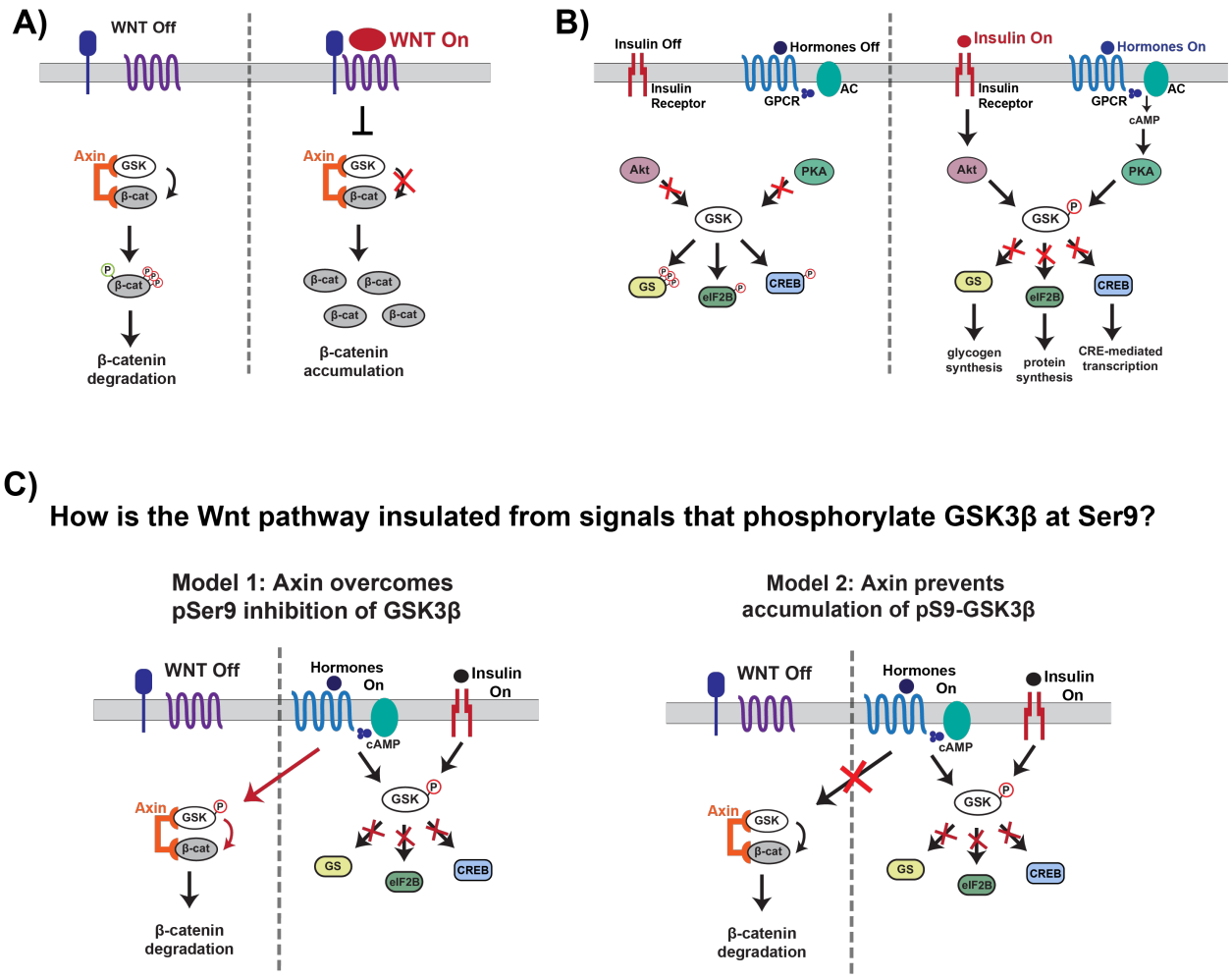

Figure 3.1. Wnt signaling is insulated from signals that phosphorylate GSK3β at Ser9
A) In the Wnt pathway, the scaffold protein Axin coordinates a GSK3β complex that phosphorylates β-catenin, which is then degraded. When a Wnt signal arrives, this machinery is disabled, and β-catenin levels rise and initiate a transcriptional program. B) In other signaling pathways, upstream signals regulate GSK3β through phosphorylation at Ser9 which blocks substrate binding, inhibiting its activity towards downstream substrates, and activates downstream signaling. C) The scaffold protein Axin may insulate Wnt-associated GSK3β from Ser9 inhibition by restoring β-catenin binding to pS9-GSK3β (Model 1) or by preventing accumulation of pS9-GSK3β in the Wnt destruction complex (Model 2).

Despite sharing the same central kinase, Wnt signals do not activate other GSK3β-dependent pathways and vice versa (Ding et al., 2000; McManus et al., 2005; Ng et al., 2009). Our previous work demonstrated that Axin increases the specificity of GSK3β specificity towards β-catenin

(Gavagan et al., 2020), which supports the idea that Wnt signals could regulate Axin to inhibit Wnt-associated GSK3β without affecting GSK3β reactions in other pathways (Beurel et al., 2015). Activation of the Wnt pathway does not lead to GSK3β phosphorylation at Ser9 (Tejeda-Muñoz et al., 2016, Ding et al., 2000; McManus et al., 2005), consistent with the idea that Wnt signals instead regulate the Wnt-specific destruction complex.

The molecular mechanism that prevents crosstalk from other GSK3β-dependent pathways into the Wnt pathway is less clear. In response to growth factors and hormones such as insulin, the kinases PKA and PKB/Akt phosphorylate GSK3β at Ser9 (Sutherland et al., 1993; Cross et al., 1995; Fang et al., 2000). The phosphorylated N-terminus is thought to inhibit GSK3β by acting as a pseudosubstrate, binding in the priming pocket and blocking substrate binding (Frame et al., 2001; Dajani et al., 2001; Stamos et al., 2014; ter Haar et al., 2001) (Figure 1B). Although we might expect that phosphorylation of Ser9 would lead to widespread inhibition of GSK3β activity, *in vivo* experiments demonstrate that insulin and growth factor signals do not activate the Wnt pathway (Ng et al., 2009; Ding et al., 2000). Thus, there must be mechanisms in cells that prevent Wnt pathway activation when pS9-GSK3β accumulates in cells.

Previous work in the field suggests two potential mechanisms that could insulate the Wnt pathway from insulin and growth factor signals. First, by tethering GSK3β and its substrates together, the Axin scaffold could overcome the inhibitory effects of Ser9 phosphorylation. Early work in the field suggested that Axin-mediated tethering could overcome the phosphopriming requirement for GSK3β substrates (Frame et al., 2001). A similar mechanism could allow pS9-GSK3β to efficiently react with Axin-tethered β-catenin even if the GSK3β priming pocket is blocked (Beurel et al., 2015) (Figure 1C). However, the model that Axin overcomes

phosphopriming requirements was initially proposed before β-catenin was found to also require phosphopriming (Liu et al., 2002), and our subsequent work confirmed that the Axin-mediated GSK3β reaction is far slower with unprimed β-catenin than with phosphoprimed pS45-β-catenin (Gavagan et al., 2020). Thus, there is no strong evidence supporting the model that Axin can overcome the GSK3β phosphopriming requirement. However, the effect of Axin on pS9-GSK3β activity has not been directly tested.

A second possible mechanism for Wnt pathway insulation is that the Axin scaffold prevents accumulation of pS9-GSK3β in the destruction complex (Figure 1C). This model is supported by *in vivo* experiments showing that in insulin-treated cells, Ser9 phosphorylation increases in the total GSK3β population but is unchanged in the Axin-associated GSK3β pool (Ding et al., 2000; Ng et al., 2009). Most simply, this effect could arise if Axin-bound GSK3β is inaccessible to the kinases that phosphorylated Ser9. More complex mechanisms involving Axin-associated phosphatases could also act to prevent pS9-GSK3β accumulation in the destruction complex.

To distinguish between these possible models, we have quantitatively evaluated the effect of Axin on pS9-GSK3β formation and activity in a minimal, *in vitro* reconstituted biochemical system. We find that in the presence of Axin, pS9-GSK3β activity towards β-catenin remains significantly impaired compared to unphosphorylated GSK3β, suggesting that Axin does not overcome GSK3β substrate priming requirements. Instead, we observe that Axin protects GSK3β from phosphorylation at Ser9 by upstream kinases, which provides biochemical evidence supporting the idea that scaffold proteins can shield bound proteins from reactions with other signaling enzymes.

3.3 Results

Biochemical Reconstitution of GSK3β reactions

To test models for how GSK3β activity is regulated, we biochemically reconstituted a minimal reaction system with the kinase GSK3β, the substrate pS45-β-catenin, and the Axin scaffold. We purified maltose binding protein (MBP) fusions of β-catenin and full length Axin as described previously (Gavagan et al., 2020). MBP-GSK3β expressed in *E. coli* is partially phosphorylated on Ser9. To obtain GSK3β in well-defined phosphorylation states, we first co-expressed GSK3β with lambda phosphatase (λPP), a serine/threonine phosphatase. The purified GSK3β from this co-expression system is fully dephosphorylated at Ser9 and remains phosphorylated at the activating site Tyr216 (Gavagan et al., 2020). The observed value of k_{cat}/K_M for GSK3β without λPP treatment is ~5-fold lower than the λPP-treated GSK3β (Table 1 & Gavagan et al., 2020).

To produce pS9-GSK3β, we incubated GSK3β with PKA, which phosphorylates GSK3β to completion at Ser9. We used affinity chromatography with amylose resin to separate MBP-tagged GSK3β from PKA (see Methods). We also expressed and purified GSK3β_S9A, which cannot be phosphorylated on Ser9, in both λPP-treated and PKA-treated forms. This mutant will allow us to distinguish effects specific to Ser9 phosphorylation from any effects that might arise from non-specific λPP-dephosphorylation or PKA phosphorylation at other GSK3β residues.

Phosphorylation at Ser9 inhibits GSK3β with a large increase in K_M

It is well established that Ser9 phosphorylation inhibits GSK3β activity, but quantitative measurements of the inhibitory effect are limited and variable (Sutherland et al., 1993; Stambolic et al., 1994; Frame et al., 2001). To evaluate how GSK3β is affected by Ser9 phosphorylation, we measured initial rates for the reaction of GSK3β with pS45-β-catenin using a quantitative western blot assay. The initial rates were used to determine the steady state Michaelis-Menten kinetic parameters k_{cat}, K_M, and k_{cat}/K_M as described previously (Gavagan et al., 2020). Using this system, we found that phosphorylation of GSK3β at Ser9 strongly inhibits its activity towards pS45-β-catenin, with a ~200-fold decrease in k_{cat}/K_M compared with non-phosphorylated or mutant S9A GSK3β (Figure 2B & Table 1). The observed rates for non-phosphorylated GSK3β and PKA-treated GSK3β_S9A are indistinguishable, indicating that the large rate decrease in pS9-GSK3β is from phosphorylation specifically at Ser9, not any other unknown PKA phosphosites.

The observed rates for the pSer9-GSK3β reaction increase linearly with pS45-β-catenin concentration with no detectable saturation up to 2 μM substrate (Figure 2B). We can estimate a conservative limit that $K_M \geq 2$ μM, which is >7-fold larger than the K_M of 0.28 μM for both non-phosphorylated GSK3β and mutant GSK3β_S9A. This K_M increase is consistent with the model that phosphorylation of Ser9 inhibits GSK3β by interfering with substrate binding, although we cannot rule out the possibility that pS9 inhibition also produces k_{cat} effects.

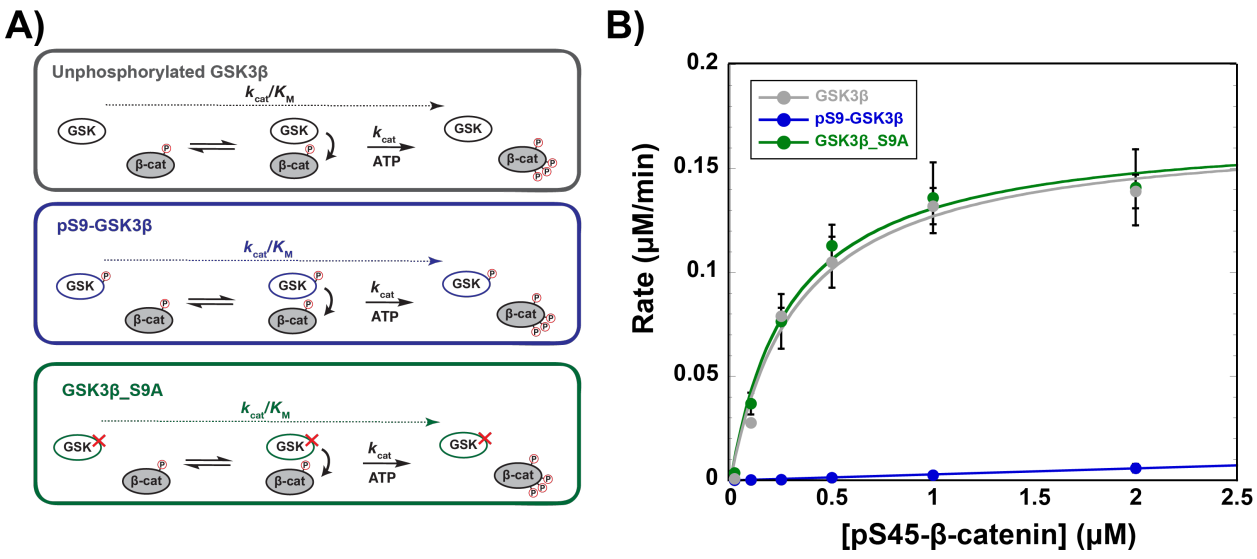

Figure 3.2. Phosphorylation at Ser9 inhibits GSK3β activity towards pS45-β-catenin
A) Minimal kinetic scheme for the reaction of non-phosphorylated GSK3β, pS9-GSK3β, and GSK3β_S9A with pS45-β-catenin. GSK3β phosphorylates pS45-β-catenin at three sites: S33, S37, and T41. B) Michaelis-Menten plot of V_{obs} versus [pS45-β-catenin] at 10 nM non-phosphorylated GSK3β, pS9-GSK3β, and GSK3β_S9A. Values are mean ± SD for at least 3 measurements. See Table 1 for values of fitted kinetic parameters. The pS9-GSK3β reaction does not detectably saturate at high [pS45-β-catenin], which means that only the value of k_{cat}/K_M can be accurately determined. We can estimate a conservative limit that $K_M \geq 2$ μM, substantially higher than the K_M for non-phosphorylated GSK3β and GSK3β_S9A.

The scaffold protein Axin cannot overcome pS9-GSK3β inhibition

To test the model that Axin-mediated tethering overcomes pS9 inhibition of the GSK3β phosphopriming site, we measured reaction rates for pS9-GSK3β, non-phosphorylated GSK3β, or PKA-treated GSK3β_S9A with pS45-β-catenin in the presence and absence of Axin. These reactions were performed at Axin concentrations where all of the GSK3β is bound to Axin, which allows direct comparisons of rate constants for GSK3β and Axin-GSK3β reactions (Gavagan et al., 2020). Addition of Axin to reactions with non-phosphorylated GSK3β and PKA-treated GSK3β_S9A produced modest ~2-fold increases in k_{cat}/K_M arising from small

changes to both the k_{cat} and the K_M, consistent with previous results (Gavagan et al., 2020). Axin produced a

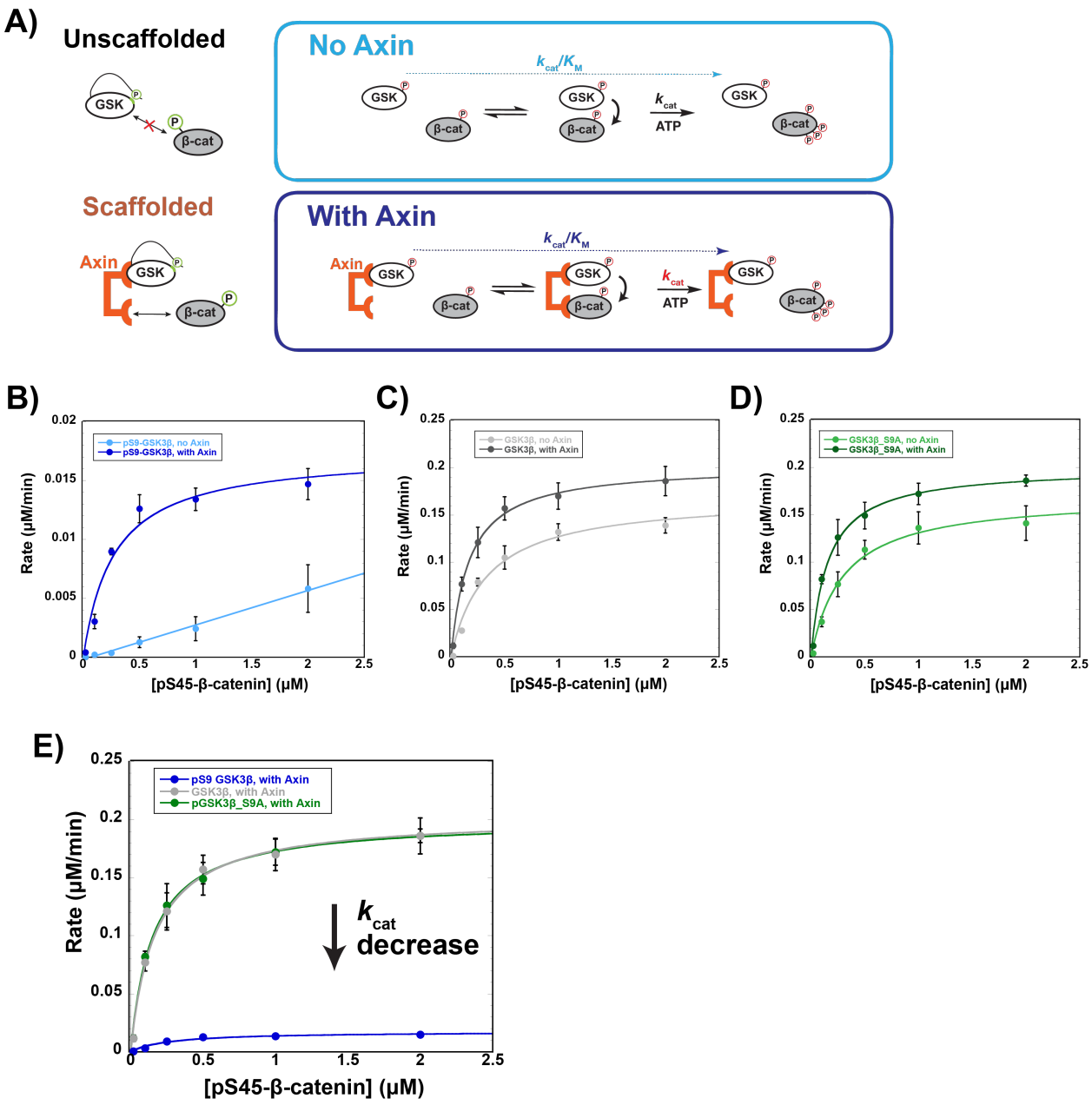

Figure 3.3. Axin restores the K_M for β-catenin but cannot overcome pS9-GSK3β inactivation
A) Minimal kinetic scheme for the reaction of pS9-GSK3β with pS45-β-catenin in the presence and absence of Axin. At the Axin concentrations used in these experiments all the GSK3β is bound to Axin (Gavagan et al., 2020). B-D) Michaelis-Menten plots of V_{obs} versus [pS45-β-catenin] in the presence and absence of 500 nM Axin with 10 nM pS9-GSK3β (B), non-phosphorylated GSK3β (C) or GSK3β_S9A (D). E) Michaelis-Menten plots of V_{obs} versus [pS45-β-catenin] in the presence of Axin with pS9-GSK3β,

non-phosphorylated GSK3β and GSK3β_S9A are plotted together as in Figure 2B. Although Axin fully rescues the K_M effect from Ser9 phosphorylation, there is still a substantial ~10-fold k_{cat} decrease in the pS9-GSK3β reaction compared to non-phosphorylated GSK3β and GSK3β_S9A. Values are mean ± SD for at least 3 measurements. See Table 1 for values of fitted kinetic parameters.

much larger ~20-fold k_{cat}/K_M increase in the pS9-GSK3β reaction. Notably, this k_{cat}/K_M increase is primarily due to rescue of the K_M. Addition of Axin results in a decrease in the observed K_M to 0.27 μM, similar to the K_M values for non-phosphorylated GSK3β and GSK3β_S9A. This result suggests that Axin can compensate for the inhibitory effect of pS9-GSK3β on substrate binding, possibly because the Axin binding site for β-catenin allows formation of an Axin•GSK3β•β-catenin ternary complex even when the GSK3β priming pocket is blocked.

Although Axin appears to fully rescue the K_M effect from Ser9 phosphorylation, there is still a substantial ~10-fold k_{cat} decrease in the pS9-GSK3β reaction compared to non-phosphorylated GSK3β. Thus, despite apparently rescuing substrate binding, Axin cannot fully restore pS45-β-catenin phosphorylation rates. The simplest interpretation of this result is that Axin assembles a non-productive pS9-GSK3β•β-catenin complex that is still inhibited by pSer9 occupying the priming pocket.

The large k_{cat} effect suggests that pS9 inhibition of GSK3β may be more mechanistically complex than previously thought. The available crystal structures of Axin-bound pS9-GSK3β do not provide a clear explanation for this behavior (Stamos et al., 2014). One possibility is that although Axin restores pS45-β-catenin binding to pS9-GSK3β, it results in a distinct binding mode/substrate confirmation that has slower turnover. Another possibility is that binding of primed substrates in the priming pocket affects the catalytic step in addition to the K_M. Substrate docking sites have been shown to play dual roles, both controlling substrate binding and specificity and allosterically modulating kinase activity (Schulze et al., 2016).

Although Axin produces large rate increases in the pS9-GSK3β reaction, there is still a large, >10-fold k_{cat} decrease, and corresponding >10-fold rate decrease across all pS45-β-catenin concentrations when GSK3β is phosphorylated (Figure 3 & Table 1). This rate drop is likely sufficient to activate Wnt outputs since stimulation with high levels of Wnt ligand can produce ~5-fold decreases in GSK3β phosphorylation of β-catenin, with corresponding ~5-10-fold increases in total β-catenin levels (Hernández et al., 2012; Hannoush, 2008). *In vivo* changes in β-catenin levels as low as 2-fold can have measurable effects on transcription of Wnt output genes (Jacobsen et al., 2016). Thus, if pS9-GSK3β accumulates in the Axin-mediated destruction complex, inhibition of β-catenin phosphorylation and improper activation of the Wnt pathway is likely to occur.

Axin prevents accumulation of pS9-GSK3β in the destruction complex

To test the model that Axin prevents upstream kinases from phosphorylating GSK3β, we evaluated the effect of Axin on the PKA-mediated phosphorylation of GSK3β at Ser9. We recombinantly purified the kinase PKA and performed *in vitro* reactions with non-phosphorylated GSK3β, both with and without Axin. We measured initial rates for pS9-GSK3β formation through quantitative western blotting using an antibody that recognizes pS9-GSK3β and determined Michaelis-Menten kinetic parameters, as before. We found that adding Axin to the reaction produced a 7-fold drop in the k_{cat}/K_M for PKA mediated phosphorylation of GSK3β. The 7-fold drop in k_{cat}/K_M is primarily a K_M effect, with a 4-fold increase in K_M when Axin is present. This K_M increase indicates that Axin interferes with formation of the PKA-GSK3β enzyme substrate complex, consistent with Axin blocking access to the N-terminus of GSK3β.

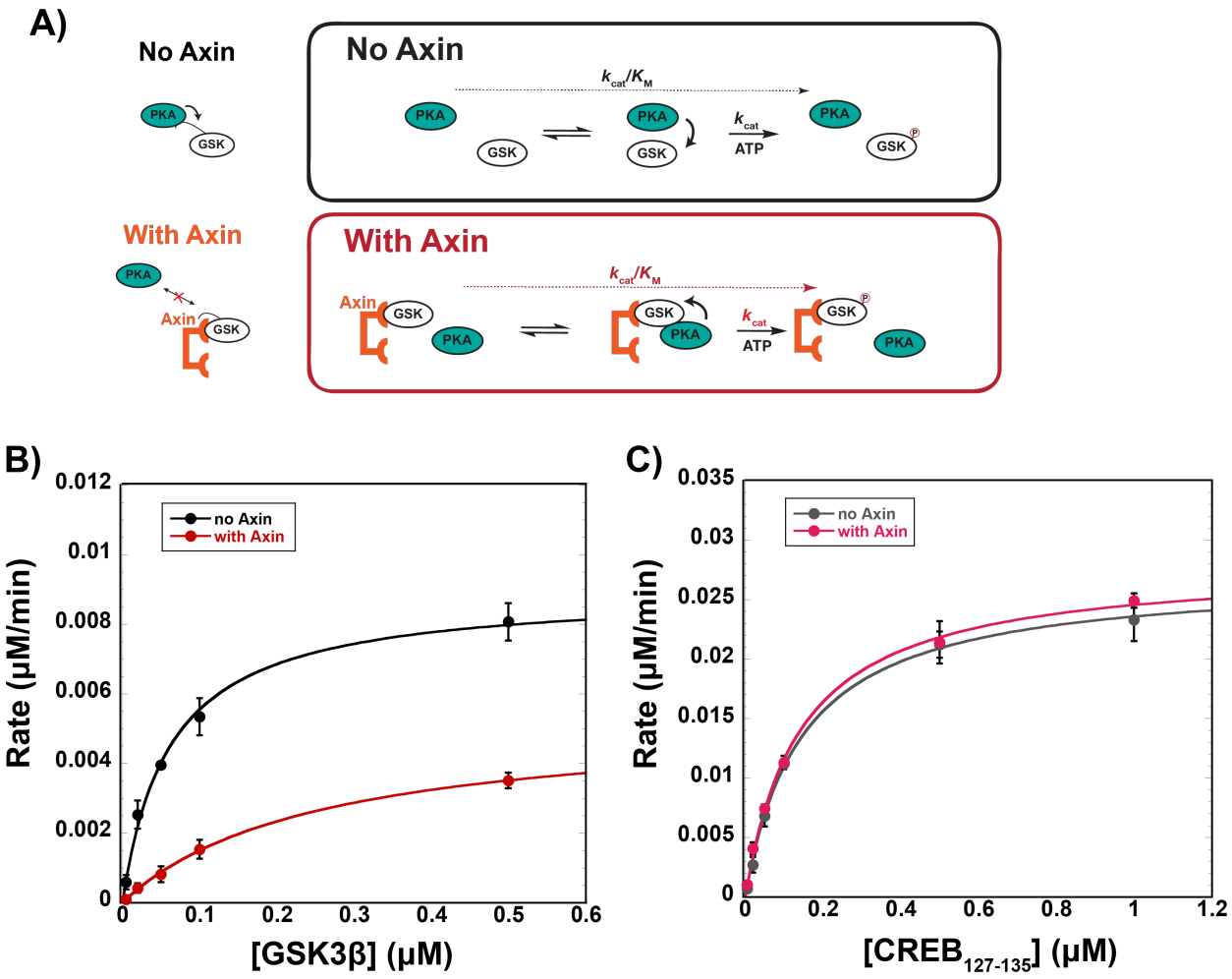

Figure 3.4. Axin prevents phosphorylation of GSK3β at Ser9
A) Minimal kinetic scheme for the reaction of PKA with pS9-GSK3β in the presence and absence of Axin. At the Axin concentrations used in these experiments all the GSK3β is bound to Axin (Gavagan et al., 2020). B) Michaelis-Menten plots of V_{obs} versus [GSK3β] with 20 nM PKA in the presence and absence of 500 nM Axin. Axin produces a 7-fold drop in the k_{cat}/K_M for PKA mediated phosphorylation of GSK3β. C) Michaelis-Menten plots of V_{obs} versus [CREB$_{127-135}$] with 20 nM PKA in the presence and absence of 500 nM Axin. Axin does not decrease PKA activity towards CREB$_{127-135}$, suggesting that the Axin•GSK3β interaction is responsible for the decrease in PKA phosphorylation of GSK3β at Ser9. Values are mean ± SD for at least 3 measurements. See Table 1 for values of fitted kinetic parameters.

An alternative explanation for the observed k_{cat}/K_M decrease is that Axin is also a substrate for PKA, and simply acts as a non-specific competitive inhibitor of the *in vitro* GSK3β phosphorylation reaction. If this model is correct, then the Axin-mediated k_{cat}/K_M decrease would

not arise specifically from the interaction between Axin and GSK3β, but would instead occur for any PKA substrate, To test this possibility, we recombinantly purified the PKA substrate CREB as a short MBP fusion peptide (MBP-$CREB_{127-135}$). CREB is phosphorylated by PKA at Ser133 (Fiol et al., 1994; Naqvi et al., 2014; Gavagan et al., 2020). When we add Axin to the PKA phosphorylation of $CREB_{127-135}$ we see no change in observed rates or in the value of k_{cat}/K_M. This result indicates that Axin is not a competitive inhibitor of PKA at the concentrations used in our assays and that the Axin•GSK3β interaction is responsible for the decrease in PKA phosphorylation of GSK3β at Ser9. This decrease in pSer9 phosphorylation of GSK3β is consistent with literature reports that the Axin-bound pool of GSK3β does not become phosphorylated at Ser9 *in vivo* (Ng et al., 2009; Ding et al, 2000).

3.4 Discussion

To understand how the scaffold protein Axin insulates Wnt signaling from GSK3β phosphoregulation associated with other signaling pathways, we biochemically reconstituted pathway reactions in a minimal, *in vitro* reconstituted biochemical system. We evaluated how Axin affects two distinct reaction steps: the activity of pSer9-GSK3β towards downstream substrates and the activity of upstream kinases that inhibit GSK3β. We observed that S9 phosphorylation has large, detrimental effects on GSK3β activity and while Axin can rescue the K_M for pS45-β-catenin, the observed k_{cat} remains impaired (Figure 2 & Table 1). Even when bound to Axin, GSK3β phosphorylation at Ser9 produces ~10-fold rate decreases which are likely sufficient to activate Wnt outputs (Hernández et al., 2012; Hannoush, 2008; Jacobsen et

al., 2016). Thus, if pSer9-GSK3β is present in the Wnt-associated Axin-GSK3β complex, then activity towards downstream substrates will be impaired, which would improperly activate the Wnt pathway. Instead, we found that Axin protects GSK3β from phosphorylation at Ser9 by upstream kinases. Adding Axin produced a 7-fold drop in the k_{cat}/K_M of PKA-mediated phosphorylation of GSK3β. This decrease in pS9 phosphorylation of GSK3β is consistent with literature reports that the Axin-bound pool of GSK3β does not become phosphorylated at Ser9 *in vivo* (Ng et al., 2009; Ding et al, 2000) and suggests that scaffold proteins can insulate signaling pathways by protecting bound kinases from negative regulators associated with other pathways (Perlson et al., 2006; Greenwald et al., 2014; Su et al., 2016).

The Axin-mediated drop in k_{cat}/K_M for the PKA-reaction with GSK3β at Ser9 is primarily due to a 4-fold increase in K_M. There are several plausible models for how Axin might disrupt the PKA interaction with the N-terminus of GSK3β. The simplest model is that Axin sterically occludes upstream kinases from accessing the Ser9 site on GSK3β. The Axin binding site on GSK3β does not directly overlap with Ser9, nor is it immediately adjacent, but Axin is a large, disordered protein and could potentially extend towards the N-terminus of GSK3β. Another possibility is that Axin binding produces allosteric changes in the N-terminus of GSK3β that make it less accessible to upstream kinases. There are several crystal structures of GSK3β available, both with and without an Axin peptide bound. These crystal structures do not indicate any obvious changes at the Ser9 site or in the region near the N-terminus of GSK3β. However, the N-terminus of GSK3β is believed to be disordered and is not visible or is only partially visible in the available crystal structures of Axin-bound GSK3β and free GSK3β (Stamos et al., 2014; ter Haar et al., 2001; Dajani et al., 2003; 2001).

Other mechanisms could also contribute to preventing accumulation of pS9-GSK3β in the Wnt destruction complex. Axin has been shown to interact with several phosphatases, including PP2A (Ikeda et al., 2000; Seeling et al., 1999, Hsu et al., 1999), PP1 (Luo et al., 2007), and PP2C (Strovel et al., 2000), and Axin can promote PP2A-mediated dephosphorylation of pS9-GSK3β (Cantoria et al., 2022). Axin recruitment of PP2A into the destruction complex could remove the inhibitory Ser9 phosphorylation from the Wnt-associated pool of GSK3β. A phosphatase-mediated mechanism could be important if exchange between the cellular pools of Axin-bound and free GSK3β is relatively fast compared to the timescale of signaling (Zalatan et al., 2012). Even if Axin protects bound GSK3β from upstream kinases, as we have observed here, if the unphosphorylated GSK3β dissociates and is replaced by pS9-GSK3β then Wnt outputs could still be improperly activated. Further experiments will be needed to quantitively evaluate the effect of Axin on PP2A activity towards pS9-GSK3β.

Another mechanism that could contribute to pathway insulation is if Wnt-associated GSK3β is physically separated from free GSK3β in localized or phase separated compartments. Liquid-liquid phase separation is thought to promote signaling by spatially organizing signaling pathways (Banani et al., 2017; Lyon et al., 2021). Phase separated droplets have been shown to exclude negative regulators from signaling complexes (Su et al., 2016). Wnt pathway proteins also phase separate (Schaefer et al., 2018; Nong et al., 2021), which could exclude kinases like Akt and PKA from accessing Wnt-associated GSK3β. Alternatively, insulin and growth factor signals might only act on a separate, highly-localized pool of GSK3β. Such behavior has been observed in other PKA-dependent pathways, with cAMP-associated microdomains allowing multiple pathways to use PKA to process distinct signals (Anton et al., 2022; Zhang et al., 2020; Bock et al., 2020). Formation of these cAMP microdomains may be mediated in part by the

action of phosphodiesterases, and a similar role for phosphatases might be important for physical separation of GSK3β pools.

Over the past 20 years new models have emerged to suggest that scaffold proteins are more than static binding platforms. These models propose an astounding array of scaffold behaviors. Scaffolds have been proposed to spatially organize and insulate signaling across a vast range of length scales from molecular mechanisms that modulate the rate and localization of one specific chemical reaction, to coordinating positive and negative regulation within signaling pathways or shared signaling nodes, to organizing large structures such as membraneless organelles (Good et al., 2011; Langeberg et al., 2015; Pan et al., 2012; Banani et al., 2017). Dissecting the underlying mechanisms behind these behaviors requires the intersection of fields with similarly varied length scales; techniques in genetics, cell biology, and quantitative biochemistry build on one another to propose and test scaffold mechanisms. Here we provide biochemical evidence for one potential mechanism of scaffold contribution to pathway insulation. Biochemical reconstitution of pathway reactions *in vitro* allowed us to rigorously test how Axin could prevent non-Wnt GSK3β regulation from activating downstream Wnt outputs. Future experiments that expand on this work by exploring the role of phosphatases and phase separation in Axin insulation of Wnt signals will likely provide further insights and reveal additional complexity.

Methods

Protein Expression Constructs

The proteins Axin, pS45-β-catenin, PKA, and the $CREB_{127-135}$ peptide ILSRRPSYR were cloned and expressed as previously described (Gavagan et al., 2020). In short, all sequences except PKA were cloned into *E. coli* expression vectors containing an N-terminal maltose binding protein (MBP) and a C-terminal His6 tag. The catalytic subunit of mouse PKA was expressed from pET15b with an N-terminal His-tag (addgene #14921)(Narayana et al., 1997). pS45-β-catenin was produced by coexpression with CK1α. Lambda phosphatase (λPP) was cloned with an N-terminal GST tag and a C-terminal His6 tag; the human λPP sequence was obtained from VMG950 (Good et al., 2009). Dephosphorylated GSK3β was produced by coexpression with λPP. The coexpression plasmid for GSK3β and λPP was constructed by inserting the GST-λPP expression cassette (without the His6 tag) into the MBP-GSK3β-His plasmid. GSK3β point mutants and Axin truncations were constructed by assembling PCR fragments. Unless otherwise noted, all wt and mutant GSK3β constructs in this study were coexpressed with λPP to ensure they are unphosphorylated.

Protein Expression and Purification

For quantitative kinetic and binding assays, all Wnt pathway, CREB, and PKA proteins were expressed in Rosetta (DE3) pLysS *E. coli* cells by inducing with 0.5 mM IPTG overnight at 18 ºC. Constructs with N-terminal MBP and C-terminal His6 tags (GSK3β, pS45-β-catenin, Axin, and $CREB_{127-135}$) were affinity purified with HisPur Ni-NTA resin (Thermo Scientific) and amylose resin (NEB). The PKA catalytic subunit was purified on Ni-NTA resin. Purified

proteins were dialyzed into 20 mM Tris-HCl pH 8.0, 150 mM NaCl, 10% glycerol, and 2 mM DTT at 4 °C, aliquoted and stored at -80 °C. If necessary, proteins were concentrated using 10000 or 30000 MWCO Amicon Ultra-15 Centrifugal Filter devices at 4 °C, 2000×g. Protein concentrations were determined using a Bradford assay (Thermo Scientific). pS45-β-catenin was further purified by size exclusion chromatography using a Superdex 200 Increase 10/300 GL column (GE Healthcare) to remove a copurifying fragment before being dialyzed into 20 mM Tris-HCl pH 8.0, 150 mM NaCl, 10% glycerol, and 2 mM DTT, aliquoted, and stored at -80 °C.

Quantitative Kinetic Assays

In vitro kinetic assays were conducted in kinase assay buffer [40 mM HEPES pH 7.4, 50 mM NaCl, 10 mM $MgCl_2$, and 0.05% IGEPAL] at 25 ºC in 60 µL total volume. Reactions were initiated by adding ATP to a final concentration of 100 µM. Reaction timepoints for initial rate kinetics were obtained at 10, 30, 60, and 90 seconds (pS45-β-catenin reactions with unphosphorylated GSK3β and GSK3β_S9A); 1, 2, 5, and 10 minutes (pS45-β-catenin reactions with pS9-GSK3β); and 0.5, 1, 2, and 4 minutes (vary [GSK3β] $CREB_{127-135}$] reactions with PKA). 10 µL aliquots were quenched by boiling in 5X SDS loading buffer. Samples were analyzed by SDS-PAGE and quantitative western blotting as described above. For reactions with pS45-β-catenin, all gel samples were diluted 5-fold in 1X SDS loading buffer to prevent a gel smearing artifact that occurs with [pS45-β-catenin] ≥ 500 nM. For reactions with PKA

phosphorylation of GSK3β, samples were diluted 4-fold (500nM GSK3β reactions without Axin) or 2-fold (all other GSK3β concentrations) to prevent signal saturation of the western blot scan.

GSK3β-phosphorylated β-catenin was detected using a primary anti-Phospho-β-Catenin (Ser33/37/Thr41) antibody (Cell Signaling Technology #9561). PKA-phosphorylated GSK3β was detected using a primary anti-phospho-GSK3β (Ser9) antibody (Cell Signaling Technology #5558) that recognizes phospho-S9-GSK3β. PKA-phosphorylated $CREB_{127\text{-}135}$ was detected using a primary anti-phospho-CREB (Ser133) antibody (Cell Signaling Technology #9198). For all reactions, the secondary antibody was IRDye 800CW Goat Anti-Rabbit IgG antibody (Li-Cor #926-32211).

Concentrations of phosphorylated product in each reaction were determined by comparing western blot signal intensities to an endpoint standard containing 50 nM product phosphorylated to completion. For pS45-β-catenin reactions the endpoint is pS45-β-catenin phosphorylated to completion by GSK3β as previously described (Gavagan et al., 2020). The pS45-β-catenin standard was prepared in a reaction with 50 nM pS45-β-catenin, 100 nM GSK3β, and 100 μM ATP in kinase assay buffer at 25 ºC for 15 min. For PKA phosphorylation of GSK3β reactions the endpoint is pS9-GSK3β, phosphorylated to completion by PKA. The pS9-GSK3β standard was prepared in a reaction with 50 nM dephosphorylated GSK3β, 100nM PKA, and 500 μM ATP in kinase assay buffer at 25 ºC for 24 hours. To prevent signal saturation of the western blot scan, the pS9-GSK3β standard was diluted 4-fold in 1x SDS loading dye, to a final concentration of 12.5nM pS9-GSK3β. For $CREB_{127\text{-}135}$ reactions the endpoint is pS133-$CREB_{127\text{-}135}$, phosphorylated to completion by PKA. The pS133-$CREB_{127\text{-}135}$ standard was prepared in a

reaction with 50 nM $CREB_{127\text{-}135}$, 100nM PKA, and 200 μM ATP in kinase assay buffer at 25 ºC for 20 hours.

Initial rate measurements were performed in triplicate. Phosphorylated product levels from quantitative western blots were analyzed using Image Studio Lite 5.2.5 (Li-Cor) and kinetic parameters were determined by fitting to the Michaelis-Menten equation or to a linear fit using Kaleidagraph 4.1.3. Initial rates for each reaction were determined by fitting a linear model to a graph of [product] vs time. Kinetic parameters were determined by fitting plots of initial rates (V_{obs}) vs. [substrate] to the Michaelis-Menten equation $V_{obs} = k_{cat}[E]_0[S]/(K_M + [S])$. Standard errors for k_{cat} and K_M reported in Tables 1 and 2 are from non-linear least squares fits to this equation. Standard errors for k_{cat}/K_M were obtained by fitting an alternative form of the equation $V_{obs} = (k_{cat}/K_M)[E]_0[S]/\left(1 + ([S]/K_M)\right)$. For the pS9-GSK3β reactions without Axin, which did not detectably saturate, the value of k_{cat}/K_M was obtained from the slope of linear fit to the plot of V_{obs} vs. [substrate].

Table 1. Kinetic parameters for pS45-β-catenin reactions, related to Figures 2-3.

Enzyme	**Reaction**	k_{cat} (s^{-1})	K_M (μM)	k_{cat}/K_M ($M^{-1}s^{-1}$)
pS9-GSK3β	–Axin	n.d.	n.d. (≥ 2 μM)	$(4.9 \pm 0.1) \times 10^3$
	+full length Axin	$(2.9 \pm 0.3) \times 10^{-2}$	0.29 ± 0.08	$(1.1 \pm 0.3) \times 10^5$
GSK3β	–Axin	$(2.8 \pm 0.2) \times 10^{-1}$	0.33 ± 0.08	$(8.5 \pm 2.1) \times 10^5$
	+full length Axin	$(3.4 \pm 0.1) \times 10^{-1}$	0.17 ± 0.02	$(2.0 \pm 0.2) \times 10^6$
GSK3β_S9A	–Axin	$(2.8 \pm 0.2) \times 10^{-1}$	0.27 ± 0.05	$(9.5 \pm 1.8) \times 10^5$
	+full length Axin	$(3.3 \pm 0.1) \times 10^{-1}$	0.16 ± 0.02	$(2.1 \pm 0.3) \times 10^6$

Table 2. Kinetic parameters for PKA reactions, related to Figure 4.

Substrate	**Reaction**	k_{cat} (s^{-1})	K_M (μM)	k_{cat}/K_M ($M^{-1}s^{-1}$)
GSK3β	–Axin	$(7.5 \pm 0.3) \times 10^{-3}$	0.062 ± 0.007	$(1.2 \pm 0.1) \times 10^5$
	+full length Axin	$(4.4 \pm 0.1) \times 10^{-3}$	0.25 ± 0.02	$(1.7 \pm 0.1) \times 10^4$
$CREB_{127-135}$	–Axin	$(2.3 \pm 0.04) \times 10^{-2}$	0.15 ± 0.009	$(1.5 \pm 0.1) \times 10^5$
	+full length Axin	$(2.3 \pm 0.05) \times 10^{-2}$	0.14 ± 0.010	$(1.6 \pm 0.1) \times 10^5$

Bibliography

Adams, J.A., Taylor, S.S., 1993. Phosphorylation of peptide substrates for the catalytic subunit of cAMP-dependent protein kinase. J. Biol. Chem. 268, 7747–7752.

Amit, S., Hatzubai, A., Birman, Y., Andersen, J.S., Ben-Shushan, E., Mann, M., Ben-Neriah, Y., Alkalay, I., 2002. Axin-mediated CKI phosphorylation of β-catenin at Ser 45: a molecular switch for the Wnt pathway. Genes Dev. 16, 1066–1076. doi:10.1101/gad.230302

Anastas, J.N., Moon, R.T., 2013. WNT signalling pathways as therapeutic targets in cancer. Nat. Rev. Cancer 13, 11–26. doi:10.1038/nrc3419

Anton, S.E., Kayser, C., Maiellaro, I., Nemec, K., Möller, J., Koschinski, A., Zaccolo, M., Annibale, P., Falcke, M., Lohse, M.J., Bock, A., 2022. Receptor-associated independent cAMP nanodomains mediate spatiotemporal specificity of GPCR signaling. Cell 185, 1130-1142.e11. https://doi.org/10.1016/j.cell.2022.02.011

Anvarian, Z., Nojima, H., van Kappel, E.C., Madl, T., Spit, M., Viertler, M., Jordens, I., Low, T.Y., van Scherpenzeel, R.C., Kuper, I., Richter, K., Heck, A.J.R., Boelens, R., Vincent, J.-P., Rüdiger, S.G.D., Maurice, M.M., 2016. Axin cancer mutants form nanoaggregates to rewire the Wnt signaling network. Nat. Struct. Mol. Biol. 23, 324–332. doi:10.1038/nsmb.3191

Banani, S.F., Lee, H.O., Hyman, A.A., Rosen, M.K., 2017. Biomolecular condensates: organizers of cellular biochemistry. Nat Rev Mol Cell Biol 18, 285–298. https://doi.org/10.1038/nrm.2017.7

Beck, M., Schmidt, A., Malmstroem, J., Claassen, M., Ori, A., Szymborska, A., Herzog, F., Rinner, O., Ellenberg, J., Aebersold, R., 2011. The quantitative proteome of a human cell line. Mol. Syst. Biol. 7, 549. doi:10.1038/msb.2011.82

Beurel, E., Grieco, S.F., Jope, R.S., 2015. Glycogen synthase kinase-3 (GSK3): regulation, actions, and diseases. Pharmacol. Ther. 148, 114–131. doi:10.1016/j.pharmthera.2014.11.016

Bhat, R.V., Andersson, U., Andersson, S., Knerr, L., Bauer, U., Sundgren-Andersson, A.K., 2018. The Conundrum of GSK3 Inhibitors: Is it the Dawn of a New Beginning? JAD 64, S547–S554. doi.org/10.3233/JAD-179934

Bock, A., Annibale, P., Konrad, C., Hannawacker, A., Anton, S.E., Maiellaro, I., Zabel, U., Sivaramakrishnan, S., Falcke, M., Lohse, M.J., 2020. Optical Mapping of cAMP Signaling at the Nanometer Scale. Cell 182, 1519-1530.e17. https://doi.org/10.1016/j.cell.2020.07.035

Burack, W.R., Shaw, A.S., 2000. Signal transduction: hanging on a scaffold. Curr. Opin. Cell Biol. 12, 211–216.

Burack, W.R., Sturgill, T.W., 1997. The activating dual phosphorylation of MAPK by MEK is nonprocessive. Biochemistry 36, 5929–5933. doi:10.1021/bi970535d

Cantoria, M.J., Alizadeh, E., Ravi, J., Bunnag, N., Kettenbach, A.N., Ahmed, Y., Paek, A.L., Tyson, J.J., Doubrovinski, K., Lee, E., Thorne, C.A., 2022. Feedback in the β-catenin destruction complex imparts bistability and cellular memory (preprint). Cell Biology. https://doi.org/10.1101/2022.01.28.478206

Choi, H.-J., Huber, A.H., Weis, W.I., 2006. Thermodynamics of β-catenin-ligand interactions: the roles of the N- and C-terminal tails in modulating binding affinity. J. Biol. Chem. 281, 1027–1038. doi:10.1074/jbc.M511338200

Cross, D.A.E., Alessi, D.R., Cohen, P., Andjelkovich, M., Hemmings, B.A., 1995. Inhibition of glycogen synthase kinase-3 by insulin mediated by protein kinase B. Nature 378, 785–789.

https://doi.org/10.1038/378785a0
Dajani, R., Fraser, E., Roe, S.M., Yeo, M., Good, V.M., Thompson, V., Dale, T.C., Pearl, L.H., 2003. Structural basis for recruitment of glycogen synthase kinase 3β to the axin-APC scaffold complex. EMBO J. 22, 494–501. doi:10.1093/emboj/cdg068
Dajani, R., Fraser, E., Roe, S.M., Young, N., Good, V., Dale, T.C., Pearl, L.H., 2001. Crystal structure of glycogen synthase kinase 3β: structural basis for phosphate-primed substrate specificity and autoinhibition. Cell 105, 721–732. doi:10.1016/s0092-8674(01)00374-9
Ding, V.W., Chen, R.H., McCormick, F., 2000. Differential regulation of glycogen synthase kinase 3β by insulin and Wnt signaling. J. Biol. Chem. 275, 32475–32481. doi:10.1074/jbc.M005342200
El-Gebali, S., Mistry, J., Bateman, A., Eddy, S.R., Luciani, A., Potter, S.C., Qureshi, M., Richardson, L.J., Salazar, G.A., Smart, A., Sonnhammer, E.L.L., Hirsh, L., Paladin, L., Piovesan, D., Tosatto, S.C.E., Finn, R.D., 2019. The Pfam protein families database in 2019. Nucleic Acids Res. 47, D427–D432. doi:10.1093/nar/gky995
Eldar-Finkelman, H., Martinez, A., 2011. GSK-3 Inhibitors: Preclinical and Clinical Focus on CNS. Front. Mol. Neurosci. 4. https://doi.org/10.3389/fnmol.2011.00032
Fang, X., Yu, S.X., Lu, Y., Bast, R.C., Woodgett, J.R., Mills, G.B., 2000. Phosphorylation and inactivation of glycogen synthase kinase 3 by protein kinase A. PNAS 97, 11960–11965. https://doi.org/10.1073/pnas.220413597
Ferrell, J.E., Bhatt, R.R., 1997. Mechanistic studies of the dual phosphorylation of mitogen-activated protein kinase. J. Biol. Chem. 272, 19008–19016. doi:10.1074/jbc.272.30.19008
Fersht, A.R., 1999. Structure and Mechanism in Protein Science. W.H. Freeman and Company.
Fiol, C.J., Mahrenholz, A.M., Wang, Y., Roeske, R.W., Roach, P.J., 1987. Formation of protein kinase recognition sites by covalent modification of the substrate. Molecular mechanism for the synergistic action of casein kinase II and glycogen synthase kinase 3. J. Biol. Chem. 262, 14042–14048.
Fiol, C.J., Wang, A., Roeske, R.W., Roach, P.J., 1990. Ordered multisite protein phosphorylation. Analysis of glycogen synthase kinase 3 action using model peptide substrates. J. Biol. Chem. 265, 6061–6065.
Fiol, C.J., Williams, J.S., Chou, C.H., Wang, Q.M., Roach, P.J., Andrisani, O.M., 1994. A secondary phosphorylation of CREB^{341} at Ser^{129} is required for the cAMP-mediated control of gene expression. A role for glycogen synthase kinase-3 in the control of gene expression. J. Biol. Chem. 269, 32187–32193.
Frame, S., Cohen, P., Biondi, R.M., 2001. A common phosphate binding site explains the unique substrate specificity of GSK3 and its inactivation by phosphorylation. Mol. Cell 7, 1321–1327. doi:10.1016/S1097-2765(01)00253-2
Fraser, E., Young, N., Dajani, R., Franca-Koh, J., Ryves, J., Williams, R.S.B., Yeo, M., Webster, M.-T., Richardson, C., Smalley, M.J., Pearl, L.H., Harwood, A., Dale, T.C., 2002. Identification of the Axin and Frat binding region of Glycogen Synthase Kinase-3. J. Biol. Chem. 277, 2176–2185. doi:10.1074/jbc.M109462200
Gavagan, M., Fagnan, E., Speltz, E.B., Zalatan, J.G., 2020. The Scaffold Protein Axin Promotes Signaling Specificity within the Wnt Pathway by Suppressing Competing Kinase Reactions. Cell Systems 10, 515-525.e5. https://doi.org/10.1016/j.cels.2020.05.002
Geiger, T., Wehner, A., Schaab, C., Cox, J., Mann, M., 2012. Comparative proteomic analysis of eleven common cell lines reveals ubiquitous but varying expression of most proteins. Mol Cell Proteomics 11, M111.014050. doi:10.1074/mcp.M111.014050

Golden, R.J., Chen, B., Li, T., Braun, J., Manjunath, H., Chen, X., Wu, J., Schmid, V., Chang, T.-C., Kopp, F., Ramirez-Martinez, A., Tagliabracci, V.S., Chen, Z.J., Xie, Y., Mendell, J.T., 2017. An Argonaute phosphorylation cycle promotes microRNA-mediated silencing. Nature 542, 197–202. doi:10.1038/nature21025

Good, M., Tang, G., Singleton, J., Reményi, A., Lim, W.A., 2009. The Ste5 scaffold directs mating signaling by catalytically unlocking the Fus3 MAP kinase for activation. Cell 136, 1085–1097. doi:10.1016/j.cell.2009.01.049

Good, M.C., Zalatan, J.G., Lim, W.A., 2011. Scaffold proteins: hubs for controlling the flow of cellular information. Science 332, 680–686. doi:10.1126/science.1198701

Greenwald, E.C., Redden, J.M., Dodge-Kafka, K.L., Saucerman, J.J., 2014. Scaffold State Switching Amplifies, Accelerates, and Insulates Protein Kinase C Signaling. Journal of Biological Chemistry 289, 2353–2360. https://doi.org/10.1074/jbc.M113.497941

Guo, X., Wang, X.-F., 2009. Signaling cross-talk between TGF-β/BMP and other pathways. Cell Res 19, 71–88. https://doi.org/10.1038/cr.2008.302

Ha, N.-C., Tonozuka, T., Stamos, J.L., Choi, H.-J., Weis, W.I., 2004. Mechanism of phosphorylation-dependent binding of APC to β-catenin and its role in β-catenin degradation. Mol. Cell 15, 511–521. doi:10.1016/j.molcel.2004.08.010

Hannoush, R.N., 2008. Kinetics of Wnt-driven β-catenin stabilization revealed by quantitative and temporal imaging. PLoS ONE 3, e3498. doi:10.1371/journal.pone.0003498

Hart, M.J., de los Santos, R., Albert, I.N., Rubinfeld, B., Polakis, P., 1998. Downregulation of β-catenin by human Axin and its association with the APC tumor suppressor, β-catenin and GSK3β. Curr. Biol. 8, 573–581.

He, X., Saint-Jeannet, J.P., Woodgett, J.R., Varmus, H.E., Dawid, I.B., 1995. Glycogen synthase kinase-3 and dorsoventral patterning in *Xenopus* embryos. Nature 374, 617–622. doi:10.1038/374617a0

Hernández, A.R., Klein, A.M., Kirschner, M.W., 2012. Kinetic responses of β-catenin specify the sites of Wnt control. Science 338, 1337–1340. doi:10.1126/science.1228734

Hinoi, T., Yamamoto, H., Kishida, M., Takada, S., Kishida, S., Kikuchi, A., 2000. Complex formation of adenomatous polyposis coli gene product and axin facilitates glycogen synthase kinase-3β-dependent phosphorylation of β-catenin and down-regulates β-catenin. J. Biol. Chem. 275, 34399–34406. doi:10.1074/jbc.M003997200

Hsu, W., Zeng, L., Costantini, F., 1999. Identification of a Domain of Axin That Binds to the Serine/Threonine Protein Phosphatase 2A and a Self-binding Domain. Journal of Biological Chemistry 274, 3439–3445. https://doi.org/10.1074/jbc.274.6.3439

Ikeda, S., Kishida, S., Yamamoto, H., Murai, H., Koyama, S., Kikuchi, A., 1998. Axin, a negative regulator of the Wnt signaling pathway, forms a complex with GSK-3β and β-catenin and promotes GSK-3β-dependent phosphorylation of β-catenin. EMBO J. 17, 1371–1384. doi:10.1093/emboj/17.5.1371

Ikeda, S., Kishida, M., Matsuura, Y., Usui, H., Kikuchi, A., 2000. GSK-3β-dependent phosphorylation of adenomatous polyposis coli gene product can be modulated by β-catenin and protein phosphatase 2A complexed with Axin. Oncogene 19, 537–545. https://doi.org/10.1038/sj.onc.1203359

Itzhak, D.N., Tyanova, S., Cox, J., Borner, G.H., 2016. Global, quantitative and dynamic mapping of protein subcellular localization. eLife 5, e16950. doi:10.7554/eLife.16950

Jacobsen, A., Heijmans, N., Verkaar, F., Smit, M.J., Heringa, J., van Amerongen, R., Feenstra, K.A., 2016. Construction and experimental validation of a Petri net model of Wnt/β-Catenin

signaling. PLoS ONE 11, e0155743. doi:10.1371/journal.pone.0155743
Ji, L., Lu, B., Wang, Z., Yang, Z., Reece-Hoyes, J., Russ, C., Xu, W., Cong, F., 2018. Identification of ICAT as an APC inhibitor, revealing Wnt-dependent inhibition of APC-Axin interaction. Mol. Cell 72, 37–47.e4. doi:10.1016/j.molcel.2018.07.040
Jope, R.S., Johnson, G.V.W., 2004. The glamour and gloom of glycogen synthase kinase-3. Trends in Biochemical Sciences 29, 95–102. https://doi.org/10.1016/j.tibs.2003.12.004
Kaidanovich-Beilin, O., Woodgett, J.R., 2011. GSK-3: Functional insights from cell biology and animal models. Front. Mol. Neurosci. 4, 40. doi:10.3389/fnmol.2011.00040
Kim, E., Ilic, N., Shrestha, Y., Zou, L., Kamburov, A., Zhu, C., Yang, X., Lubonja, R., Tran, N., Nguyen, C., Lawrence, M.S., Piccioni, F., Bagul, M., Doench, J.G., Chouinard, C.R., Wu, X., Hogstrom, L., Natoli, T., Tamayo, P., Horn, H., Corsello, S.M., Lage, K., Root, D.E., Subramanian, A., Golub, T.R., Getz, G., Boehm, J.S., Hahn, W.C., 2016. Systematic Functional Interrogation of Rare Cancer Variants Identifies Oncogenic Alleles. Cancer Discov 6, 714–726. doi:10.1158/2159-8290.CD-16-0160
Kim, S.-E., Huang, H., Zhao, M., Zhang, X., Zhang, A., Semonov, M.V., MacDonald, B.T., Zhang, X., Garcia Abreu, J., Peng, L., He, X., 2013. Wnt stabilization of β-catenin reveals principles for morphogen receptor-scaffold assemblies. Science 340, 867–870. doi:10.1126/science.1232389
Kimelman, D., Xu, W., 2006. β-catenin destruction complex: insights and questions from a structural perspective. Oncogene 25, 7482–7491. doi:10.1038/sj.onc.1210055
Kishida, S., Yamamoto, H., Ikeda, S., Kishida, M., Sakamoto, I., Koyama, S., Kikuchi, A., 1998. Axin, a negative regulator of the Wnt signaling pathway, directly interacts with adenomatous polyposis coli and regulates the stabilization of β-catenin. J. Biol. Chem. 273, 10823–10826. doi:10.1074/jbc.273.18.10823
Langeberg L.K., Scott J.D., 2015. Signalling scaffolds and local organization of cellular behaviour. Nat. Rev. Mol. Cell Biol. 16, 232 doi:10.1038/nrm3966
Lee, E., Salic, A., Krüger, R., Heinrich, R., Kirschner, M.W., 2003. The roles of APC and Axin derived from experimental and theoretical analysis of the Wnt pathway. PLoS Biol. 1, E10. doi:10.1371/journal.pbio.0000010
Levchenko, A., Bruck, J., Sternberg, P.W., 2000. Scaffold proteins may biphasically affect the levels of mitogen-activated protein kinase signaling and reduce its threshold properties. Proc. Natl. Acad. Sci. USA 97, 5818–5823. doi:10.1073/pnas.97.11.5818
Liu, C., Li, Y., Semenov, M., Han, C., Baeg, G.H., Tan, Y., Zhang, Z., Lin, X., He, X., 2002. Control of β-catenin phosphorylation/degradation by a dual-kinase mechanism. Cell 108, 837–847. doi:10.1016/s0092-8674(02)00685-2
Liu, J., Xing, Y., Hinds, T.R., Zheng, J., Xu, W., 2006. The third 20 amino acid repeat is the tightest binding site of APC for β-catenin. J. Mol. Biol. 360, 133–144. doi:10.1016/j.jmb.2006.04.064
Luo, W., Peterson, A., Garcia, B.A., Coombs, G., Kofahl, B., Heinrich, R., Shabanowitz, J., Hunt, D.F., Yost, H.J., Virshup, D.M., 2007. Protein phosphatase 1 regulates assembly and function of the β-catenin degradation complex. EMBO J 26, 1511–1521. https://doi.org/10.1038/sj.emboj.7601607
Lyon, A.S., Peeples, W.B., Rosen, M.K., 2021. A framework for understanding the functions of biomolecular condensates across scales. Nat Rev Mol Cell Biol 22, 215–235. https://doi.org/10.1038/s41580-020-00303-z
MacDonald, B.T., Tamai, K., He, X., 2009. Wnt/β-catenin signaling: components, mechanisms,

and diseases. Dev. Cell 17, 9–26. doi:10.1016/j.devcel.2009.06.016
McManus, E.J., Sakamoto, K., Armit, L.J., Ronaldson, L., Shpiro, N., Marquez, R., Alessi, D.R., 2005. Role that phosphorylation of GSK3 plays in insulin and Wnt signalling defined by knockin analysis. EMBO J. 24, 1571–1583. doi:10.1038/sj.emboj.7600633
McNeill, H., Woodgett, J.R., 2010. When pathways collide: collaboration and connivance among signalling proteins in development. Nat. Rev. Mol. Cell Biol. 11, 404–413. doi:10.1038/nrm2902
Mendoza, M.C., Er, E.E., Blenis, J., 2011. The Ras-ERK and PI3K-mTOR pathways: cross-talk and compensation. Trends in Biochemical Sciences 36, 320–328. https://doi.org/10.1016/j.tibs.2011.03.006
Milo, R., Jorgensen, P., Moran, U., Weber, G., Springer, M., 2010. BioNumbers-the database of key numbers in molecular and cell biology. Nucleic Acids Res. 38, D750–3. doi:10.1093/nar/gkp889
Moon, R.T., Kohn, A.D., De Ferrari, G.V., Kaykas, A., 2004. WNT and β-catenin signalling: diseases and therapies. Nat. Rev. Genet. 5, 691–701. doi:10.1038/nrg1427
Nagaraj, N., Wisniewski, J.R., Geiger, T., Cox, J., Kircher, M., Kelso, J., Pääbo, S., Mann, M., 2011. Deep proteome and transcriptome mapping of a human cancer cell line. Mol. Syst. Biol. 7, 548. doi:10.1038/msb.2011.81
Narayana, N., Cox, S., Shaltiel, S., Taylor, S.S., Xuong, N., 1997. Crystal structure of a polyhistidine-tagged recombinant catalytic subunit of cAMP-dependent protein kinase complexed with the peptide inhibitor PKI(5-24) and adenosine. Biochemistry 36, 4438–4448. doi:10.1021/bi961947
Naqvi, S., Martin, K.J., Arthur, J.S.C., 2014. CREB phosphorylation at Ser133 regulates transcription via distinct mechanisms downstream of cAMP and MAPK signalling. Biochem J 458, 469–479. https://doi.org/10.1042/BJ20131115
Ng, S.S., Mahmoudi, T., Danenberg, E., Bejaoui, I., de Lau, W., Korswagen, H.C., Schutte, M., Clevers, H., 2009. Phosphatidylinositol 3-kinase signaling does not activate the Wnt cascade. J. Biol. Chem. 284, 35308–35313. doi:10.1074/jbc.M109.078261
Nong, J., Kang, K., Shi, Q., Zhu, X., Tao, Q., Chen, Y.-G., 2021. Phase separation of Axin organizes the β-catenin destruction complex. Journal of Cell Biology 220. https://doi.org/10.1083/jcb.202012112
Nusse, R., Clevers, H., 2017. Wnt/β-Catenin Signaling, Disease, and Emerging Therapeutic Modalities. Cell 169, 985–999. doi:10.1016/j.cell.2017.05.016
Pan, C.Q., Sudol, M., Sheetz, M., Low, B.C., 2012. Modularity and functional plasticity of scaffold proteins as p(l)acemakers in cell signaling. Cellular Signalling 24, 2143–2165. https://doi.org/10.1016/j.cellsig.2012.06.002
Park, S.-H., Zarrinpar, A., Lim, W.A., 2003. Rewiring MAP kinase pathways using alternative scaffold assembly mechanisms. Science 299, 1061–1064. doi:10.1126/science.1076979
Pawson, T., Nash, P., 2003. Assembly of cell regulatory systems through protein interaction domains. Science 300, 445–452. doi:10.1126/science.1083653
Perlson, E., Michaelevski, I., Kowalsman, N., Ben-Yaakov, K., Shaked, M., Seger, R., Eisenstein, M., Fainzilber, M., 2006. Vimentin Binding to Phosphorylated Erk Sterically Hinders Enzymatic Dephosphorylation of the Kinase. Journal of Molecular Biology 364, 938–944. https://doi.org/10.1016/j.jmb.2006.09.056
Peterson-Nedry, W., Erdeniz, N., Kremer, S., Yu, J., Baig-Lewis, S., Wehrli, M., 2008. Unexpectedly robust assembly of the Axin destruction complex regulates Wnt/Wg signaling

in Drosophila as revealed by analysis in vivo. Dev. Biol. 320, 226–241. doi:10.1016/j.ydbio.2008.05.521
Polakis, P., 2000. Wnt signaling and cancer. Genes Dev. 14, 1837–1851.
Satoh, S., Daigo, Y., Furukawa, Y., Kato, T., Miwa, N., Nishiwaki, T., Kawasoe, T., Ishiguro, H., Fujita, M., Tokino, T., Sasaki, Y., Imaoka, S., Murata, M., Shimano, T., Yamaoka, Y., Nakamura, Y., 2000. AXIN1 mutations in hepatocellular carcinomas, and growth suppression in cancer cells by virus-mediated transfer of AXIN1. Nat. Genet. 24, 245–250. doi:10.1038/73448
Schaefer, K.N., Bonello, T.T., Zhang, S., Williams, C.E., Roberts, D.M., McKay, D.J., Peifer, M., 2018. Supramolecular assembly of the beta-catenin destruction complex and the effect of Wnt signaling on its localization, molecular size, and activity in vivo. PLoS Genet. 14, e1007339. doi:10.1371/journal.pgen.1007339
Schulze, J.O., Saladino, G., Busschots, K., Neimanis, S., Süß, E., Odadzic, D., Zeuzem, S., Hindie, V., Herbrand, A.K., Lisa, M.-N., Alzari, P.M., Gervasio, F.L., Biondi, R.M., 2016. Bidirectional Allosteric Communication between the ATP-Binding Site and the Regulatory PIF Pocket in PDK1 Protein Kinase. Cell Chemical Biology 23, 1193–1205. https://doi.org/10.1016/j.chembiol.2016.06.017
Seeliger, M.A., Young, M., Henderson, M.N., Pellicena, P., King, D.S., Falick, A.M., Kuriyan, J., 2005. High yield bacterial expression of active c-Abl and c-Src tyrosine kinases. Protein Sci 14, 3135–3139. doi:10.1110/ps.051750905
Seeling, J.M., Miller, J.R., Gil, R., Moon, R.T., White, R., Virshup, D.M., 1999. Regulation of beta-catenin signaling by the B56 subunit of protein phosphatase 2A. Science 283, 2089–2091. https://doi.org/10.1126/science.283.5410.2089
Selenko, P., Frueh, D.P., Elsaesser, S.J., Haas, W., Gygi, S.P., Wagner, G., 2008. *In situ* observation of protein phosphorylation by high-resolution NMR spectroscopy. Nat. Struct. Mol. Biol. 15, 321–329. doi:10.1038/nsmb.1395
Shaywitz, A.J., Greenberg, M.E., 1999. CREB: a stimulus-induced transcription factor activated by a diverse array of extracellular signals. Annu. Rev. Biochem. 68, 821–861. doi:10.1146/annurev.biochem.68.1.821
Sobrado, P., Jedlicki, A., Bustos, V.H., Allende, C.C., Allende, J.E., 2005. Basic region of residues 228-231 of protein kinase CK1α is involved in its interaction with Axin: binding to Axin does not affect the kinase activity. J. Cell. Biochem. 94, 217–224. doi:10.1002/jcb.20350
Speltz, E.B., Zalatan, J.G., 2020. The relationship between effective molarity and affinity governs rate enhancements in tethered kinase-substrate reactions. bioRxiv. doi:10.1101/2020.03.12.989012
Stambolic, V., Woodgett, J.R., 1994. Mitogen inactivation of glycogen synthase kinase-3 beta in intact cells via serine 9 phosphorylation. Biochem J 303, 701–704.
Stamos, J.L., Chu, M.L.-H., Enos, M.D., Shah, N., Weis, W.I., 2014. Structural basis of GSK-3 inhibition by N-terminal phosphorylation and by the Wnt receptor LRP6. eLife 3, e01998. doi:10.7554/eLife.01998
Stamos, J.L., Weis, W.I., 2013. The β-catenin destruction complex. Cold Spring Harb. Perspect. Biol. 5, a007898. doi:10.1101/cshperspect.a007898
Strovel, E.T., Wu, D., Sussman, D.J., 2000. Protein Phosphatase 2Cα Dephosphorylates Axin and Activates LEF-1-dependent Transcription *. Journal of Biological Chemistry 275, 2399–2403. https://doi.org/10.1074/jbc.275.4.2399

Su, X., Ditlev, J.A., Hui, E., Xing, W., Banjade, S., Okrut, J., King, D.S., Taunton, J., Rosen, M.K., Vale, R.D., 2016. Phase separation of signaling molecules promotes T cell receptor signal transduction. Science aad9964. https://doi.org/10.1126/science.aad9964

Sutherland, C., Leighton, I.A., Cohen, P., 1993. Inactivation of glycogen synthase kinase-3β by phosphorylation: new kinase connections in insulin and growth-factor signalling. Biochemical Journal 296, 15–19. https://doi.org/10.1042/bj2960015

Sutherland, C., 2011. What are the *bona fide* GSK3 substrates? Int J Alzheimers Dis 2011, 505607. doi:10.4061/2011/505607

Tejeda-Muñoz, N., González-Aguilar, H., Santoyo-Ramos, P., Castañeda-Patlán, M.C., Robles-Flores, M., 2016. Glycogen Synthase Kinase 3␣ Is Positively Regulated by Protein Kinase C␣-Mediated Phosphorylation Induced by Wnt Agonists. Molecular and Cellular Biology 36, 11.

ter Haar, E., Coll, J.T., Austen, D.A., Hsiao, H.-M., Swenson, L., Jain, J., 2001. Structure of GSK3β reveals a primed phosphorylation mechanism. Nature Structural Biology 8, 593–596. https://doi.org/10.1038/89624

Thompson, J., Williams, C., 2018. Protein Phosphatase 2A in the Regulation of Wnt Signaling, Stem Cells, and Cancer. Genes 9, 121. https://doi.org/10.3390/genes9030121

Thornton, T.M., Pedraza-Alva, G., Deng, B., Wood, C.D., Aronshtam, A., Clements, J.L., Sabio, G., Davis, R.J., Matthews, D.E., Doble, B., Rincon, M., 2008. Phosphorylation by p38 MAPK as an alternative pathway for GSK3beta inactivation. Science 320, 667–670. https://doi.org/10.1126/science.1156037

Tullai, J.W., Chen, J., Schaffer, M.E., Kamenetsky, E., Kasif, S., Cooper, G.M., 2007. Glycogen synthase kinase-3 represses cyclic AMP response element-binding protein (CREB)-targeted immediate early genes in quiescent cells. J. Biol. Chem. 282, 9482–9491. doi:10.1074/jbc.M700067200

Wang, D., Eraslan, B., Wieland, T., Hallström, B., Hopf, T., Zolg, D.P., Zecha, J., Asplund, A., Li, L.-H., Meng, C., Frejno, M., Schmidt, T., Schnatbaum, K., Wilhelm, M., Ponten, F., Uhlén, M., Gagneur, J., Hahne, H., Kuster, B., 2019. A deep proteome and transcriptome abundance atlas of 29 healthy human tissues. Mol. Syst. Biol. 15, e8503. doi:10.15252/msb.20188503

Wang, Q.M., Fiol, C.J., DePaoli-Roach, A.A., Roach, P.J., 1994. Glycogen synthase kinase-3β is a dual specificity kinase differentially regulated by tyrosine and serine/threonine phosphorylation. J. Biol. Chem. 269, 14566–14574. doi:10.3892/ijo.2015.3135

Willert, K., Shibamoto, S., Nusse, R., 1999. Wnt-induced dephosphorylation of Axin releases β-catenin from the Axin complex. Genes Dev. 13, 1768–1773. doi:10.1101/gad.13.14.1768

Wisniewski, J.R., Ostasiewicz, P., Duś, K., Zielińska, D.F., Gnad, F., Mann, M., 2012. Extensive quantitative remodeling of the proteome between normal colon tissue and adenocarcinoma. Mol. Syst. Biol. 8, 611. doi:10.1038/msb.2012.44

Xing, Y., Clements, W.K., Kimelman, D., Xu, W., 2003. Crystal structure of a β-catenin/Axin complex suggests a mechanism for the β-catenin destruction complex. Genes Dev. 17, 2753–2764. doi:10.1101/gad.1142603

Xing, Y., Clements, W.K., Le Trong, I., Hinds, T.R., Stenkamp, R., Kimelman, D., Xu, W., 2004. Crystal structure of a β-catenin/APC complex reveals a critical role for APC phosphorylation in APC function. Mol. Cell 15, 523–533. doi:10.1016/j.molcel.2004.08.001

Zalatan, J.G., Coyle, S.M., Rajan, S., Sidhu, S.S., Lim, W.A., 2012. Conformational control of the Ste5 scaffold protein insulates against MAP kinase misactivation. Science 337, 1218–

1222. doi:10.1126/science.1220683
Zeng, L., Fagotto, F., Zhang, T., Hsu, W., Vasicek, T.J., Perry, W.L., Lee, J.J., Tilghman, S.M., Gumbiner, B.M., Costantini, F., 1997. The mouse Fused locus encodes Axin, an inhibitor of the Wnt signaling pathway that regulates embryonic axis formation. Cell 90, 181–192. doi:10.1016/s0092-8674(00)80324-4
Zhang, F., Phiel, C.J., Spece, L., Gurvich, N., Klein, P.S., 2003. Inhibitory phosphorylation of glycogen synthase kinase-3 (GSK-3) in response to lithium. Evidence for autoregulation of GSK-3. J. Biol. Chem. 278, 33067–33077. doi:10.1074/jbc.M212635200
Zhang, J.Z., Lu, T.-W., Stolerman, L.M., Tenner, B., Yang, J.R., Zhang, J.-F., Falcke, M., Rangamani, P., Taylor, S.S., Mehta, S., Zhang, J., 2020. Phase Separation of a PKA Regulatory Subunit Controls cAMP Compartmentation and Oncogenic Signaling. Cell 182, 1531-1544.e15. https://doi.org/10.1016/j.cell.2020.07.043
Zhu, G., Liu, Y., Shaw, S., 2005. Protein Kinase Specificity: A Strategic Collaboration between Kinase Peptide Specificity and Substrate Recruitment. Cell Cycle 4, 52–56. https://doi.org/10.4161/cc.4.1.1353